APPENDICES

Evaluation of Missouri's NBI Data to Predict the Deterioration of Bridges
TR202012

Principal Investigator
Glenn Washer, Ph.D., P.E., Professor
University of Missouri

Co-Principal Investigator
John Myers, PhD, PE
Missouri University of Science and Technology

Henry Brown, P.E., Research Engineer
University of Missouri

Post-Doctoral Associate
Mohammad Hammed, P.E., Ph.D.
University of Missouri

Authors
Glenn Washer, John Myers, Mohammad Hammed, and Henry Brown

A report from
Missouri Center for Transportation Innovation
University of Missouri
Civil and Environmental Engineering
E2509 Lafferre Hall
Columbia, Missouri 65211

TABLE OF CONTENTS

LIST OF FIGURES

LIST OF TABLES

APPENDIX A. DESCRIPTION OF THE STATISTICAL METHODS

The deterioration modeling for the project was conducted using two separate methodologies. The Kaplan-Meier (K-M) method of survival analysis was used to determine the overall characteristics of deterioration in terms of the time-in-condition rating (TICR) for culverts and bridge components of deck, superstructure, and substructure. This analysis was used to characterize the reliability of structures in terms of how rapidly components' condition rating (CR) decreased over time based on historical inspection records that were obtained for the project.

Cox regression or Cox proportional hazard was used to assess the effect of independent variables such as span length, application of deicing chemicals, etc. on bridge components and culverts' deterioration. This methodology is optimum for assessing multiple independent variables that might influence the deterioration of structures, how these variables interact, and which variables have a significant influence on bridge deterioration.

The contents of this section were summarized in the main body of the report. Additional details on the modeling methodologies used can be found in Appendix C and validation methodologies for testing the applicability of the models can be found in Appendix G.

Kaplan-Meier Survival Analysis

Before introducing the statistical methods used in this research in detail, providing the definition of the terms that are used in subsequent sections of the report would be helpful. The first term is dependent variable also called an outcome variable defined as "any outcome variable associated with some measure" such as the CR of a bridge component or culvert recorded at some inspection intervals [1]. The dependent variable in this research is the time or duration a bridge component or culvert stayed in a CR. For example, a bridge superstructure is rated in CR 7 for 15 years, therefore this superstructure has a time in condition rating (TICR) of 15 in CR 7. Say this superstructure then transitioned to CR 6 and stayed in CR 6 for nine years, then the superstructure has a TICR of 9 in CR 6 and so on. The duration a bridge component or culvert is in service is called survival time. The survival time can be subdivided into survival time for each CR since each CR has distinct definition.

The second term is *covariate*, also called an explanatory variable, defined as "any variable that is measurable and considered to have a statistical relationship with the dependent variable" [1]. Examples of the covariates considered in this project and speculated to have relationship with the dependent variable are snow days, freeze/thaw cycles, Average Daily Traffic (ADT), Average Daily Truck Traffic (ADTT), and

so on. Covariates are divided into *continuous* and *categorical* families. *Continuous* covariates are those that can take any numeric values such as ADT or number of snow days in a given year. *Categorical* covariates are those that are qualitative without any numeric value such as the location of a bridge in any of seven districts of Missouri, or the subdivision of bridge superstructures into subgroups such as prestressed concrete girders and steel girders. Categorical covariates have two or more levels or categories.

The current approach is to perform survival analysis, known in engineering as reliability analysis or time to failure analysis, employing statistical methods to study the incidence and *time of events* [2]. One of the methods for time to failure analysis is the K-M estimator or the product-limit method. The K-M method is a nonparametric maximum likelihood estimator of *time to event data* (i.e., component transitioning to a different CR) and is a common method for treating discontinuous reliability data [2, 3].

Reliability data can be calculated using the K-M estimator by equation (A-1).

$$\hat{S}(t) = \prod_{j:t_j \le t} (1 - \frac{d_j}{n_j}) \text{ for } t_1 \le t \le t_k \qquad \textbf{(A-1)}$$

In equation (A-1), $\hat{S}(t)$ is the K-M estimator, d_j is the number of bridge components for which the event occurred (transitioned to the lower CR) at time t_j, n_j is the number of bridge components at risk of event at time t_j, and t_1, t_k are the boundary for *k* distinct event times. The K-M estimator is accompanied by statistics such as the mean, median, confidence interval for the median, standard error of the mean, and hazard rate that can be used to analyze results.

The *hazard* or *failure* rate is the number of bridge components per unit of time (year) to transition from one CR to the lower one (assuming the rate is constant during the year). The hazard rate can be computed instantaneously, cumulatively, or averaged within a certain time interval [4]. The instantaneous hazard rate is the number of bridge components that transition to a lower CR in a unit of time (year) and this quantity varies from one year to the next. This estimate can be computed for $t_j \le t \le t_{j+1}$ using equation (A-2) in which $\tau_j = t_{j+1} - t_j$ [5].

$$\hat{h}(t) = \frac{d_j}{n_j \cdot \tau_j} \qquad \textbf{(A-2)}$$

The cumulative failure rate is the integral of the instantaneous hazard rate within the interval of 0 to *t*, and this quantity could be computed as $H(t) = -\ln(\hat{S}(t))$. Similarly, average failure rate (AFR) could be computed within any two time-intervals. Since instantaneous failure rate is variable and changes in each unit of time, the AFR could be used to give a single number to indicate the average number of bridge components in a given CR per year to transition to the lower CR during the years the data are available for analysis.

Finally, the K-M estimator can be used to study the effect of time-invariant covariates (explanatory variables) on bridge performance such as bridge families with different ADT, span length, location, and environmental conditions, and so on. Or bridges can be grouped based on construction era (1980 – 2000 vs. 2000 – 2017) by time-blocking to study the effect of higher standards and improved construction material on bridge performance with those of the old standards and lower quality material. Other parameters described in Objective 3 can also be studied in this way. In this research, the K-M method has been used to study certain covariates, such as the material of construction for superstructure components (e.g., steel, PSC, etc.) and deterioration patterns among districts. However, the K-M estimator is not effective for analyzing the potential interactions between multiple covariates, such as the effect of deicing chemical application, snowy days, and ADT in combination. For this reason, Cox regression analysis has been used to study these covariates, as will be described in further sections of the report.

Figure A-1 shows the deterioration model for steel superstructures in Missouri. These data indicate the TICR in years for bridges with different CRs ranging from 8 to 3. Figure A-1A shows the reliability (probability) of a component transitioning from one CR to another. The red line in the figure illustrates the median transition time. For example, for CR 5 (+), 50% of the components will transition to CR 4 after about 7 years in CR 5. Figure A-1B illustrates the deterioration rate of the component which is the compliment of the reliability.

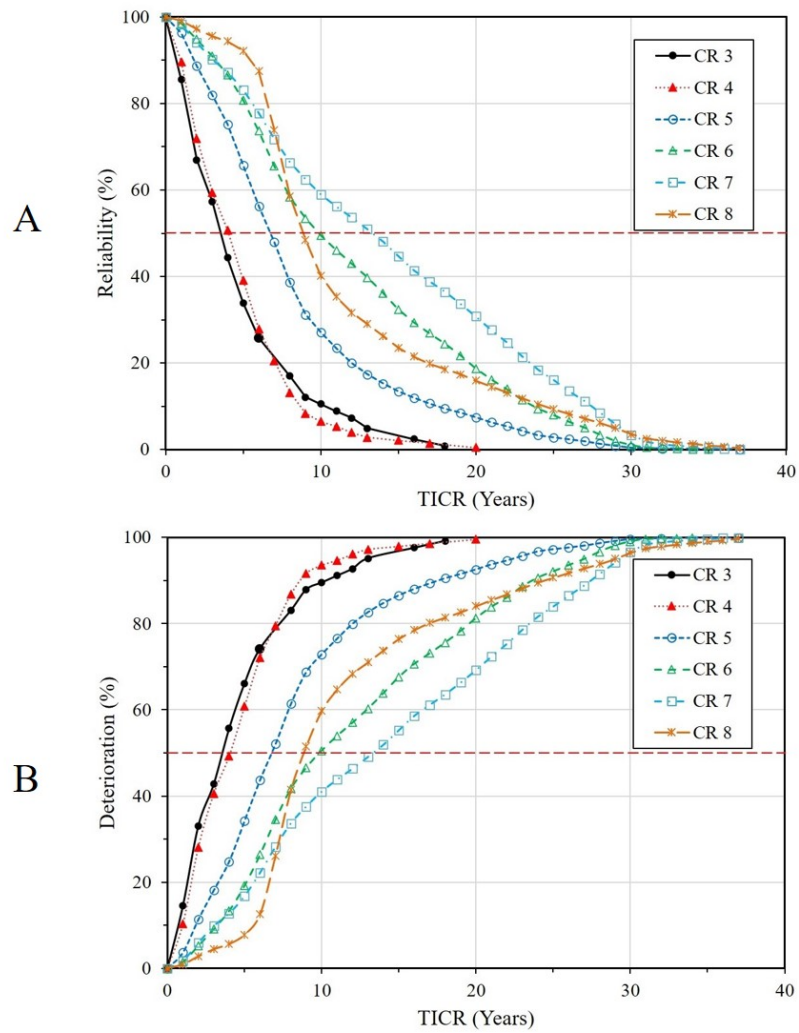

Figure A-1. K-M deterioration models for steel superstructures in Missouri.

The K-M method is only capable of analyzing survival data or the dependent variable alone to describe the reliability and deterioration patterns for bridge components and culverts. To investigate the effect of covariates on the reliability or deterioration of the bridge components or culverts another statistical method called *Cox proportional hazard* method or *Cox regression* is used.

Cox Regression Analysis

Cox proportional hazards model or Cox regression is semi-parametric method used for analyzing the effect of explanatory variable on the survival data [6]. This method is called semi-parametric as it has "a fully parametric regression structure but leaves their dependence on time unspecified" [7]. The equation for the Cox regression model is shown in equation (A-3).

$$h(t, X, \beta) = \lambda_0(\mathrm{t}) \times \exp(\beta_1 X_1 + \beta_2 X_2 + \cdots) \quad \textbf{(A-3)}$$

In equation (A-3), h(t, X, β) is the dependent variable as a function of time and covariates (X, β). The dependent variable corresponds to the NBI CR assigned by inspectors to each one of the bridge components (deck, superstructure, and substructure) and culverts. The CR changes as bridges/culverts deteriorate, typically dropping to the next lower CR. Deterioration of the bridges/culverts and changes in CR are caused by factors such as salt used for deicing purposes, ADT, snow days, freeze/thaw cycles, and so on. These parameters believed to affect the deterioration patterns for bridge components and culverts are called *covariates*. The dependent variable is the product of the hazard function $\lambda_0(\mathrm{t})$ that "characterizes how the hazard function changes as a function of time" and the exponentiated linear function of the covariates, $\exp(\beta_1 X_1 + \beta_2 X_2 + \cdots)$ [7]. As shown, the hazard is a function of time, but the covariates are time independent – the covariates do not change with respect to time. The β's are unknown parameters computed based on the available data for each covariate, X_n. No assumption is made about the shape of the hazard function $\lambda_0(\mathrm{t})$, and that is why Cox regression is called semi-parametric. If all covariates are equal to zero, then exp(0) equals a value of 1, leaving only the baseline hazard function, $\lambda_0(\mathrm{t})$. The baseline hazard function is analogous to the intercept or the constant term in ordinary regression [7].

The parameter estimate for each covariate, β, is calculated using the method of partial maximum likelihood for each covariate. One of the properties of the Cox regression is that it can be stratified across variables not considered as a covariate such as the CR 3 - 8. In the case of stratified Cox regression, a single parameter is estimated by pooling the information from all strata – one parameter is estimated for CRs 3 – 8 of bridge components or culverts. Hence, as will be shown later, sample size in a given CR, especially in CR 3, may negatively affect the parameter estimate.

The hazard ratio for two subjects (bridges or culverts) with covariate x_0 and x_1 using equation (A-3) only depends on (X,β) as the hazard functions cancels out each other as shown in equation (A-4). In this way, the hazard ratio

$$HR(t, x, \beta) = \frac{\exp(\beta_1 X_1)}{\exp(\beta_0 X_0)} \quad \textbf{(A-4)}$$

can be used to compare the effect of one covariate to another. For example, this could be used to compare bridge performance in one district as compared to a different district.

Model Development

Before embarking to model building for Cox proportional hazard method, the covariates were studied together to determine if there is any collinearity or multicollinearity, which is the case "in many nonexperimental situations" [8]. Collinearity or multicollinearity is defined as the correlation between the explanatory variables (i.e., *covariates*) available for model-building and those that are left out or neglected [8]. Multicollinearity between the explanatory variables poses problems that need to be addressed as outlined below [8, 9].

1. Presence of multicollinearity does not "inhibit our ability to obtain good fit nor does it tend to affect inference about the mean responses or predictions of new observations, provided these inferences are made within the region of observations."
2. "The estimated regression coefficients tend to vary widely from one sample to the next when the predictor variables are highly correlated. As a result, only imprecise information may be available about the individual true regression coefficients."
3. The interpretation of the regression coefficients to find out the effect of an explanatory variable on the response variable by increasing one covariate by one unit and holding all other covariates constant "is not fully applicable". For example, to study the effect of bridge deterioration based on the number of snow days and the amount of salt used for deicing purposes, it is unrealistic to increase one covariate and keep the other one constant, because increasing one covariate inherently means the increase in use of the other covariate. Or ADTT is recorded as a percentage of ADT in the SI&A guide and the increase in ADT would cause the ADTT to increase proportionally.
4. "A regression coefficient does not reflect any inherent effect of the particular predictor variable on the response variable, but only a marginal or partial effect, given whatever other predictor variables are included in the model. Or correlated covariates "contains much of the same information".
5. The parameter estimate for the covariate is not significant even though the variable should be highly correlated with the response variable, the TICR.
6. Addition or deletion of a covariate changes other regression coefficients "dramatically."
7. The sign of the regression coefficient is the opposite of the reality or prior experience.

There are two ways to check for collinearity or multicollinearity. As an informal method, the simple correlation between the covariates using the pairwise correlation is helpful, but to unearth multicollinearity among several covariates, variance inflation factor (VIF) is effective. VIF is a measure of "how much the variance of an estimated regression coefficient increases" if the covariates are correlated [9]. The VIF for uncorrelated explanatory variables is equal to 1, and a greater VIF shows multicollinearity among predictor variables. There are different recommendations in the literature about ranking the severity of VIF. VIF of less than 4 is considered moderate and VIF between 4 to 10 is considered high. A VIF greater than 10 indicates that the "regression coefficients are poorly estimated due to multicollinearity" [8-10].

Table A-1 contains the VIF for the continuous covariates that would be used to build Cox regression model for cast-in-place (CIP) decks. In this table, each covariate is regressed on all other continuous covariates. Each column lists the covariate number against which each of the numbered covariates are regressed. For example, the first column lists the VIF result for the case where age in TICR is regressed on all other covariates. As shown in Table A-1, the VIF for the structure length is low (1.97) and the VIF for ADT and ADTT are high (close to 10). The VIF for the freeze/thaw and snow is about 2.5 or greater when both of the covariates are together, but when either one of the covariates are removed from the model - as shown in column 4 and 5 – the VIF is reduced for the other covariate, to a value of ~1.1 in this case.

Table A-1. Variance Inflation Factor (VIF) for continuous covariates for CIP decks.

Covariate No.	Covariate Name	1	2	3	4	5	6	7	8
1	Age in TICR		1.25	1.23	1.14	1.22	1.25	1.25	1.22
2	Structure length (ft.)	1.97		1.04	1.97	1.97	1.97	1.97	1.97
3	Max. span length (ft.)	2.01	1.07		2.04	2.04	2.04	2.04	2.03
4	Freeze/thaw (days/year)	2.54	2.78	2.78		1.11	2.78	2.79	2.62
5	Snow (days/year)	2.75	2.82	2.82	1.13		2.80	2.82	2.44
6	ADT	9.62	9.63	9.63	9.61	9.57		1.30	9.13
7	ADTT	9.18	9.19	9.20	9.20	9.20	1.24		9.14
8	Salt (tons/lane miles)	1.41	1.45	1.44	1.36	1.26	1.38	1.44	

The following are the remedial actions recommended in the literature for lessening the effects of multicollinearity [8-10].

1. Drop one or more predictors from the regression model to minimize the effect of multicollinearity.
2. "Restrict the use of the fitted regression model to inferences for values of the predictor variables that follow the same pattern of multicollinearity."
3. Use centered data for covariates – subtract the mean of a covariate from all observations – included in the analysis.
4. Model the response variable on different explanatory variables of the same data set.
5. Use Principal Component Analysis (PCA) to select the number of covariates that explain the majority of the error for the response variable.

In this report a combination of recommendations 1 and 4 are employed to select the explanatory variables. For example, a Cox regression model is built by including ADT and another Cox regression is built by including ADTT, or similarly, two separate Cox regressions are built for the covariates of maximum span length and structure length. Recommendation 1 would be applied using the VIF criterion for correlated covariates. Since the VIF is calculated by regressing one explanatory variable on all other covariates and it is not related to the response variable and "the functional form of the model for the dependent variable is irrelevant to the estimation of collinearity," it is applicable to Cox regression as well [11].

Based on recommendation 1, dropping either one of the correlated covariates would lessen the effect of multicollinearity, and based on recommendation 4, we can build two models with different covariates of the same effect on the response variable, TICR.

As mentioned before, partial maximum likelihood method is used to estimate the parameters associated with each of the covariates considered for each bridge component or culverts. The maximum likelihood estimate ($\hat{L}$) shows "the extent to which the data are fitted by a particular model" and for a model the larger this statistic "the better is the agreement between the model and the observed data" [5].

$$L(\beta) = \prod_{j=1}^{r} \frac{\exp\,(\acute{\beta}\, x_{(j)})}{\sum_{l \in R(t_{(j)})} \exp\,(\acute{\beta}\, x_l)} \qquad \textbf{(A-5)}$$

In equation (A-5), x is the vector of the covariates and β is the parameter estimate for the covariates. The summation in the denominator is the sum of the values of exp $(\acute{\beta}\, x_l)$ over all bridges at risk at time $t_{(j)}$, and $R(t_{(j)})$ is the bridge set at risk of transitioning to the lower CR. As shown in equation (A-5), the maximum likelihood will be smaller than unity as it is the product of several conditional probabilities. Consequently, "-2log L will always be positive, and for a given data set, the smaller the value of -2log L, the better the model." [5]

Table C-1 contains the statistic -2log L, and the likelihood ratio test which compares the model with a covariate with the null model using equation (A-6).

$$Likelihood\ ratio = -2\log\frac{L_1}{L_2} \qquad \textbf{(A-6)}$$

In equation (A-6), L1 is the null model and L2 is the model with the covariate. The likelihood ratio test is asymptotically a chi-square distribution under the null hypothesis that the coefficient of the added covariate(s) is zero. The degree of freedom (DOF) for this distribution is equal to the difference between the number of covariates for the two models. If the value of this ratio is not large, the two models could be judged to be the same, but if the ratio is large, it indicates that the addition of the new covariate is needed in the model. The likelihood ratio test is compared with the theoretical chi-squared distribution with the same number of DOF and a predefined decision rule (say 5%). If the likelihood ratio test is larger than the critical value of the theoretical chi-squared distribution or alternatively the probability value associated with the likelihood ratio test is smaller than the predefined decision rule value, it shows that the extra covariate is needed in the model. For the cases where each covariate is added to the model one by one, the null model is compared with the new model with only one covariate (DOF=1) and the critical value for chi-square

distribution with one DOF is 3.84. Therefore, any likelihood ratio greater than 3.84 or any probability value smaller than the 0.05 indicates that the added covariate is statistically significant and needed in the model. Similarly, any value smaller than 3.84 indicates that the covariate is not significant when considered individually but may be significant when considered along with other covariates.

Model development recommended by Collett (and outlined below) was followed for developing the model for bridge components and culverts and was supplemented by automatic variable selection [5].

1. Each covariate is added to the Cox regression independently, and its effect on deterioration is calculated by comparing the likelihood ratio test of the Cox regression when the covariate is included as compared with the null Cox model without the covariate in the model. In this step the statistical significance of each covariates applied independently is assessed.
2. All covariates that were statistically significant at 15% in step 1 are modeled together. Some covariates may cease their significance in the presence of other covariates.
3. Covariates that are no longer significant in step 2 are removed from the model one at a time, and their effect is calculated by comparing the log-likelihood of the full model – all covariates from step 2 included – to the log-likelihood from the model with the insignificant covariate discarded. If the discarded covariate does not affect the likelihood ratio test, it is discarded from the model.
4. Covariates that were not significant independently in step 1 are added to the model from step 3 one at a time to check if any covariate become significant in the presence of other covariates.
5. Higher order terms of the covariates (x^2, x^3, …) and interaction terms are considered between the explanatory variables from step 3. The model from this step would be used further to verify model assumptions, goodness of fit test, and detecting outliers (if any).

Model Assumptions

There are two assumptions for the Cox regression model shown in equation (A-3). 1) the proportional hazard assumption – the hazards are not changing with time and 2) the explanatory variables are modeled with the correct functional form – x, x^2, log(x), or $\sqrt{x}$. Tests are available to verify the assumptions and to take corrective actions in case of any violation. These tests are discussed in the following paragraphs.

Proportional Hazard Assumption

The proportional hazard (PH) assumption states that the covariates are not time dependent – the hazard is the same if a bridge's TICR changes from 10 to 15 or from 30 to 35, i.e., no time dependence. There are several methods to check continuous covariates for the PH assumption: graphical, goodness-of-fit (GOF), Schoenfeld residuals, and time-dependent variable approaches [6]. The graphical and GOF has some drawbacks related to the number of observations and the censoring, but Schoenfeld residuals and the time-dependent variable approach is preferred [2]. For example, to test a continuous covariate for the PH assumption using Schoenfeld residuals, the Schoenfeld residuals are computed for continuous covariates included in the model and plotted as the Schoenfeld residual against the function of time [12]. The time could be a simple function such as (t) where it corresponds to TICR for bridge components and culverts or

other functions of the time such as log (TICR). Fitting a curve on the scatter plot of the Schoenfeld residuals would reveal if the PH holds or not. A flat smooth curve near zero would suggest that the PH assumption is valid for the covariate.

Another way of using the Schoenfeld residuals is to calculate its correlation coefficient with the function of time such as TICR, log (TICR), or $TICR^2$ [2]. In this case, the assumption is that the Schoenfeld residuals are independent of time, therefore there should not be a statistically significant correlation coefficient. Here the null hypothesis is that there is no correlation between the function of time and the Schoenfeld residuals calculated for each continuous covariate at a specified significance level, say 5%. Hence, the alternate hypothesis is that correlation exists between the Schoenfeld residuals and the function of time. Thus, any correlation coefficient for a covariate smaller than 5% indicates that the PH does not hold for that covariate and correction measures should be employed.

The PH assumption for categorical covariates is assessed using the K-M curve constructed for all the levels of the covariate included in the model [12]. For the PH assumption for the categorical covariates to hold, the levels of the covariates should not cross each other, look parallel, and be of a similar shape [12]. A different way than the graphical test would be to request test statistics across all the levels.

Covariates Functional Form

In the Cox regression model shown in equation (A-3), the covariates are assumed to be related to the hazard function as a simple linear function. This assumption should be verified before interpretating the Cox regression results. Martingale residuals is one of the most common ways to check the functional form of the continuous covariates [13]. "The residual can be interpreted as the difference over time of the observed number of events minus the expected number of events under the assumed Cox model" [13]. To find the functional form of a continuous covariate, the Cox model is fitted to all other covariates in the model except the covariate for which the functional form is to be determined. The Martingale residual is then plotted against the values of the covariate not included in the model and a smoothed curve is fitted to the scatter plot. The shape of the smoothed curve defines the actual functional form of the covariate to be included in the model [13]. Another common practice is to fit a null model – a model without any covariate - and output the Martingale residuals against each of the continues covariates identified for the model [12]. A smoothed curve fitted on the Martingale residuals indicate the functional form of the covariate to be used for building the model. A straight line or nearly straight line indicates that a linear relationship, x, hold between the independent variable and the covariate [12].

Detecting Influential Observations and Outliers

Detecting influential observations on the parameter estimates (β) and outliers are two issues to be studied once a Cox regression model is fit. To detect the influence of each observation on a parameter estimate "is to compare the estimate β one obtains by estimating β from all the data, to the estimate $\beta_{(j)}$ obtained from the data with the given observation deleted from the sample" [13]. To determine the influence of an observation, $\beta - \beta_{(j)}$, also known as dfbeta, *dfβ,* is calculated and if the value is close to zero, there is no influence from observation j on the parameter estimate, but if the value is large, it suggests an influence on the parameter estimate from observation j [13]. Another way to check for influence of individual observation is to compare *dfβ* with the parameter estimate. Influential observations could be detected by the score residuals, where it approximates $b - b_{(j)}$, and a plot of this residual against each covariate X_{jk} would reveal the effect of the jth observation on the covariate k [13]. A positive value of the *dfβ*, indicates that the exclusion of an observation reduces the parameter estimate and this implies that inclusion of an observation increases the parameter estimate [12]. In other words, *dfβ* is the measurement of the effect of an observation on the parameter estimate when the observation is included in the model [12].

Assessment of the Overall Model Fit

There may be interest on the assessment of influential observations and outliers on parameter estimate for each covariate included in the model, but also on the overall fit of the model. To assess the effect of observations on the overall fit of the model, likelihood displacement could be generated from the model and then plotted against TICR for bridge components and culverts [12]. "The likelihood displacement score quantifies how much the likelihood of the model, which is affected by all coefficients, changes when the observation is left out." [12]

Predictive Accuracy of the Cox Regression

"The predictive accuracy of a statistical model can be measured by the agreement between observed and predicted outcome." [14] In Cox regression, *concordance statistics,* also called *C-statistic*, is one measure of accuracy. "The concept underlying concordance is that a subject who experiences a particular outcome has a higher predicted probability of that outcome than a subject who does not experience the outcome. The C-statistic can be calculated as the proportion of pairs of subjects whose observed and predicted outcomes agree (are concordant) among all possible pairs in which one subject experiences the outcome of interest and the other one does not. The number of pairs is calculated using $\binom{n}{2}$, where n is the number of observations in the data set. The higher the C-statistic, the better the model can discriminate between subjects who do experience the outcome of interest and subjects who do not." [14] Harrell's C-statistic is one of several concordance formulations that are used for survival analysis. The concordance statistics can

be calculated by using equation (A-7) where n_c is the number of concordance observations, n_t is the number of tied observations (same time events or identical covariates), and n_d is the number of discordant observations.

$$C = \frac{n_c + 0.5 \times n_t}{n_c + n_d + n_t} \qquad \textbf{(A-7)}$$

Another way of measuring the predictive accuracy of Cox regression is the receiver operator characteristic (ROC) and area under the ROC curve (AUC). "Time-dependent ROC curves and AUC functions characterize how well the fitted model can distinguish between subjects who experience an event from subjects who are event-free. Whereas C-statistics provide overall measures of predictive accuracy, time-dependent ROC curves and AUC functions summarize the predictive accuracy <u>at specific times</u>. In practice, it is common to use several time points within the support of the observed event times. " [14]

APPENDIX B. SUPERSTRUCTURE TYPES LISTED IN THE NBI

Materials and Type of Construction

Structure Kind and Structure Type

Structure kind (043A) and structure type (043B) variables describe the materials of construction (e.g., steel, reinforced concrete, prestressed concrete, etc.) and construction type (e.g., simply supported, continuous, truss, girder, etc.). The combination of these two items was used to identify families of bridges with similar material and construction type for analysis.

Table B-1 lists the number and kinds of state-owned bridge families. There were 56 different combinations of structure type and kind found in the inventory. The most common structure overall was found to be a continuous concrete culvert with 3,310 structures. The most common bridge types were bridges with steel superstructures, either continuous (2,645) or simple span (1,602), followed by prestressed concrete continuous structures (1,262).

The three most common materials for bridge superstructure construction were steel, reinforced concrete (RC), and prestressed concrete (PSC). Considering all structure types for each of these materials, there were 4,836 steel bridge, 5,558 RC bridges and culverts and 2,601 prestressed PSC bridges.

It should be noted that the table includes all of the structures considered in the research, which included NBI records that spanned 37 yrs. The values shown in the table are not the current number of bridge or culverts, but rather the number of bridges and culverts included in the NBI over the 37 yrs addressed through the research.

Table B-1. Table list of different structures by type and kind.

SI&A items		SI&A description	No.	SI&A items		SI&A description	No.
43A	43B			43A	43B		
2	19	Concrete continuous culvert	3,310	2	5	Concrete continuous box beam or girder - multiple	12
4	2	Steel continuous stringer/multi beam girder	2,645	8	19	Masonry culvert	9
3	2	Steel stringer/multi beam girder	1,602	3	12	Steel arch – thru	7
6	2	Prestressed concrete continuous stringer/multi beam girder	1,262	3	9	Steel truss – deck	6
1	4	Concrete tee beam	790	6	1	Prestressed concrete continuous slab	6
2	1	Concrete continuous slab	767	1	6	Concrete box beam or girders - single or spread	5
3	10	Steel truss – thru	423	4	14	Steel continuous stayed girder	5
5	5	Prestressed concrete box beam or girder - multiple	384	2	7	Concrete continuous frame (except frame culverts)	4
6	4	Prestressed concrete continuous tee beam	344	3	0	Steel other	4
1	1	Concrete slab	247	0	2	Other stringer stringer/multi-beam or girder	3
5	6	Prestressed concrete box beam or girder – single	201	4	12	Steel continuous arch – thru	3
2	6	Concrete continuous box beam or girders - single or spread	193	4	6	Steel continuous box beam or girders - single or spread	3
5	2	Prestressed concrete stringer/multiple-beam or girder	174	1	5	Concrete box beam or girders - multiple	2
5	4	Prestressed concrete tee beam	169	2	2	Concrete continuous stringer/multi-beam or girder	2
1	22	Concrete channel beam	120	4	19	Steel continuous culvert (includes frame culverts)	2
4	3	Steel continuous girder and floor beam system	44	4	7	Steel continuous frame (except frame culverts)	2
1	11	Concrete arch – deck	34	4	9	Steel continuous truss – deck	2
7	2	Timber stringer/multi-beam or girder	34	0	19	Other culvert (includes frame culverts)	1
3	19	Steel culverts	33	1	3	Concrete girder and floor beam system	1
4	10	Steel continuous truss – thru	28	2	12	Concrete continuous arch - thru	1
6	6	Prestressed concrete continuous box beam or girder – single	26	3	1	Steel slab	1
3	3	Steel girder and floor beam system	25	3	13	Steel suspension	1
1	7	Concrete frame (except frame culverts)	20	3	5	Steel box beam or girders - multiple	1
2	4	Concrete continuous tee beam	20	3	7	Steel frame (except frame culverts)	1
2	11	Concrete continuous arch - deck	18	4	13	Steel continuous suspension	1
5	1	Prestressed concrete slab	18	6	21	Prestressed concrete continuous segmental box girder	1
6	5	Prestressed concrete continuous box beam or girder – multiple	16	7	0	Timber other	1
1	2	Concrete stringer/multi-beam or girder	12	8	11	Masonry arch – deck	1
						Total number of bridges and culverts	13,047

APPENDIX C. DATA ANALYSIS

This appendix includes fundamental data from the Cox regression analysis for structures. The data in this section supplements the main body of the report. Data in this appendix is primarily intended for researchers interesting in the modeling methodologies used in this research.

Reliability of CIP Bridge Decks

The -2log L and the likelihood ratio for the covariates of the Cox regression model for CIP decks is shown in Table C-1. As shown in Table C-1, except for the ADT and ADTT, all other covariates are statistically significant when examined individually. It was found that ADT and ADTT did not have a statistically significant effect on the deterioration of CIP decks.

Table C-1. Table showing maximum likelihood estimate for CIP deck covariates.

Var. No.	Variables in model	-2log $\hat{L}$	Likelihood ratio	Result
0	None	242,492.64		Null model
1	Age in TICR	242,446.15	46.49	Significant
2	Structure length (ft.)	242,479.71	13.99	Significant
3	Maximum span length (ft.)	242,435.75	56.89	Significant
4	Freeze/thaw (days/year)	242,455.34	37.30	Significant
5	Snow (days/year)	242,463.27	29.36	Significant
7	Salt (tons/lane miles)	242,419.31	73.33	Significant
8	ADT	242,492.25	0.39	Not signi.
9	ADTT	242,492.41	0.23	Not signi.
10	District	242,398.57	94.07	Significant
11	Region	242,442.91	49.73	Significant
12	Superstructure type	242,228.75	263.89	Significant

Table C-2 lists the effect of covariates on the performance of the CIP decks. This table presents the final results where all modeling steps have been completed and all assumptions and diagnosis were met. The first column lists the name of the covariate, the second column lists the parameter estimate ($\hat{\beta}$) for each covariate, the fourth column contains the standard error for the parameter estimate. The table also shows the chi-square value and probability value (p-value) comparing the chi-square from the fifth column to the critical value of theoretical chi-square value (3.84 for p-value of 0.05) for the single degree of freedom model. The p-value indicates if the covariates are statistically significant by recording the likelihood the chi-squared value exceeds the theoretical values simply by chance. Smaller values in this column indicate that the occurrence was not by chance but rather was statistically significant. Values greater than 0.5 indicate the covariate was found not to be statistically significant.

In Table C-2, the first five rows record the results for the categorical covariate *superstructure type*. The superstructure type steel cont. girders is not listed but rather acts as the reference for the other combinations of deck and superstructure type. Each of the five superstructure types shown have a parameter estimate and

associated standard error that was used to construct the confidence interval for the parameter estimate. The last column for the first five rows shows that the performance of the CIP decks on different superstructure types is different as indicated by the p-value less than 0.05 or 5%.

Row 6 lists the parameter of the age in TICR and rows 7-11 contain the interaction of age in TICR with the different superstructure types. The interaction of age in TICR with superstructure types demonstrates that age affects the performance of the CIP decks on different superstructure types differently for most superstructure types. The only exception is CIP decks on the PSC continuous girders where the p-value is greater than 0.05. This shows that the performance of the CIP deck on PSC continuous girders may not be statistically different than CIP deck on the reference superstructure type – steel continuous girders. However, these data indicate that there is a statistical difference between the effect of age on deterioration of bridge decks *(other than for PSC)*; the effect is relatively small, and the negative value for the parameter estimate indicates that the performance is better as compared to compared to CIP decks on continuous steel superstructures.

Table C-2. Table showing Cox regression model output for CIP decks.

No.	Covariate	Parameter estimate ($\hat{\beta}$)	Standard error	Chi-square	P-value
1	RCC slabs	0.197	0.049	15.83	<.0001
2	CIP deck on RCC beams	0.336	0.061	30.40	<.0001
3	CIP deck on steel girders	0.252	0.057	19.61	<.0001
4	CIP deck on PSC cont. girders	0.110	0.046	5.592	0.018
5	CIP deck on PSC box beams	0.900	0.058	239.2	<.0001
6	Age in TICR	0.022	0.001	391.7	<.0001
7	Age in TICR*RCC slabs	-0.015	0.001	101.1	<.0001
8	Age in TICR*CIP deck on RCC beams	-0.021	0.002	194.3	<.0001
9	Age in TICR*CIP deck on steel girders	-0.013	0.001	87.79	<.0001
10	Age in TICR*CIP deck on PSC cont. girders	-0.002	0.003	0.403	0.525
11	Age in TICR*CIP deck on PSC box beams	-0.028	0.004	44.34	<.0001

Table C-3. contains the effect of district on the performance of the CIP decks. The northeast (NE) district is not listed in the table because this categorical covariate was selected as the reference. From the p-value column it is evident that CIP decks located in different districts perform differently in most cases. The exception is the for the KC district that has a p-value of 0.059, which is close to 0.05. It should be noted the choosing the p-value of 0.05 is a subjective choice that is the normal convention for this type of analysis. A different value could be selected. For example, the 0.05 p-value indicates a 1 in 20 chance that differences could be the result of chance and therefore not statistically significant. If a p-value of 0.10 was chosen, it would mean that there is a 1 in 10 chance the difference could be the result of chance, a less rigorous threshold. Consequently, these data don't indicate there wasn't any difference at all between the KC district and the NE district, only that the difference did not meet the statistical test at the level being used in the analysis.

Row 7 in Table C-3. lists the effect of salt on the performance of the CIP decks and rows list the interaction of salt with each of the six levels of the district covariates, with the NE district again acting as the reference. The p-value column for rows 8-13 indicates that the effect of salt in NW, CD, and SW is different than the effect of salt in NE as demonstrated by the smaller p-values. In contrast, the effect of salt in KS, SL, and SE is not different than the effect of salt in NE as shown by the p-values greater than 0.05.

Table C-3. Table showing Cox regression analysis for districts and the effect of different levels of salt application.

No.	Covariate	Parameter estimate ($\hat{\beta}$)	Standard error	Chi-square	P-value
1	NW	-1.388	0.538	6.643	0.010
2	KC	-1.078	0.572	3.558	0.059
3	CD	-2.567	0.475	29.17	<.0001
4	SL	-1.188	0.454	6.844	0.008
5	SW	-2.365	0.475	24.78	<.0001
6	SE	1.320	0.621	4.511	0.033
7	Salt (tons/lane miles)	-0.108	0.132	0.667	0.414
8	Salt*NW	0.546	0.193	8.000	0.005
9	Salt*KC	0.212	0.161	1.732	0.188
10	Salt*CD	1.028	0.171	35.93	<.0001
11	Salt*SL	0.193	0.134	2.072	0.150
12	Salt*SW	1.240	0.191	42.16	<.0001
13	Salt*SE	-0.547	0.426	1.646	0.199

Table C-4 reports data on the effect of freeze/thaw cycles on the performance of the CIP decks. The parameter estimate for this covariate is negative, which indicates that increasing the number of freeze/thaw cycles reduces the hazard of deterioration. This result is not consistent with most experience and research that indicates increasing freeze/thaw cycles results in increased deterioration over time [15]. The increased deterioration would be expected to increase the hazard of deterioration, but the results showed the opposite. Rows 2-5 show the statistically significant interaction effect of salt and freeze/thaw cycles, snow, and the interaction effect of snow and salt. The interaction of snow and salt together also has a negative parameter estimate, indicating that when these covariates were considered together, the effect was to reduce the hazard of damage.

Table C-4. Table showing the results of the Cox regression for covariates of freeze/thaw, salt, and snow days.

No.	Covariate	Parameter estimate ($\hat{\beta}$)	Standard error	Chi-square	P-value
1	Freeze/thaw (days/year)	-0.062	0.004	198.0	<.0001
2	Salt * freeze/thaw	0.010	0.001	50.12	<.0001
3	Snow (days/year)	0.070	0.006	130.9	<.0001
4	Salt*snow	-0.012	0.002	31.50	<.0001

Statistical Data

This section documents that data on which the statistical analysis is based. These data are provided to document the project data for the record, for future researchers, and for those looking for additional insight into the characteristic of the dataset on which the analysis is based. Similar sections documenting the dataset are included in the report for superstructures, substructures, and culverts.

Table C-5 includes statistical data for the covariates used in the analysis for CIP decks on different types of superstructures. This includes the covariate name, the count or number of instances that were available for analysis, and the general statistics for each covariate. The general statistics provide an overview of the typical values and variation in the data used in the analysis. This includes the median value where 50% of the population is above and 50% below the median value, and the mean (average). The mode records the most frequently occurring value. Table C-6 shows general statistics for salt application. Other tables in this appendix address the covariate values for superstructures, substructures, and culverts.

Table C-5. Table showing general statistics for continuous covariates for CIP decks.

Superstructure type	Covariate name	Count	General statistics (year)			
			Median	Mode	Mean	STD
All (regardless of the superstructure type)	Age	8,232	50	54	47	25.3
	Structure length (ft.)		176	113	234	289.5
	Maximum span length (ft.)		60	60	67.4	37.2
	Condition rating		6	7	6.2	1.2
CIP decks on steel simple girders	Age	1,564	64	56	65.4	15.4
	Maximum span length (ft.)		41	49	43.2	21.1
	Structure length (ft.)		107	95	125.6	105.6
	Condition rating		6	6	5.6	1.2
CIP decks on steel cont. girders	Age	2626	48	50	44.3	15.1
	Maximum span length (ft.)		85	70	94.2	43.7
	Structure length (ft.)		253	264	356.3	424.2
	Condition rating		7	7	6.4	1.1
CIP decks on PSC cont. girders	Age	1,685	23	24	24.3	12.7
	Maximum span length (ft.)		66	90	68.4	18.0
	Structure length (ft)		196	146	242.5	209.0
	Condition rating		7	7	7.2	0.6
CIP decks on PSC box beams	Age	649	9	8	17.1	15.1
	Maximum span length (ft.)		69	60	75	33.6
	Structure length (ft.)		151	106	218.1	227.7
	Condition rating		7	7	7	0.7
RCC slabs	Age	989	54	51	55.4	37
	Maximum span length (ft.)		46	56	44	18.4
	Structure length (ft.)		135	67	144	132
	Condition rating		6	6	6.2	1
RCC girders	Age	1,019	65	58	67	16.4
	Maximum span length (ft.)		47	43	52.3	22.2
	Structure length (ft.)		138	128	169.3	128.7
	Condition rating		6	6	5.5	1.2

Table C-6. Table showing general statistics for salt application.

Covariate	Covariate	Count	General statistics (year)			
Salt (tons/lane mile)	NW	9,810	2.9	2.0	2.7	0.8
	NE	11,385	2.2	4.4	2.9	1.2
	KC	7,931	4.3	4.9	4.2	1.3
	CD	11,568	2.9	4.4	2.6	1.1
	SL	5,951	5.0	10	5.1	2.2
	SW	16,206	2.2	2.8	2.1	0.8
	SE	14,697	1.2	2.2	1.2	0.4

Table C-7 shows additional background data used for the analysis of CIP decks on different types of superstructures. These data illustrate the number of instances for each CR for each superstructure type. The table also records the SI&A items 43A and 43B for the superstructure type and its name. The number of instances for each CR for each superstructure type provides information on the size of the dataset used in calculating the TICR and other analysis in the report.

Table C-7. Number of different superstructure types with CIP decks in CR 3 – 8.

SI&A items		SI&A description	# of bridges/culverts in each CR						SI&A items		SI&A description	# of bridges/culverts in each CR					
43A	43B		3	4	5	6	7	8	43A	43B		3	4	5	6	7	8
4	2	St. cont. stringer/multi beam girder	324	528	856	1,629	2,039	1,072	2	5	RC cont. box beam or girder - multiple	4	8	6	3	3	0
3	2	St stringer/multi-beam girder	390	629	883	1,047	700	235	3	12	ST – thru	0	1	1	2	5	1
1	4	RC tee beam	155	279	416	461	249	51	3	9	ST truss – deck	2	1	3	2	0	1
2	1	RC cont. slab	31	83	202	537	532	269	6	1	PSC continuous slab	0	0	0	2	1	2
3	10	St. truss – thru	102	149	202	222	105	18	1	6	RC box beam or girders - single or spread	0	0	1	5	5	0
6	2	PSC cont. stringer/multi beam girder	5	6	15	132	874	638	4	14	ST cont. stayed girder	0	0	0	0	3	1
5	4	PSC tee beam	2	5	4	6	66	43	2	7	RC cont. frame (except frame culverts)	3	1	3	1	2	0
1	22	RC channel beam	16	55	71	64	37	10	3	0	ST other	0	1	0	1	0	0
2	6	RC cont. box beam or girders - single or spread	20	52	97	152	111	42	0	2	Other stringer stringer/multi-beam or girder	0	0	0	0	0	2
6	4	PSC cont. tee beam	2	8	7	27	235	95	4	12	ST cont. arch – thru	1	1	0	1	2	1
1	1	RC slab	38	60	87	120	67	18	4	6	ST cont. box beam or girders - single or spread	0	1	0	0	2	2
5	6	PSC box beam or girder – single	0	1	1	20	64	65	1	5	RC box beam or girders - multiple	0	0	0	0	0	0
5	2	PSC stringer / multiple-beam or girder	4	1	4	22	85	72	2	2	RC cont. stringer/multi-beam or girder	1	0	0	0	1	1
5	5	PSC box beam or girder - multiple	0	3	3	4	16	8	4	7	ST cont. frame (except frame culverts)	0	1	1	1	2	2
4	3	St cont. girder and floor beam system	2	7	14	27	38	17	4	9	ST cont. truss – deck	1	1	1	1	0	0
1	11	RC – deck	4	6	12	13	8	0	1	3	RC girder and floor beam system	0	1	0	0	0	0
3	3	St girder and floor beam system	6	12	15	12	4	1	2	12	RC cont. arch - thru	1	0	0	0	0	0
1	7	RC frame (except frame culverts)	2	4	9	9	11	0	3	1	ST slab	0	0	0	0	1	0
2	4	RC continuous tee beam	3	12	10	10	6	2	3	13	ST suspension	0	0	0	0	0	0
2	11	RC continuous arch - deck	3	5	9	12	3	1	3	5	ST box beam or girders - multiple	0	0	0	0	1	1
5	1	Prestressed concrete slab	0	7	6	5	2	1	3	7	ST frame (except frame culverts)	0	0	0	1	0	0
7	2	TR stringer/multi-beam or girder	0	1	3	2	0	0	4	13	ST cont. suspension	0	0	0	1	0	0
4	10	ST cont. truss – thru	6	9	9	15	12	8	6	21	PSC cont. segmental box girder	0	0	0	0	1	0
6	6	PSC cont. box beam or girder – single	0	0	0	0	9	12	7	0	TR other	0	1	0	0	0	0
6	5	PSC continuous box beam or girder – multiple	0	1	1	2	12	5	8	11	Masonry arch – deck	0	0	0	0	1	0
1	2	RC stringer / multi-beam or girder	1	2	2	5	5	0									

Reliability Analysis for Superstructures

This section of the report documents results of statistical analysis for different bridge superstructure types.

Table C-8 shows different types of superstructures, their count, and their combination for analysis. Table C-9 shows the effect of covariates on the performance of superstructures when assessed individually.

Table C-8. Table showing different types of superstructures, their count, and their combination for analysis.

SI&A items		SI&A description	Count	Analysis data set	Combined count
43A	43B				
4	2	Steel continuous stringer/multi beam girder	2,645	Steel cont. girders	2,645
3	2	Steel stringer/multi beam girder	1,602	Steel simple girders	1,602
5	2	Prestressed concrete stringer/multiple-beam or girder	174	PSC cont. girders	1,436
6	2	Prestressed concrete continuous stringer/multi beam girder	1,262		
1	1	Concrete slab	247	RCC slabs	1,014
2	1	Concrete continuous slab	767		
1	4	Concrete tee beam	790	RCC girders	1,022
2	4	Concrete continuous tee beam	20		
1	6	Concrete box beam or girders - single or spread	5		
1	5	Concrete box beam or girders - multiple	2		
2	6	Concrete continuous box beam or girders - single or spread	193		
2	5	Concrete continuous box beam or girder - multiple	12		
5	4	Prestressed concrete tee beam	169	PSC box beams	1140
6	4	Prestressed concrete continuous tee beam	344		
5	5	Prestressed concrete box beam or girder - multiple	384		
5	6	Prestressed concrete box beam or girder – single	201		
6	5	Prestressed concrete continuous box beam or girder – multiple	16		
6	6	Prestressed concrete continuous box beam or girder – single	26		
Total number					**8,859**

Table C-9. Table showing the effect of covariates on the performance of superstructures by their own.

Var. No.	Variables in model	-2log $\hat{L}$	Likelihood ratio	Result
0	None	234,158.95	-	Null model
1	District	234,030.87	128.08	Significant
2	Region	234,134.09	24.86	Significant
3	Superstructure type	233,745.38	413.57	Significant
4	Waterway	234,145.74	13.22	Significant
5	Age in TICR	234,074.55	84.40	Significant
6	Structure length (ft.)	234,135.44	23.52	Significant
7	Maximum span length (ft.)	234,110.21	48.74	Significant
8	Freeze/thaw (days/year)	233,962.90	196.06	Significant
9	Snow (days/year)	234,156.10	2.85	Not sign.
10	Salt (tons/lane miles)	234,078.35	80.60	Significant
11	ADT	234,158.67	0.28	Not sign.
12	ADTT	234,158.95	0	Not sign.

Table C-10 lists the output for the Cox regression model built for superstructures. The description of this table is similar to Table C-2 for Cox regression output for CIP decks presented earlier. For superstructures, the reference covariate was steel continuous girders, so this covariate does not appear in Table C-10. Those covariates (or combinations of covariates) that are nonsignificant are shaded in the table.

Table C-10. Table showing the Cox regression output for superstructures.

No.	Parameter	DF	Parameter estimate ($\hat{\beta}$)	Standard error	Chi-square	P-value
1	RCC slabs	1	0.346	0.113	9.385	0.002
2	RCC girders	1	0.875	0.126	46.40	<.0001
3	Steel simple girders	1	0.582	0.089	42.69	<.0001
4	PSC cont. girders	1	0.220	0.109	4.051	0.044
5	PSC box beams	1	0.304	0.104	8.492	0.004
6	Age in TICR	1	0.021	0.001	286.9	<.0001
7	Age in TICR*RCC slabs	1	-0.016	0.002	69.91	<.0001
8	Age in TICR*RCC girders	1	-0.023	0.002	145.3	<.0001
9	Age in TICR*steel girders	1	-0.010	0.002	43.03	<.0001
10	Age in TICR*PSC cont. girders	1	0.0005	0.003	0.029	0.864
11	Age in TICR*PSC box beams	1	-0.017	0.004	22.94	<.0001
12	Maximum span length	1	0.003	0.0003	114.7	<.0001
13	Maximum span length*RCC slabs	1	-0.00007	0.002	0.002	0.962
14	Maximum span length*RCC girders	1	0.006	0.001	22.09	<.0001
15	Maximum span length*Steel girders	1	-0.003	0.001	9.890	0.002
16	Maximum span length*PSC cont. girders	1	0.002	0.001	3.026	0.082
17	Maximum span length*PSC box beams	1	0.010	0.001	93.38	<.0001

Table C-11 shows the Cox regression output for superstructures in different districts, the covariate of salt application and the interaction of salt application with districts to assess if the effect of salt is different in different districts. The reference district was the NE district.

Table C-11. Table showing Cox regression analysis output for superstructures.

No.	Parameter	DF	Parameter estimate ($\hat{\beta}$)	Standard error	Chi-square	P-value
1	NW	1	-1.224	0.266	21.14	<.0001
2	KC	1	-0.645	0.649	0.988	0.320
3	CD	1	-1.917	0.538	12.70	0.0004
4	SL	1	-0.337	0.152	4.900	0.023
5	SW	1	1.434	0.195	53.68	<.0001
6	SE	1	-1.378	0.394	12.23	0.0005
7	Salt (tons/lane miles)	1	0.634	0.141	20.26	<.0001
8	Salt*NW	1	-1.224	0.266	21.14	<.0001
9	Salt*KC	1	-0.060	0.184	0.106	0.745
10	Salt*CD	1	0.790	0.192	16.82	<.0001
11	Salt*SL	1	-0.337	0.152	4.900	0.027
12	Salt*SW	1	1.434	0.196	53.68	<.0001
13	Salt*SE	1	-1.378	0.394	12.23	0.0005

Table C-12 shows the general statistics for superstructures based on the construction materials and type. These data indicate the values for the covariates used in the analysis. The values listed in the table indicate median, mode, average, and standard deviation for different covariates such as age, maximum span length, etc., subdivided by materials and construction type such as continuous steel girders, steel girders, etc.

Table C-12. Table showing general statistics for superstructures based on construction material and construction type.

Covariate name	Superstructure type	Count	General statistics			
			Median	Mode	Average	STD
Age (years)	Steel continuous girders	2,517	49	54	46	14
	Steel girders	1,562	64	58	67	15
	PSC cont. girders	1,177	25	24	26	12
	PSC box beams	658	9	8	17	15
	RCC slabs	984	53	51	55	37
	RCC beams	1,013	64	61	67	17
Maximum span length (ft.)	Steel continuous girders	2,517	83	70	93	43
	Steel girders	1,562	40	49	43	20
	PSC cont. girders	1,177	67	90	69	18
	PSC box beams	658	75	60	74	31
	RCC slabs	984	45	56	44	18
	RCC beams	1,013	47	43	52	22
Structure length (ft.)	Steel continuous girders	2,517	250	164	354	427
	Steel girders	1,562	107	107	125	106
	PSC cont. girders	1,177	202	146	251	221
	PSC box beams	658	137	90	192	206
	RCC slabs	984	135	67	144	131
	RCC beams	1,013	138	128	169	129
Number of span	Steel continuous girders	2,517	3	3	4	3
	Steel girders	1,562	3	3	3	3
	PSC cont. girders	1,177	3	3	4	3
	PSC box beams	658	3	3	3	2
	RCC slabs	984	3	3	4	2
	RCC beams	1,013	3	3	3	2
Average condition rating	Steel continuous girders	2,517	7	7	7	1
	Steel girders	1,562	7	6	6.6	1
	PSC cont. girders	1,177	7	7	7	1
	PSC box beams	658	7	7	7	1
	RCC slabs	984	6	6	6	1
	RCC beams	1,013	6	6	5.5	1
ADT	Steel continuous girders	2,517	3,500	11,000	8,386	14,747
	Steel girders	1,562	490	200	2,796	12,047
	PSC cont. girders	1,177	4,538	11,000	9,264	15,845
	PSC box beams	658	1,506	210	4,875	11,415
	RCC slabs	984	4,877	5,500	12,444	19,803
	RCC beams	1,013	2,140	5,500	8,031	15,671
ADTT	Steel continuous girders	2,517	401	1,100	1,145	1,978
	Steel girders	1,562	52	19	340	1,444
	PSC cont. girders	1,177	559	1,100	1,178	1,983
	PSC box beams	658	167	20	601	1,405
	RCC slabs	984	561	550	1,552	2,473
	RCC beams	1,013	239	550	963	1,943

Table C-13. Table showing general statistics for salt application used for superstructure analysis.

Covariate name	Superstructure type	Count	General statistics			
			Median	Mode	Average	STD
Salt (tons/lane mile)	NE	9,810	2.2	4.4	2.9	1.3
	NW	11,385	2.9	2	2.7	0.8
	KC	7,931	4.3	4.9	4.2	1.3
	CD	11,568	2.8	3.5	2.6	1.1
	SL	5,951	5	10.1	5.1	2.2
	SE	16,206	1.2	0.7	1.2	0.4
	SW	14,697	2.2	2.8	2.1	0.8

Reliability Analysis for Substructures

The final Cox regression model for substructures after investigating the influential observations and outliers are shown in Table C-14.

Table C-14. Table showing the Cox regression output for substructures.

No.	Parameter	DF	Parameter estimate ($\hat{\beta}$)	Standard error	Chi-square	P-value
1	Age in TICR	1	0.006	0.001	99.40	<.0001
2	NW	1	-2.848	0.538	28.06	<.0001
3	KC	1	-0.708	0.577	1.508	0.220
4	CD	1	-2.246	0.445	25.44	<.0001
5	SL	1	-0.0637	0.356	0.032	0.858
6	SW	1	-4.033	0.392	105.5	<.0001
7	SE	1	1.387	0.510	7.395	0.006
8	Salt (tons/lane miles)	1	0.901	0.096	90.83	<.0001
9	Salt*NW	1	1.092	0.193	32.12	<.0001
10	Salt*KC	1	-0.115	0.152	0.575	0.448
11	Salt*CD	1	0.988	0.162	37.11	<.0001
12	Salt*SL	1	-0.312	0.104	9.019	0.003
13	Salt*SW	1	2.208	0.159	193.2	<.0001
14	Salt*SE	1	-0.001	0.355	0.000	0.998
15	Structure length (ft.)	1	0.0001	0.00001	33.83	<.0001
16	Waterway	1	0.105	0.019	28.00	<.0001

The statistically significant covariates are age in TICR, salt, district, structure length, whether a bridge is located on a waterway or not, and interaction of district with salt.

The effect of the categorical covariate district is a relative effect. As shown in Table C-14, six of the seven districts are listed and district Northeast (NE) is not listed, because it is selected as a reference district and other districts are compared to NE. The parameter estimates for the six districts show the extent of hazard either larger than NE, as is the case for Southeast (SE), or smaller than NE, as is the case for all other five districts.

In row 16 of Table C-14 the covariate waterway is a categorical covariate comparing the reliability of substructure located on a waterway to those that are not located on a waterway. The reference level is substructures not located on a waterway and the parameter estimate for substructures located on a waterway is 0.105 relative to substructures not located on a waterway. The hazard ratio for these two categories of substructures is $e^{0.105}$=1.11, or substructures located on a waterway has 11% more hazard of deteriorating to lower CRs than those not located on a waterway. Inverting the hazard ratio shows that substructures not located on a waterway has 90% of the hazard of substructures located on a waterway. The hazard ratio for all covariates as well as the confidence interval for the hazard ratios are listed in the main body of the report. Table 24 shows the effect of covariates on substructures.

The general statistics for substructure are listed in Table C-15. Table C-16 shows the general statistical data related to salt application in the different districts.

Table C-15. Table showing general statistics for substructures.

Covariate name	Count	General statistics (year)			
		Median	Mode	Average	STD
Age	8,728	53	54	50.2	24.6
Structure length (ft.)	8,728	170	113	251.7	400.8
Number of spans	8,728	3	3	3.4	2.6
Average condition rating	8,728	7	7	6.6	1.2

Table C-16. Table showing the general statistical data related to salt application in the different districts.

Covariate name		Count	General statistics (year)			
			Median	Mode	Average	STD
Salt (tons/lane miles)	NE	9,810	2.2	4.4	2.9	1.2
	NW	11,385	2.9	2.0	2.7	0.8
	KC	7,931	4.3	4.9	4.2	1.3
	CD	11,568	2.8	3.5	2.6	1.1
	SL	5,951	4.9	10.1	5.1	2.2
	SE	16,206	1.2	2.2	1.2	0.4
	SW	14,697	2.2	2.8	2.2	0.8
Number of bridges over a waterway and not over a waterway						
Number of bridges over a waterway		6,227	Number of bridges not over a waterway			2,501

Reliability Analysis for Culverts

The effect of the covariates on the reliability, or survival, of the culverts are investigated using the Cox regression and presented in following paragraphs. Before beginning the statistical analysis of the effect of covariates on deterioration of the culverts, general information about the covariates is provided first in Table C-17. The distribution of the concrete continuous culverts for districts is shown in the lower part of Table C-17 as well. The covariates considered for data analysis of concrete continuous culverts are structure

length (ft.), maximum span length (ft.), amount of salt used for deicing purposes (tons/lane miles), freeze/thaw cycles (days/year), snow (days/year), ADT, ADTT, and district.

Table C-17. Table showing general statistics for culverts.

Covariate name		Count	General statistics (year)			
			Median	Mode	Average	STD
Age		3,262	62	59	61.4	22.1
Structure length (ft.)			27	25	30.6	11.0
Average condition rating			6	6	6.6	0.9
Snow (days/year)			42	41	41.4	9.4
ADT			853	754	4,662	12,901
ADTT			91	77	464	1,773
Salt (tons/lane miles)	NE	9,810	2.2	1.9	2.9	1.2
	NW	11,385	2.9	4.4	2.7	0.8
	KC	7,931	4.3	4.9	4.2	1.3
	CD	11,568	2.8	4.4	2.6	1.1
	SL	5,951	5.0	10.1	5.1	2.2
	SE	16,206	1.2	2.2	1.2	0.4
	SW	14,697	2.2	3.3	2.1	0.8

Number of culverts for districts			
District name	**Counts of culverts**	**District name**	**Counts of culverts**
Northwest	370	St. Louis	226
Northeast	419	Southwest	688
Kansas City	260	Southeast	807
Central	492		

Table C-18 shows the result of the Cox regression analysis for concrete continuous culverts for each of the covariates individually, and the result is compared with the null model (no covariate in the model). This initial analysis shows whether a covariate is statistically significant by its own, and a non-significant covariate may become significant in the presence of other covariates when all covariates are included in the model. The model building procedure described in the model development section is followed to build the Cox regression model for concrete continuous culverts.

Table C-18. Table showing the result for Cox regression analysis of individual covariates for culverts.

Var. No.	Variables in model	-2log $\hat{L}$	Likelihood ratio	Result
0	None	101,231.73	Null model	
1	Age in TICR	100,989.30	13.81	Significant
2	District	100,919.60	83.51	Significant
3	Structure length (ft.)	100,972.83	30.28	Significant
4	Maximum span length (ft.)	100,998.55	4.57	Significant
5	Freeze/thaw cycle (days/year)	101,002.41	0.71	Not sig.
6	Snow (days/year)	100,987.72	15.40	Significant
7	Salt (tons/lane miles)	100,987.16	15.95	Significant
8	ADT	101,000.34	2.77	Not sig.
9	ADTT	101,001.56	1.55	Not sig.

The final output for Cox regression model for concrete continuous culverts is shown in Table C-19. Description of Table C-19 is similar to the one provided for CIP decks in Table C-2. The parameter estimates from Table C-19 were used to calculate the hazard ratios for all covariates listed in this table and the hazard ratios are listed in Tables 26 and 27.

Table C-19. Table showing the Cox regression output for culverts.

No.	Parameter	DF	Parameter estimate ($\hat{\beta}$)	Standard error	Chi-square	Pr > chi-square
1	Age in TICR	1	0.003	0.001	17.61	<.0001
2	NW	1	1.641	1.334	1.514	0.218
3	KC	1	1.482	1.648	0.808	0.369
4	CD	1	2.698	0.837	10.39	0.001
5	SL	1	2.004	0.844	5.631	0.017
6	SW	1	5.815	0.690	70.96	<.0001
7	SE	1	5.873	0.926	40.24	<.0001
8	Salt (tons/lane miles)	1	1.533	0.198	59.73	<.0001
9	Salt*NW	1	-0.501	0.484	1.070	0.301
10	Salt*KC	1	-0.721	0.404	3.184	0.074
11	Salt*CD	1	-0.783	0.310	6.403	0.011
12	Salt*SL	1	-0.9275	0.212	19.20	<.0001
13	Salt*SW	1	-2.051	0.286	51.24	<.0001
14	Salt*SE	1	-2.716	0.661	16.89	<.0001
15	Structure length (ft.)	1	0.008	0.001	37.85	<.0001
16	Snow (days/year)	1	0.022	0.005	20.96	<.0001
17	Snow*salt	1	-0.004	0.002	4.450	0.035

APPENDIX D. RELIABILITY AND SERVICE LIFE GRAPHS FOR CIP DECKS BY MODOT DISTRICT

This appendix includes the reliability and service life graphs for CIP decks in each of the MoDOT districts.

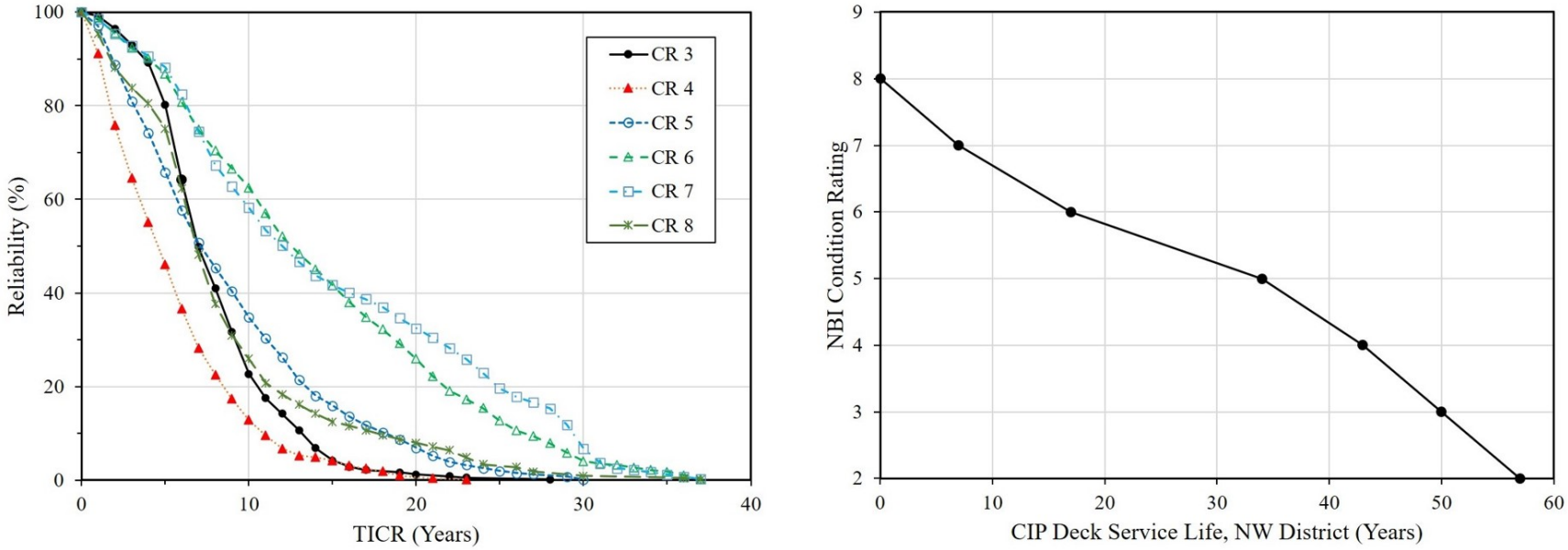

Figure D-1. Plot showing the reliability and median service life graphs for CIP decks in CR 8-3 located in Northwest district.

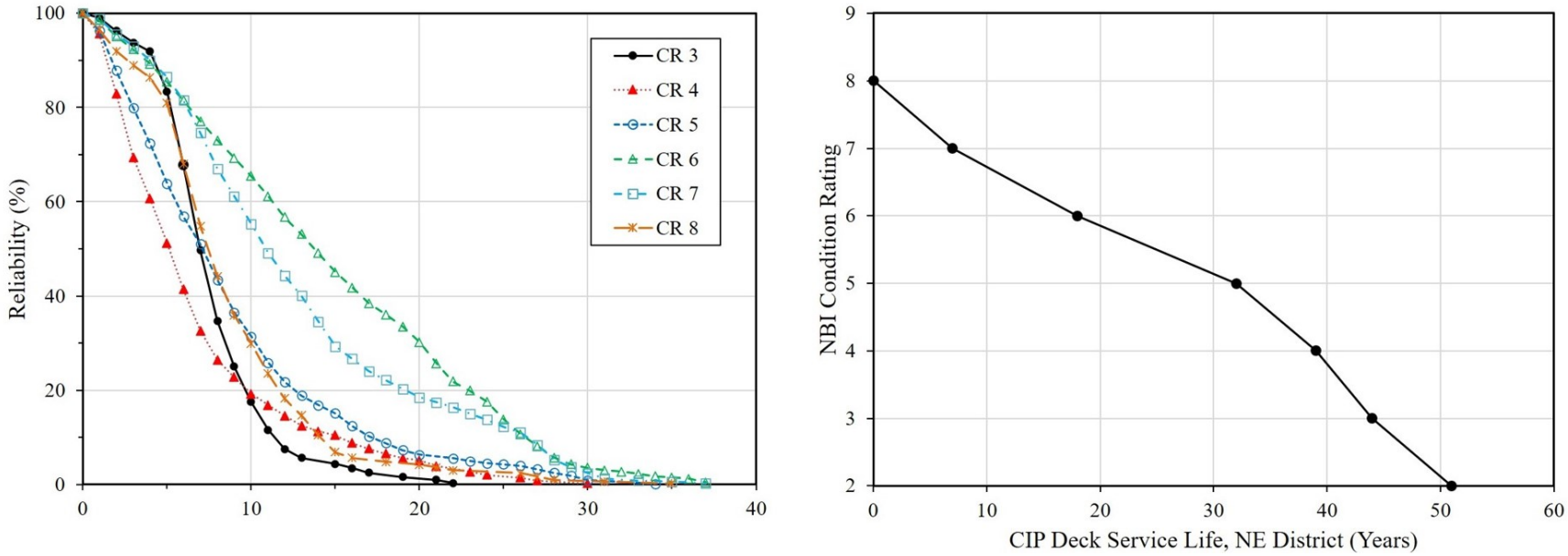

Figure D-2. Plot showing the reliability and median service life graphs for CIP decks in CR 8-3 located in Northeast district.

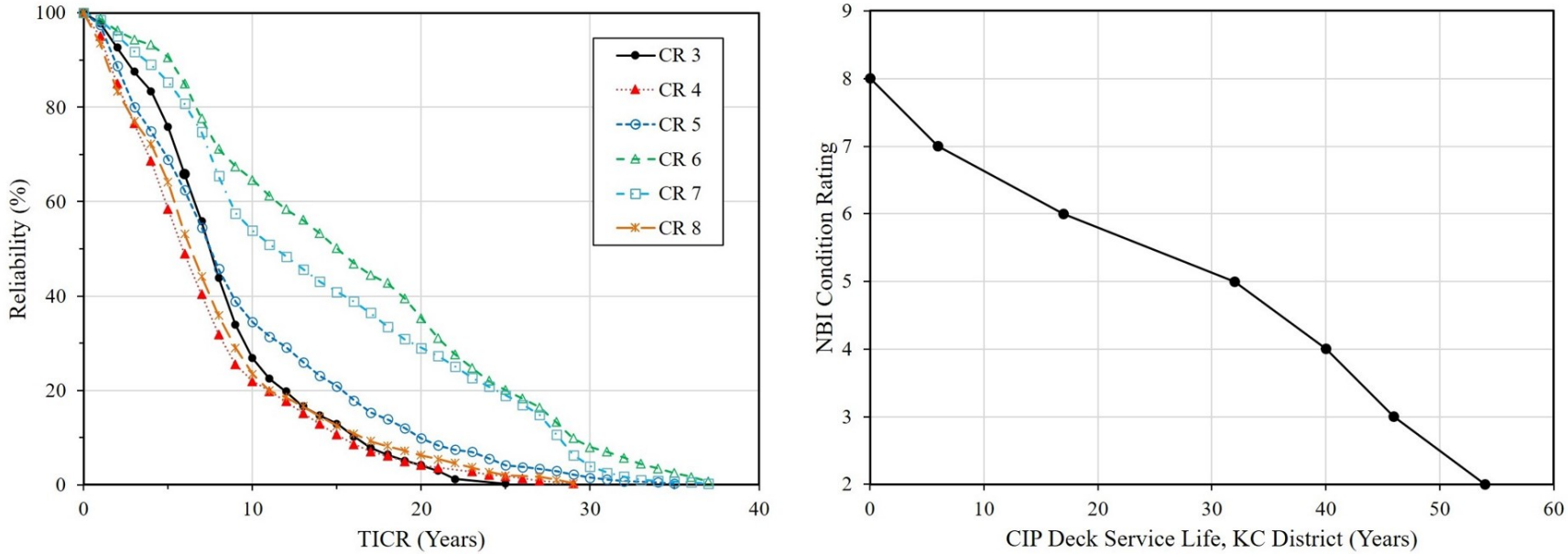

Figure D-3. Plot showing the reliability and median service life graphs for CIP decks in CR 8-3 located in Kansas City district.

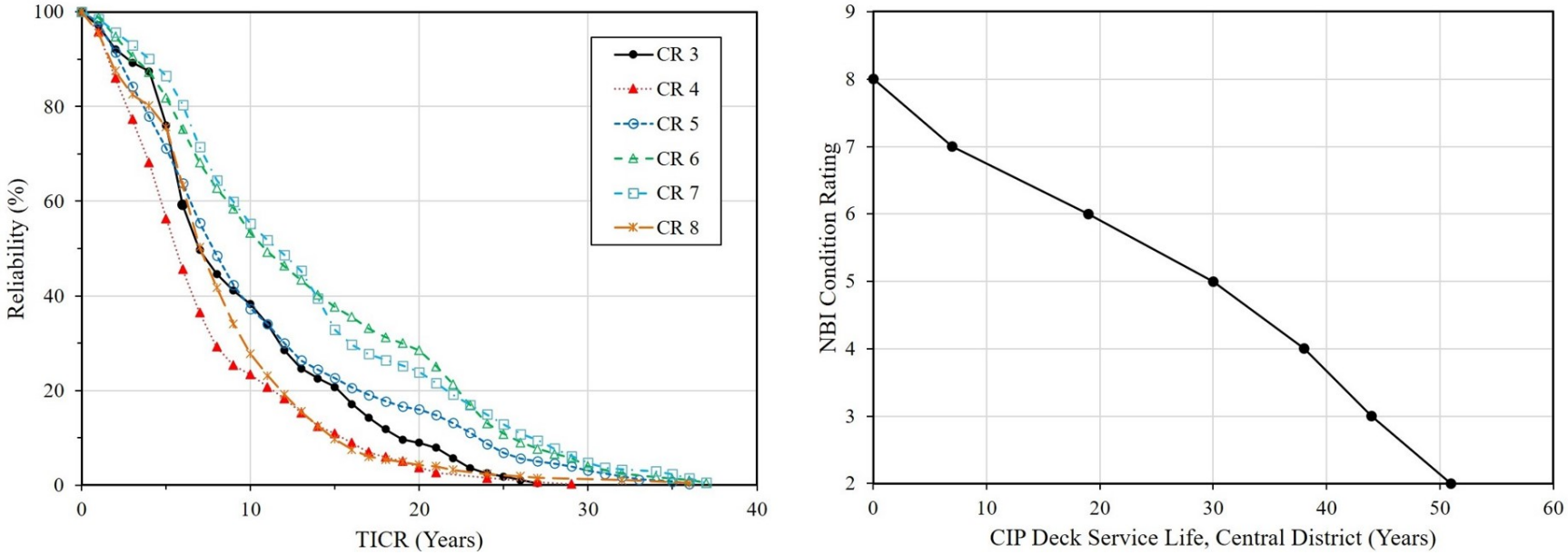

Figure D-4. Plot showing the reliability and median service life graphs for CIP decks in CR 8-3 located in Central district.

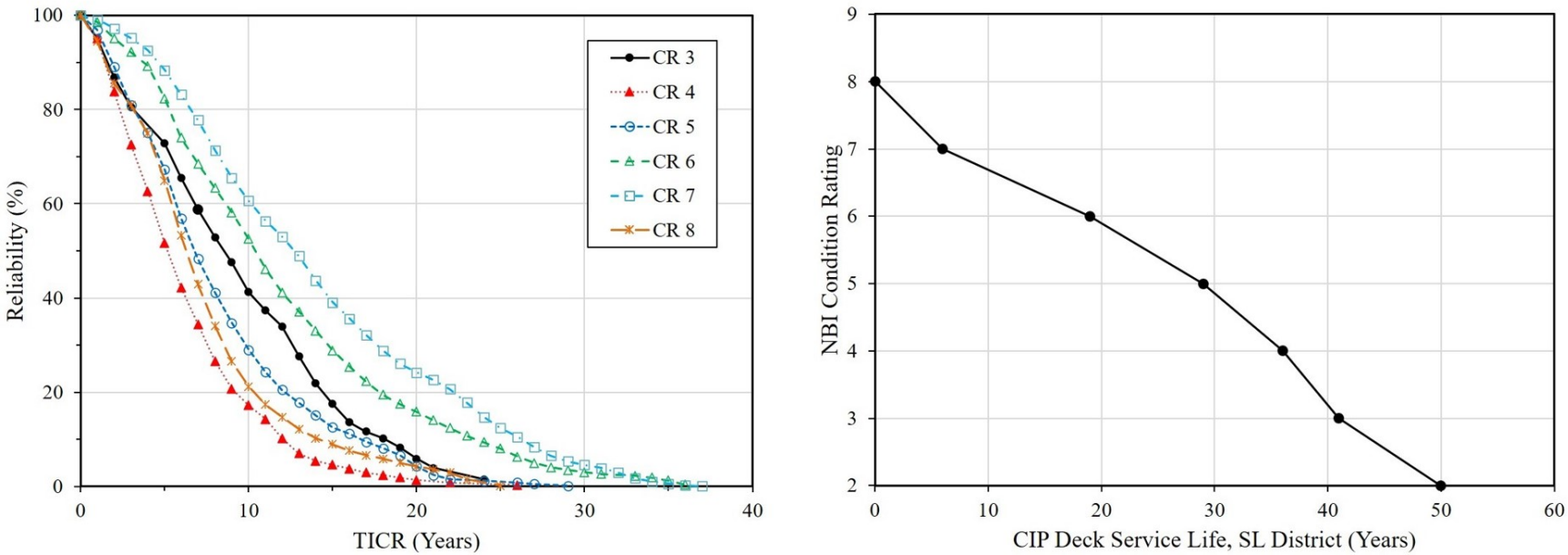

Figure D-5. Plot showing the reliability and median service life graphs for CIP decks in CR 8-3 located in St. Louis district.

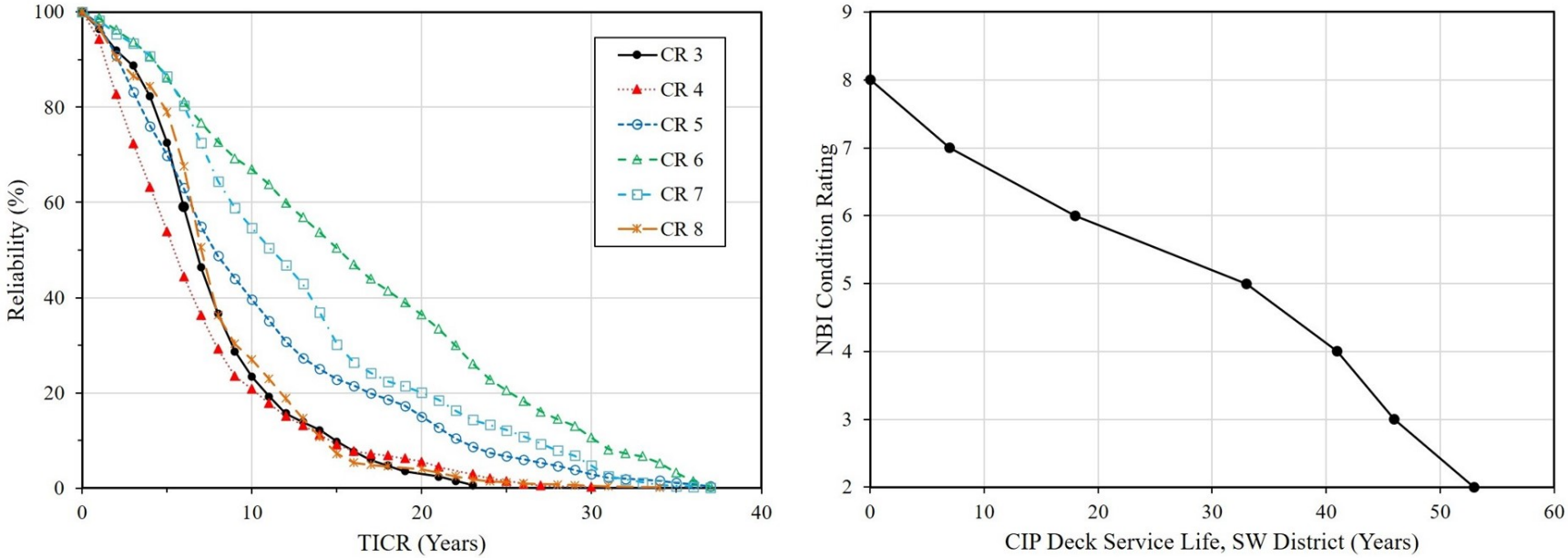

Figure D-6. Plot showing the reliability and median service life graphs for CIP decks in CR 8-3 located in Southwest district.

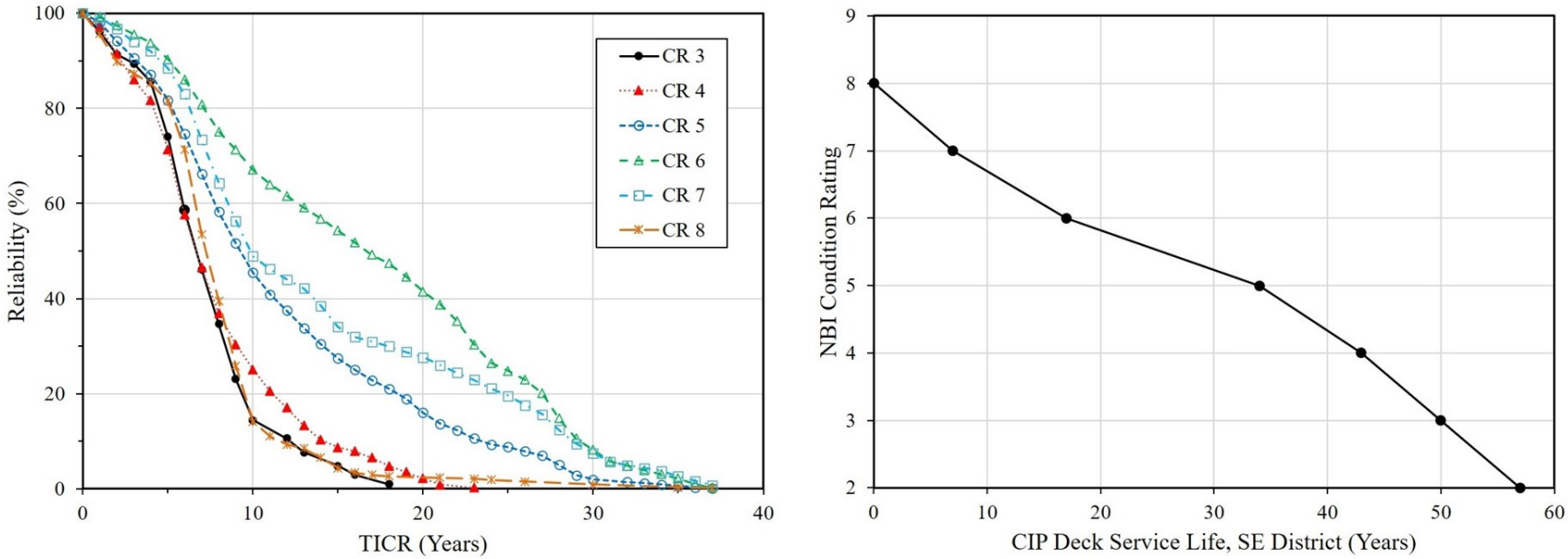

Figure D-7. Plot showing the reliability and median service life graphs for CIP decks in CR 8-3 located in Southeast district.

APPENDIX E. RELIABILITY AND SERVICE LIFE GRAPHS FOR CIP DECKS BY SUPERSTRUCTURE TYPES

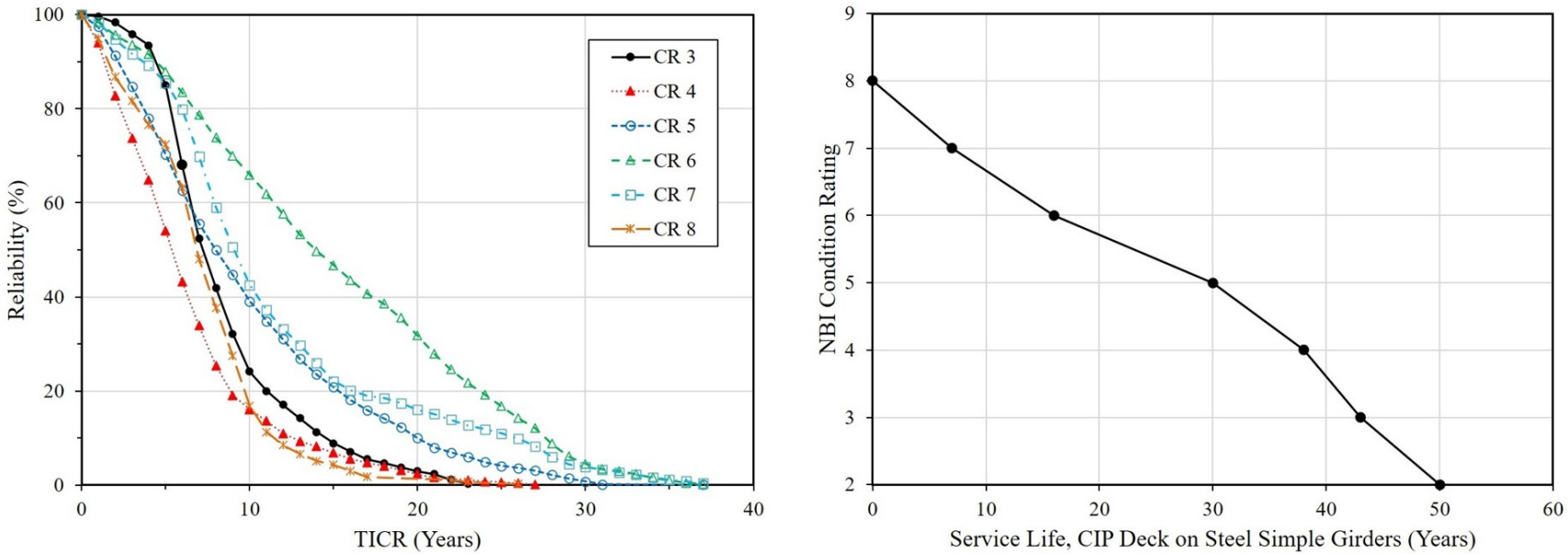

Figure E-1. Plots showing the reliability graph for CIP decks on steel simple girders (left) and service life (right).

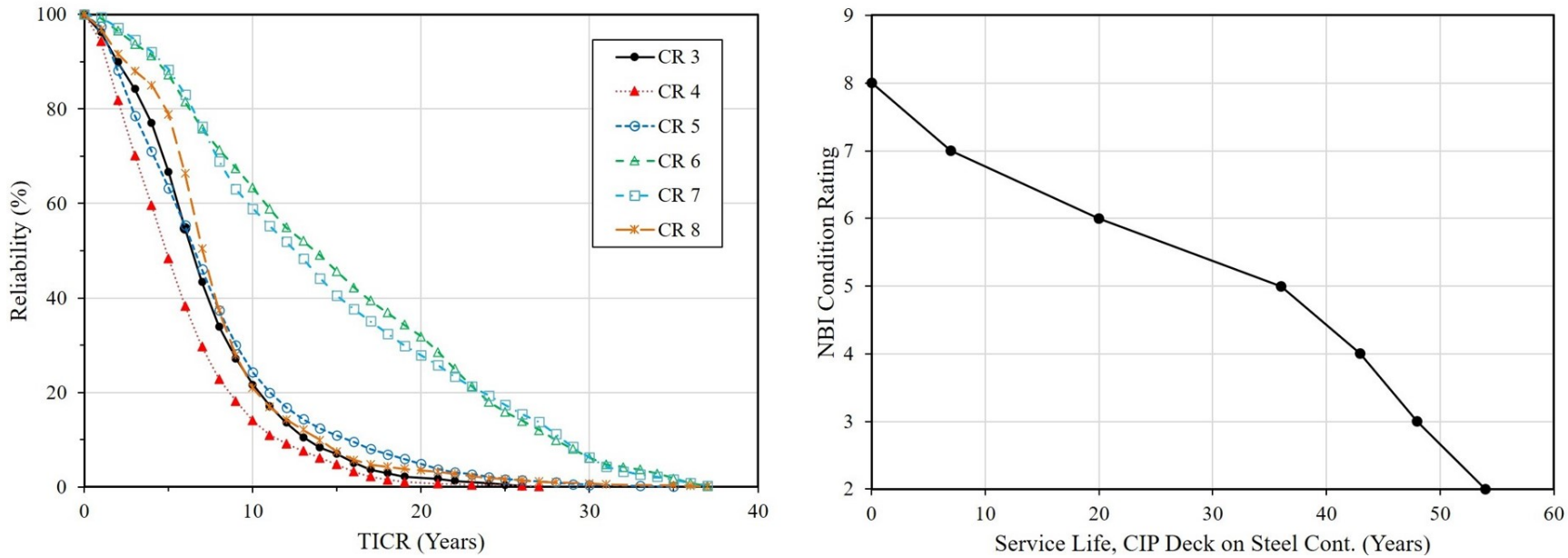

Figure E-2. Plots showing the reliability graph for CIP decks on steel continuous girders (left) and service life (right).

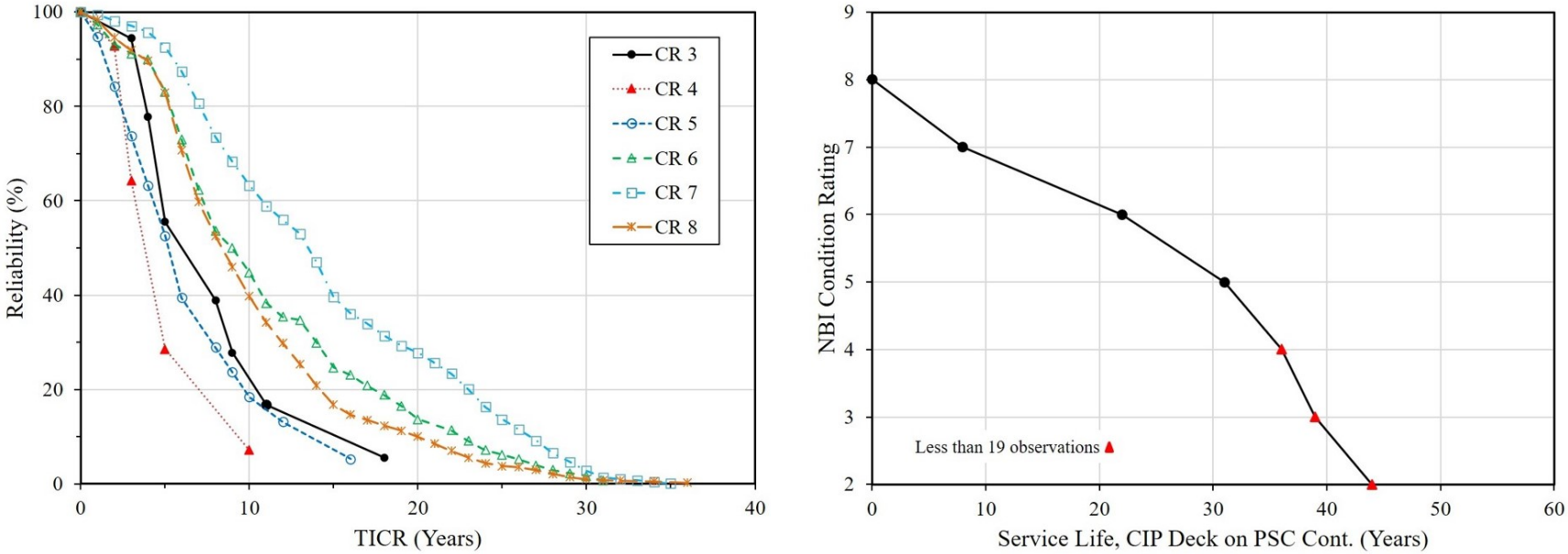

Figure E-3. Plots showing CIP decks reliability graph on PSC continuous girders (left) and service life (right).

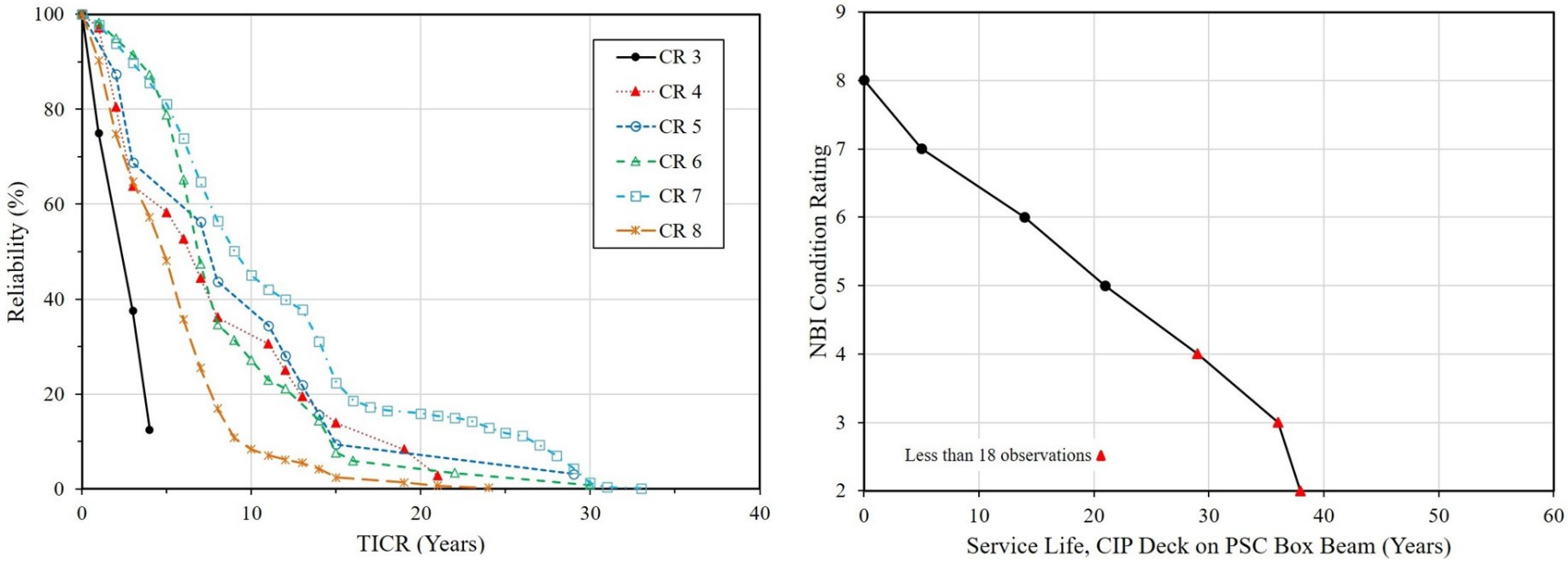

Figure E-4. Plots showing the reliability graph for CIP decks on PSC box beams (left) and service life (right).

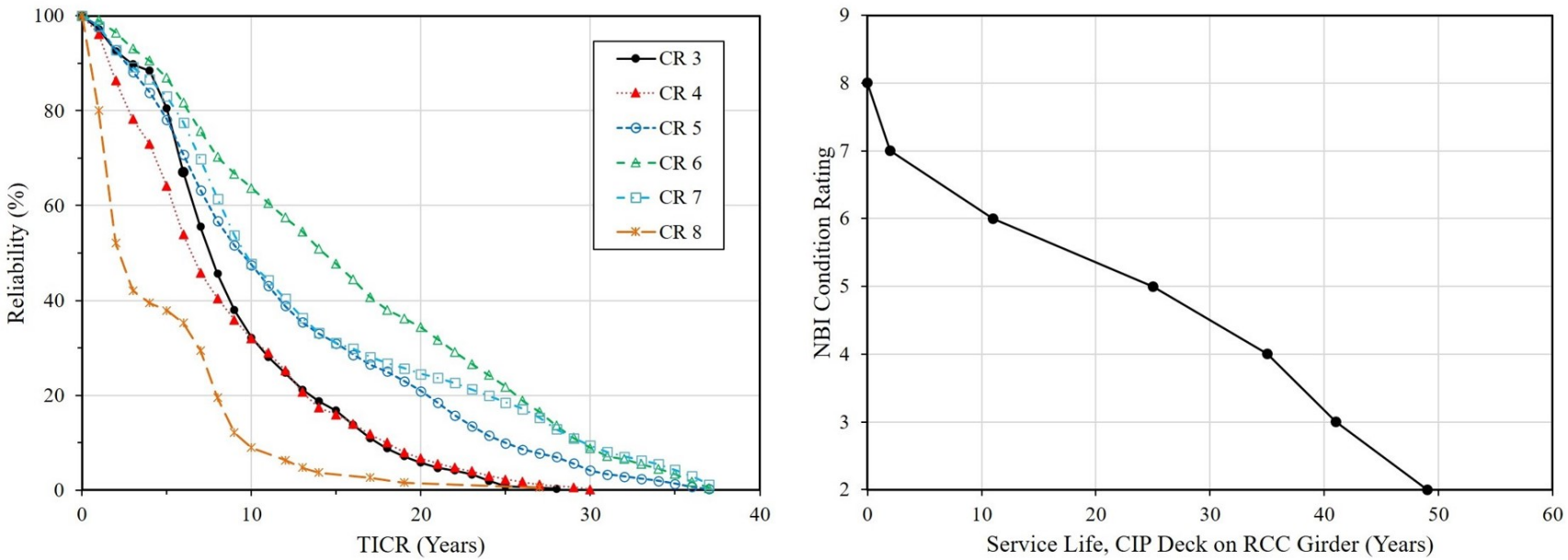

Figure E-5. Plots showing the reliability graph for CIP decks on RCC girders (left) and service life (right).

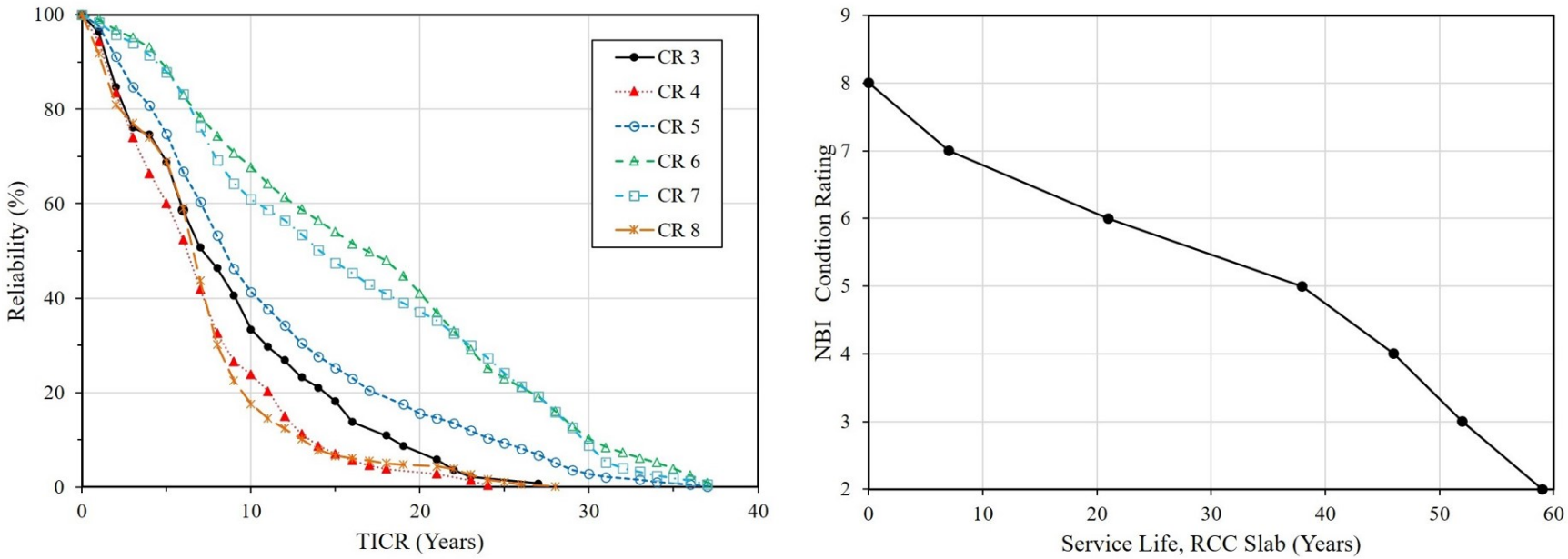

Figure E-6. Plot showing the reliability graph for RCC slabs (left) and service life (right).

APPENDIX F. RELIABILITY AND SERVICE LIFE GRAPHS FOR SUPERSTRUCTURE TYPES

This section contains the reliability and service life graphs for superstructures.

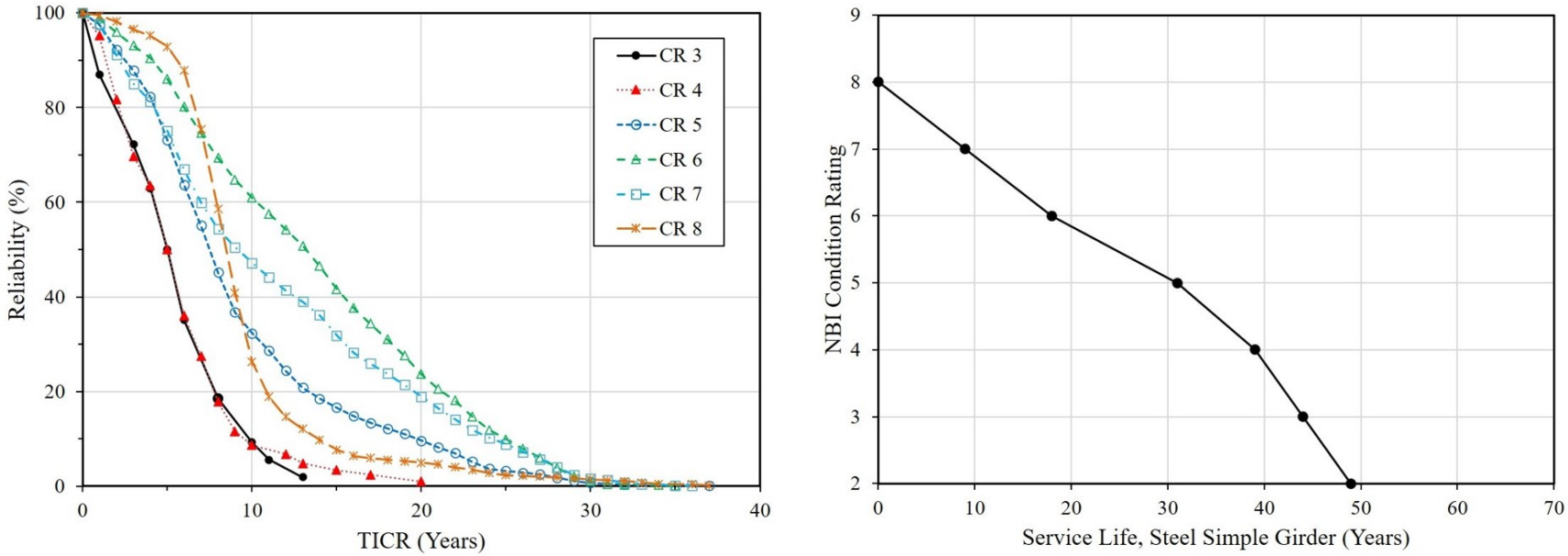

Figure F-1. Plot showing the reliability graph for steel simple girders (left) and service life (right).

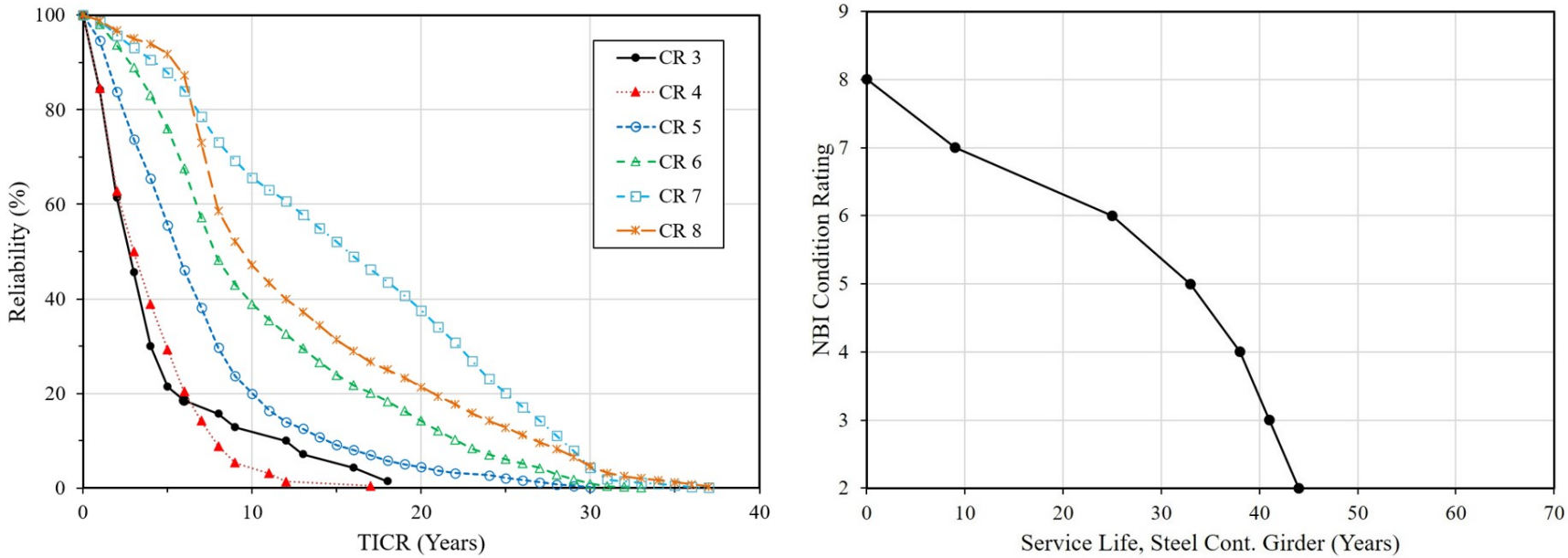

Figure F-2. Plot showing the reliability graph for steel continuous girders (left) and service life plot (right).

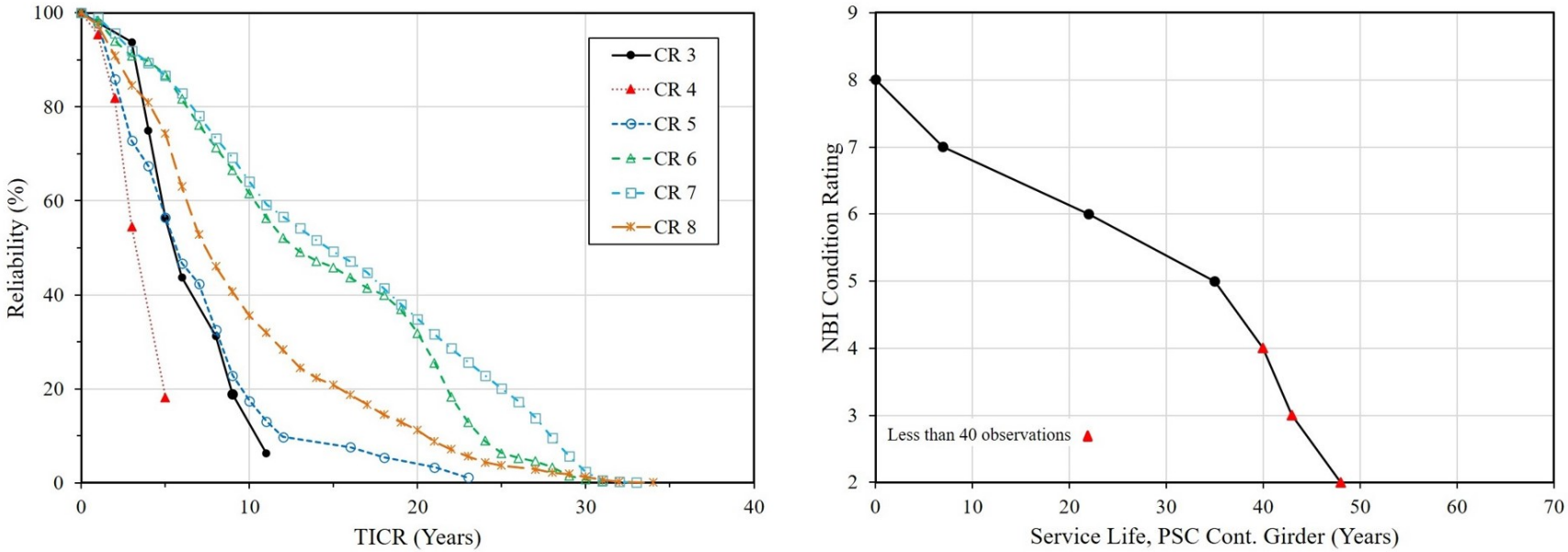

Figure F-3. Plot showing the reliability graph for PSC continuous girders (left) and service life plot (right).

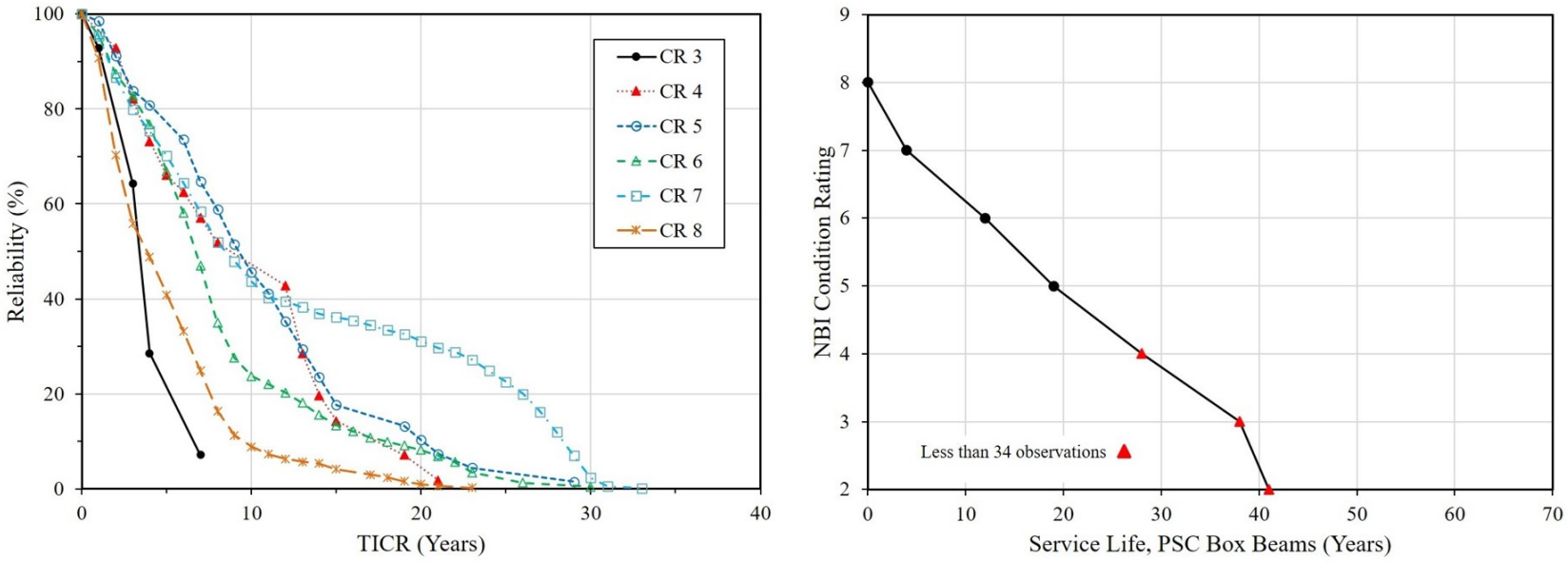

Figure F-4. Plot showing the reliability graph for PSC box beams (left) and service life plot (right).

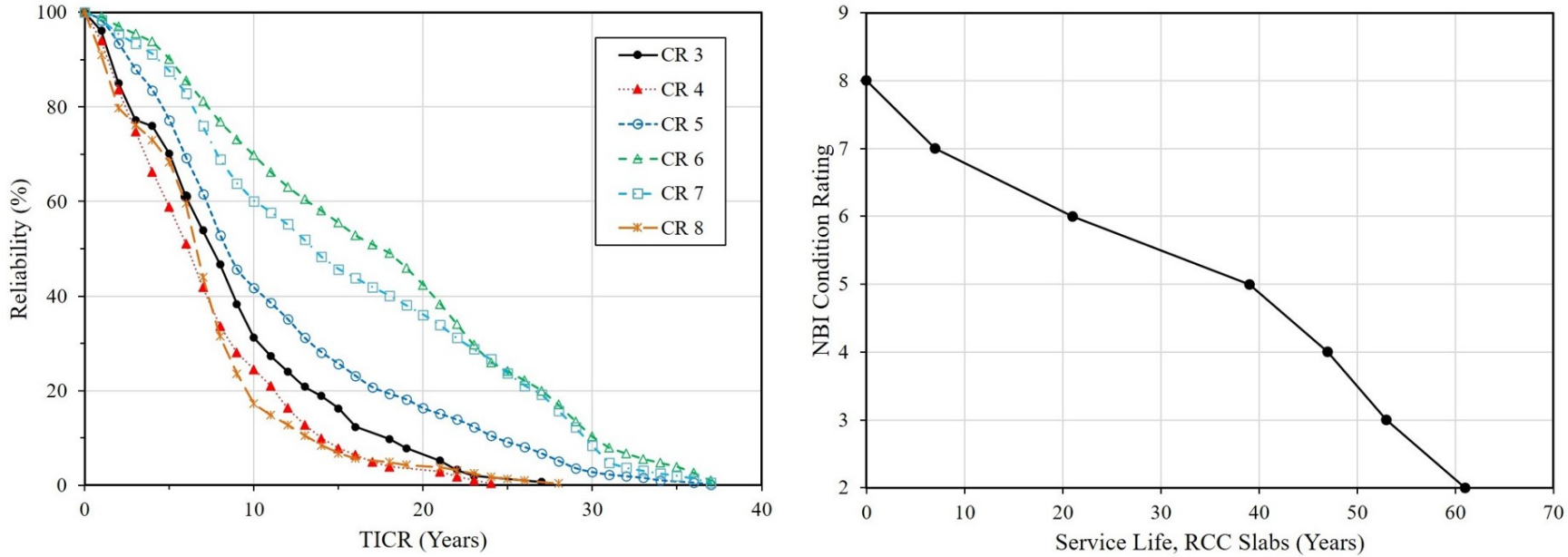

Figure F-5. Plot showing the reliability graph for RCC slabs (left) and service life plot (right).

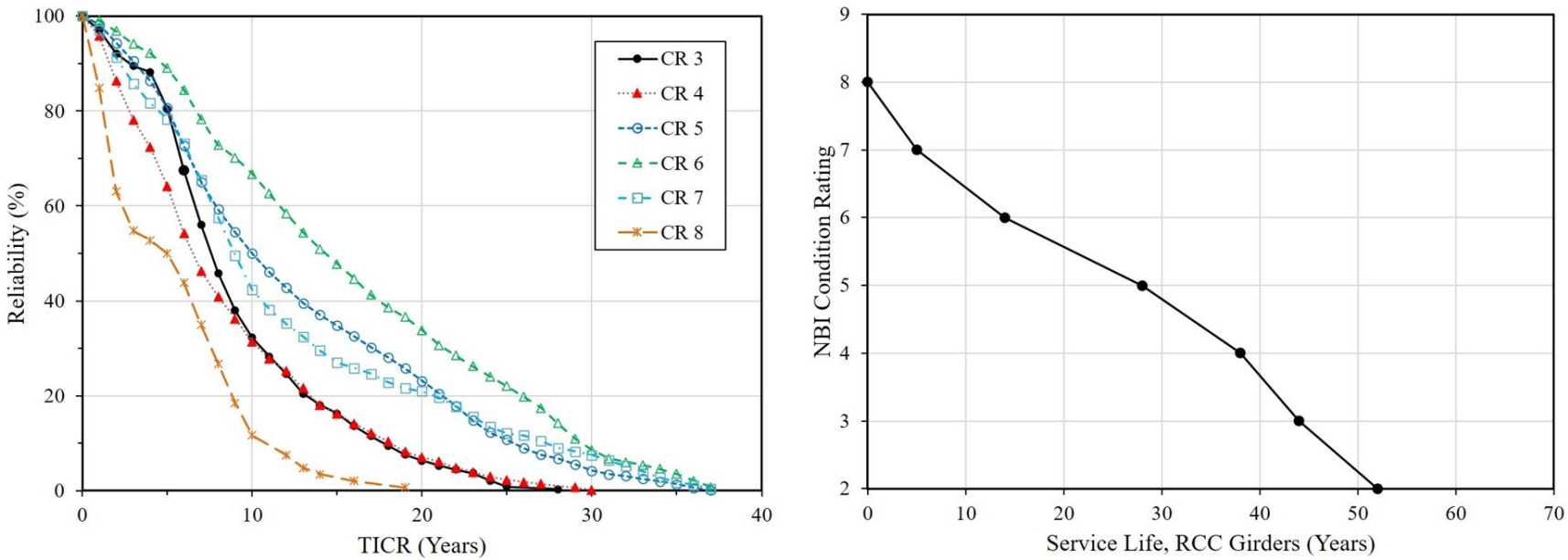

Figure F-6. Plot showing the reliability graph for RCC girders (left) and service life plot (right).

APPENDIX G. MODEL VERIFICATION

The following appendix includes the verification process for the Cox regression model used in the research. This includes verifying the functional form of the covariates, checking the proportional hazard assumption, assessing the influence of outliers, verifying the overall fit of the models, and checking the predictive accuracy of the model. The results of the verification processes are graphical in nature, and results are presented as figures illustrating the fit of the curves. The verification for the CIP deck Cox model is presented first with some text describing the results. For other bridge components and culverts, only the graphical results are presented.

The results in this appendix are provided for two reasons. First, to demonstrate that the Cox regression results presented in the research have been rigorously validated using statistical methods. Second, the results are presented for use by future researchers exploring the use of Cox regression methodologies to analyze bridge deterioration.

Checking Model Assumptions for CIP Decks

Functional Form of the Covariates

To determine the correct functional form of continuous covariates, the Martingale residual was requested from the null model for CIP decks – a model without any covariates. The residual is plotted against the covariate and a smoothed curve is fitted on the plot. The shape of the smoothed curve shows the shape of the relationship between the dependent variable and the covariate. Initially, it is assumed that the hazard is related to the exponentiated linear function of the covariates and if the smoothed curve is linear without any defined shape, then the assumption is valid. Otherwise, the shape of the smoothed curve indicates the true relationship between the dependent variable and the covariate. For reading further about this, please refer to the Appendix A section titled "MODEL ASSUMPTIONS" and the references provided therein. As shown in Figure G-1, the martingale residual is plotted against the covariate TICR, a covariate used to investigate the effect of age of the bridge components on bridge deterioration. There are four plots with different smoothing coefficients. The smoothing coefficient for top left-hand plot is 0.2, and as shown the smoothed curve is oscillating around zero and overfitting the smoothed curve [12]. But as the smoothing coefficient increases the overfitting problem is resolved and as shown in the lower right-hand plot, the smoothed plot is linear and flat for the smoothing coefficient of 0.8. This indicates that the exponentiated linear relationship between covariate for time in CR and the dependent variable TICR is valid.

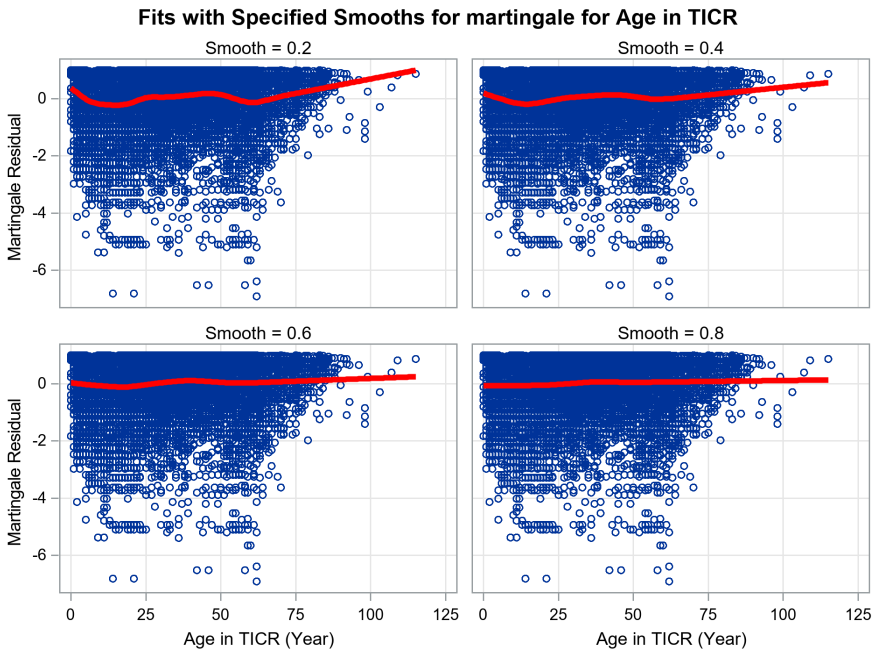

Figure G-1. Plot showing martingale residuals with smooths for age in TICR for CIP decks.

The martingale residual plot for the maximum span length, which investigates the effect on CIP deck deterioration, is shown in Figure G-2. The plot for the smoothing coefficient of 0.8 shows a flat line passing through zero, which indicates the linear relationship holds for this covariate as well.

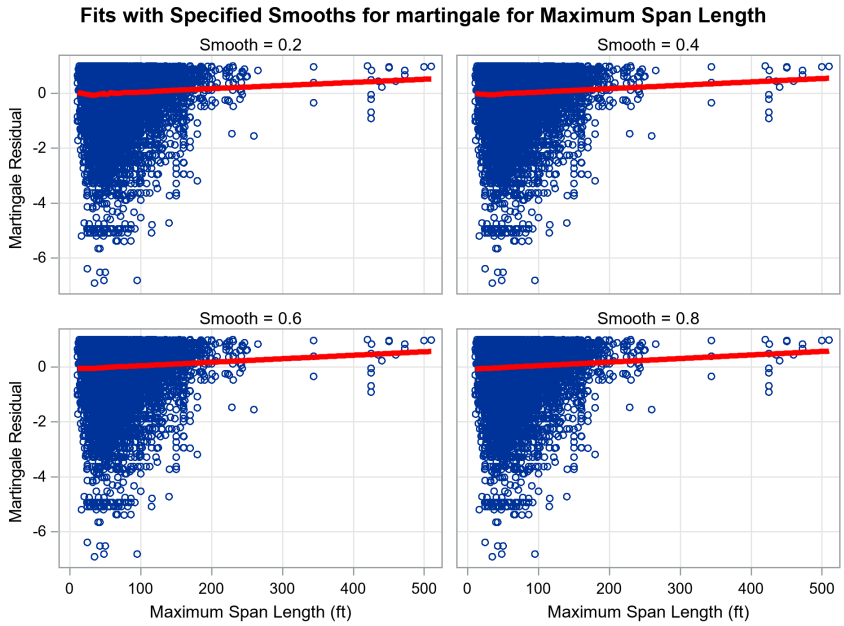

Figure G-2. Plot showing martingale residuals with smooths for CIP decks maximum span length.

Similarly, Figure G-3shows the plot for martingale residual for the covariate of salt (tons/lane mile) and its overlayed flat smoothed curve. The curve for the smoothing coefficient of 0.8 shows a little slope due to two data points for salt in St. Louis district. These data points were investigated for influential effects on parameter estimates and outliers and none of the points were identified as influential or outliers.

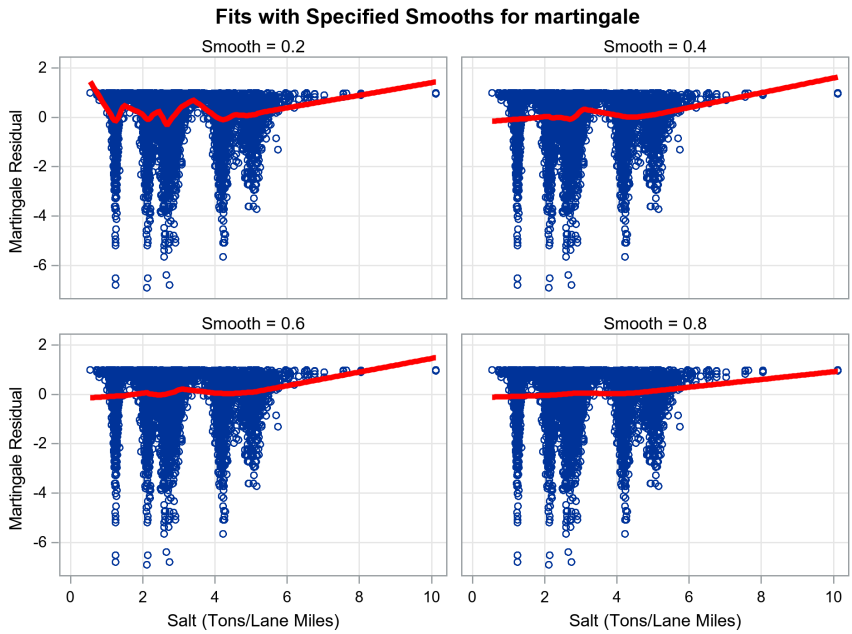

Figure G-3. Plot showing martingale residuals with smooths for salt per mile for CIP decks.

The martingale residual for the covariate of snow days is plotted in Figure G-4. As shown, for the smooth coefficient of 0.8 the curve is flat with a little bit of slope through the end. These data points were investigated for influential effects on parameter estimates and outliers and no data points were identified as such.

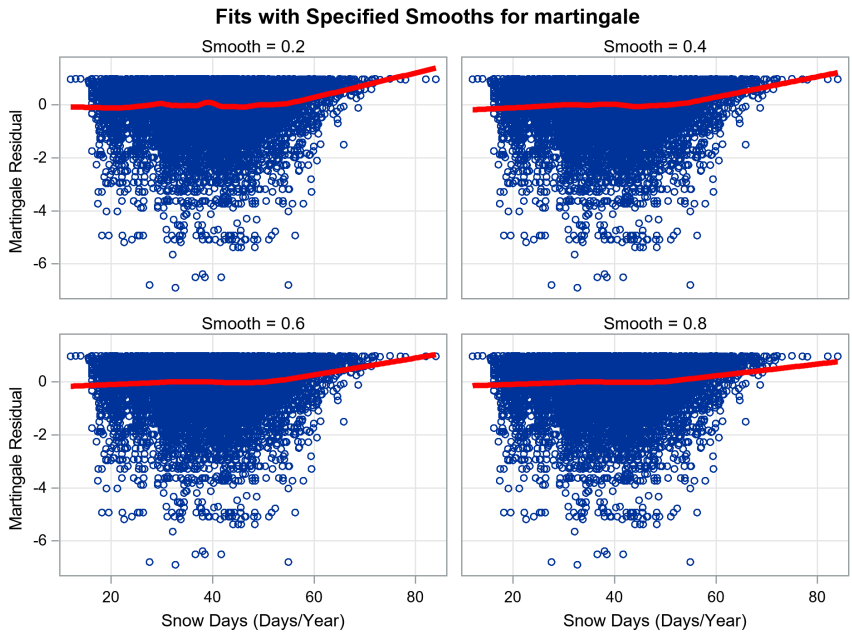

Figure G-4. Plot showing martingale residuals with smooths for snow days for CIP decks.

Proportional Hazard Assumption

The proportional hazard (PH) assumption is the second assumption in building the Cox regression model. As described in "MODEL ASSUMPTIONS" section of Appendix A, initially, it is assumed that the hazard is time independent, and it does not change with respect to the dependent variable TICR for CIP decks. To verify this assumption, the Schoenfeld residuals for individual covariate are requested and plotted against the covariate itself. A flat, smooth curve as shown in Figure G-5, for all smoothing coefficients, indicates that the PH assumption holds for the covariate age in TICR.

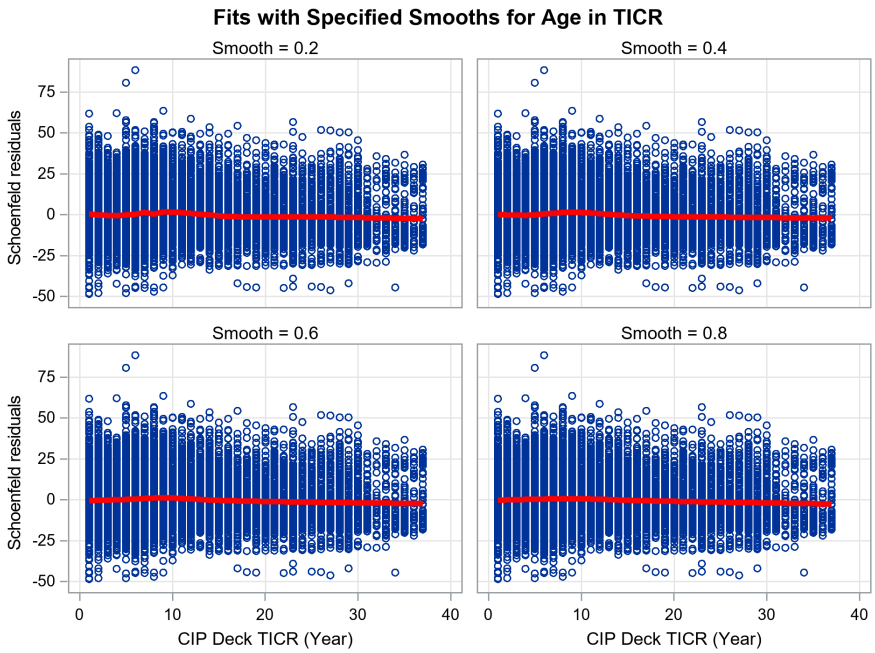

Figure G-5. Plot showing Schoenfeld residuals with smooths for age in TICR for CIP deck.

The Schoenfeld residual plotted against the maximum span length is shown in Figure G-6. The plots for all four smoothing coefficients show that the PH assumption holds for covariate maximum span length for CIP decks.

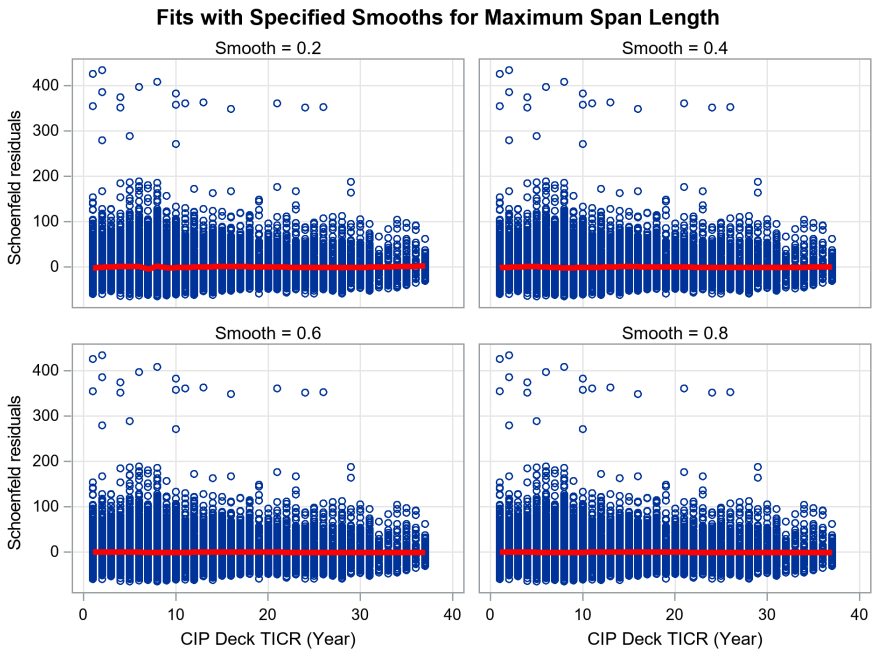

Figure G-6. Plot showing Schoenfeld residuals with smooths for maximum span length for CIP deck.

The Schoenfeld residual plotted against salt is shown in Figure G-7. The plots for all four smoothing coefficients show that the PH assumption holds for covariate salt for CIP decks.

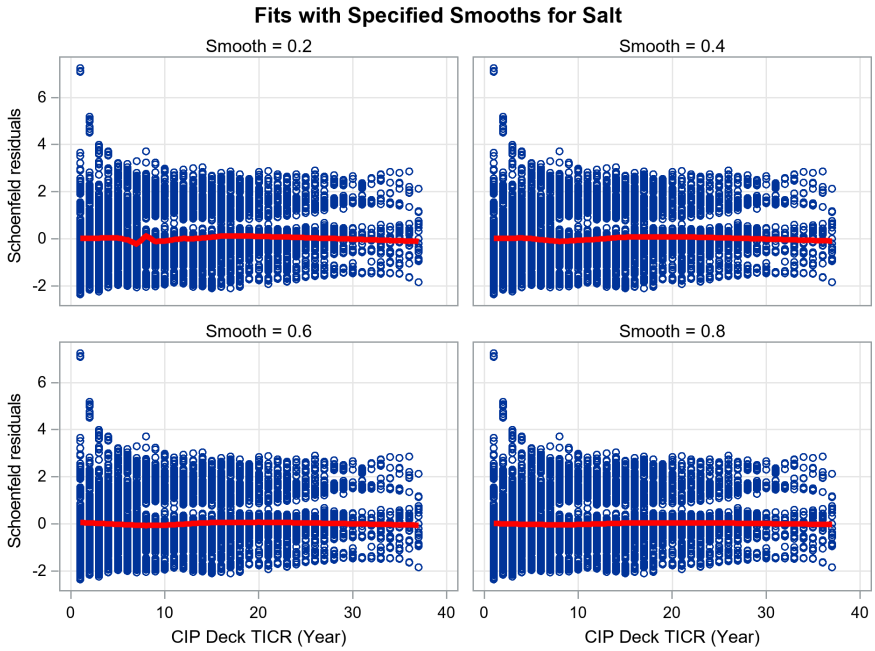

Figure G-7. Plot showing Schoenfeld residuals with smooths for salt for CIP deck.

The Schoenfeld residual for the covariate snow days is shown in Figure G-8. The fit for the plot for all four smoothing coefficients looks flat at zero, which indicates the PH assumption is met for the covariate of snow days.

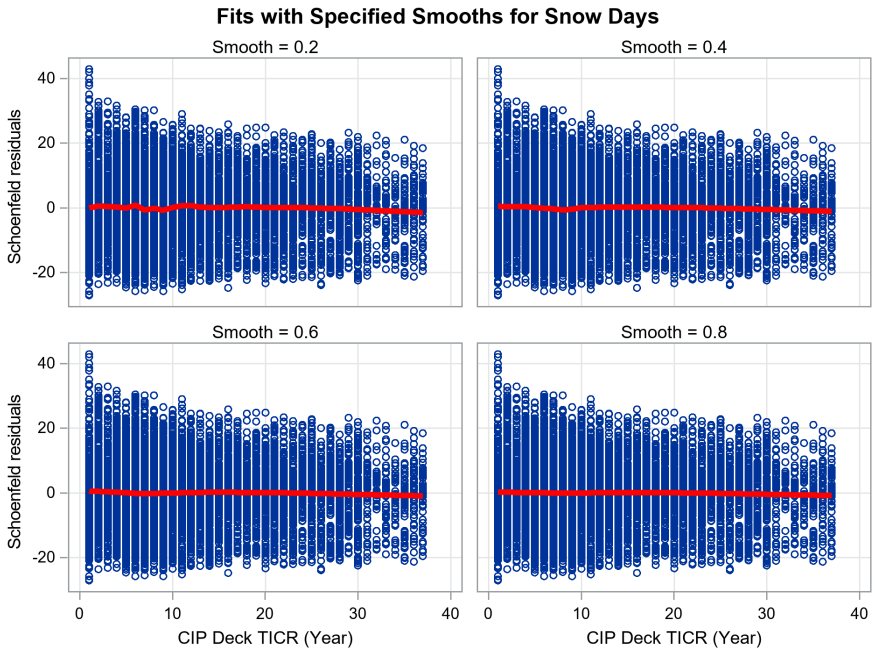

Figure G-8. Plot showing Schoenfeld residuals with smooths for snow days for CIP deck.

There is an interaction between the covariate salt and snow days in the model. The Schoenfeld residual for the interaction term is shown in Figure G-9. As shown, the fit for the smoothed curve is flat for all four different smoothing coefficients which indicate that the PH assumption for interaction term holds as well.

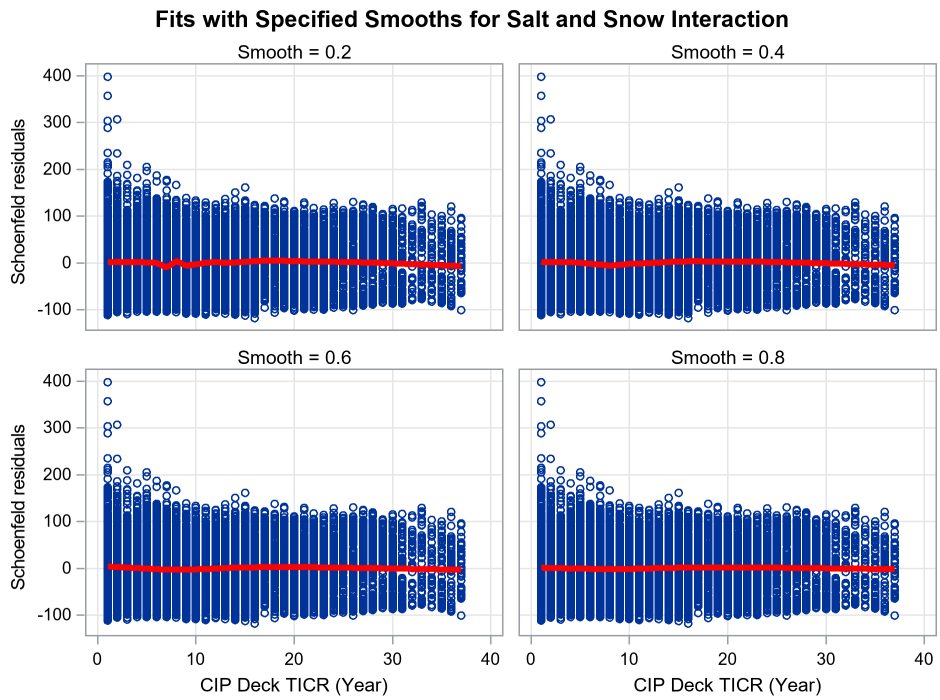

Figure G-9. Plot showing Schoenfeld residuals with smooths for salt and snow interaction for CIP deck.

Influential Observations and Outliers

Investigation of the influential observations for each continuous covariate is presented here. For this purpose, the dfbeta measure, dfβ, is calculated for each covariate and then plotted against the associated covariate to determine whether an observation has influential effects or not. For details on influential observations, please see "MODEL ASSUMPTIONS" section in this report (Appendix A). As shown in Figure G-10, the scatter plot uses the Federal ID for a bridge to determine the bridges with influential observations for covariates. The vertical axis is the dfβ, labeled as "Difference in parameter estimate for age in TICR" and the horizontal axis is the associated covariate, age in TICR. The plot also shows the symmetry grid line at ± 0.00005. A comparison of the absolute values with the parameter estimate for age in TICR (+0.01293) shows that the difference is small. Specifically, as shown, inclusion of bridge ID 10023 would decrease the parameter estimated for age in TICR by over 0.0001, which is a small amount compared to the parameter estimate. If observations for age in TICR for bridge ID 10023 are excluded from the model, the parameter would be 0.01281, or less than 1% smaller than if this observation is kept in the model. Other bridge IDs are either decreasing (falling below zero) or increasing (falling above zero) the parameter estimate by a much smaller amount compared to bridge ID 10023. Therefore, these observations are not influential, and no corrective action is required.

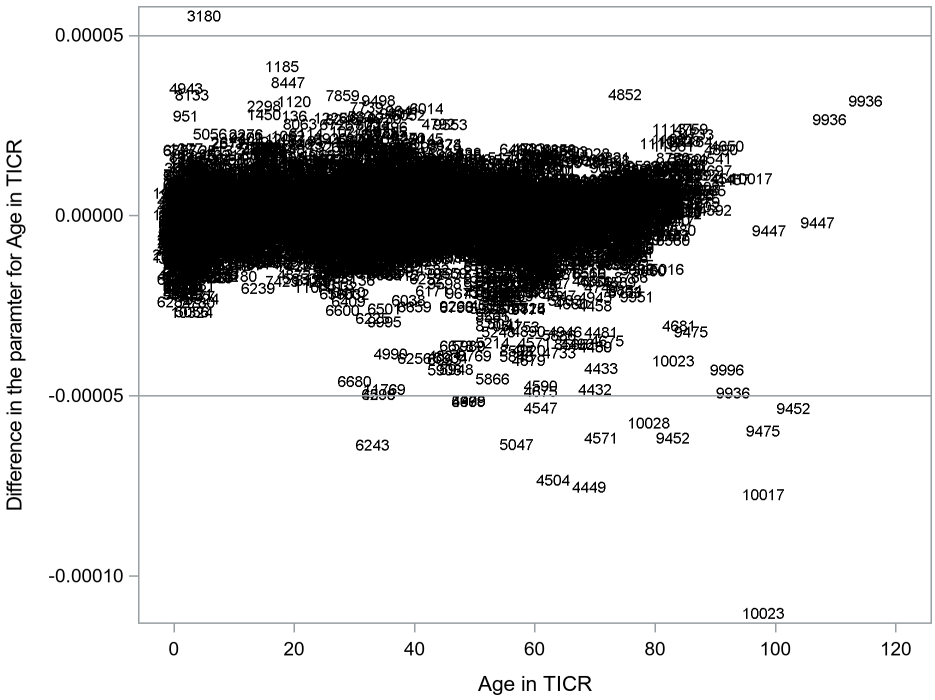

Figure G-10. Plot showing the influence of individual observations on age in TICR for CIP deck.

The dfβ for the covariate maximum span length (ft.) is shown in Figure G-11. The furthest bridge ID shown in this graph is 2780 shows that by including this observation, the parameter estimates for maximum span length would decrease by an amount of about 0.00008. Comparing this quantity with the parameter estimate for maximum span length +0.00176, it appears to reduce the parameter estimate by 4.6%. For example, if a cut off percentage point of 5% is set for detection of influential observations, even in this case, this observation is not an influential observation. Other bridge IDs are not influential compared to this bridge.

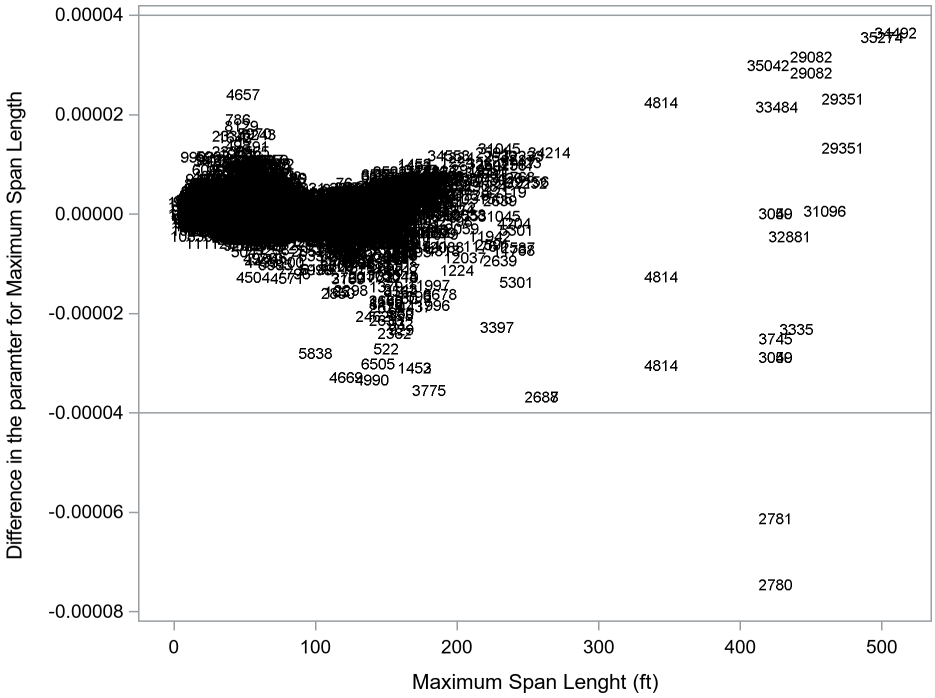

Figure G-11. Plot showing the influence of individual observations on maximum span length for CIP deck.

The *dfβ* for the covariate of salt (tons/lane miles) is shown in Figure G-12. Two bridge IDs that have the highest influence are 4950 and 3324. Including the salt data for these two bridges in the analysis would decrease the parameter estimate for salt by over 0.004 for each of the observations, individually. Comparing this quantity with the parameter estimate for salt, 0.29513, in model 3, it appears that the influence is not large enough and including these observations would decrease the parameter estimate by only about 2.6%, combined. All other observations influential effects are smaller than the bridge 4950 and 3324.

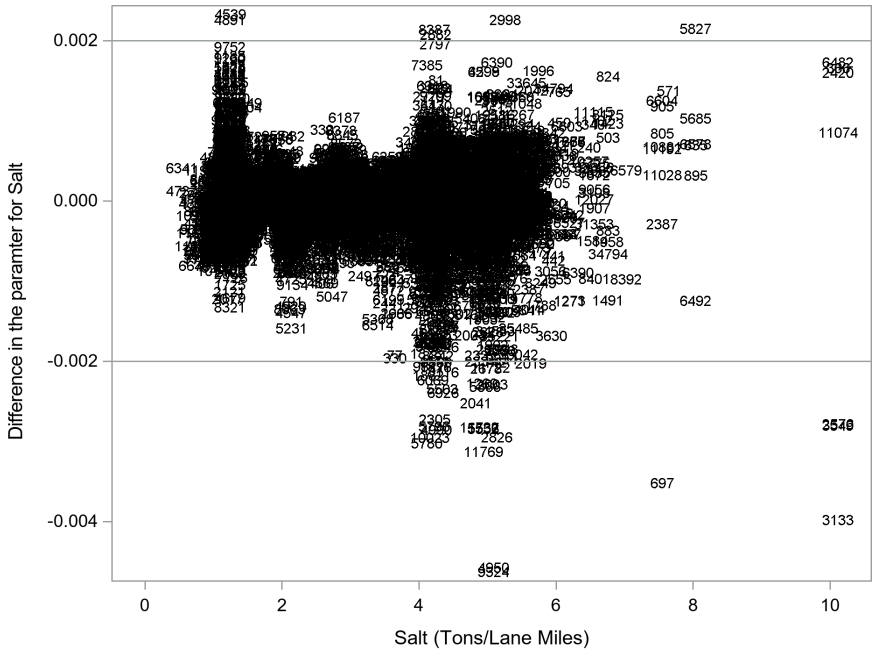

Figure G-12. Plot showing the influence of individual observations on salt for CIP deck.

The plot for investigating influential observations for the covariate of snow days is shown in Figure G-13. As shown in Figure G-13, bridge ID 3133 has the highest influence on reducing the parameter estimate if included in the model. The amount of influence from this observation is close to 0.0003. Comparing this value with the parameter estimate for snow days, 0.01735 demonstrates that the influence is not pronounced, and the observation could stay in the model without adverse effect on parameter estimate for snow days.

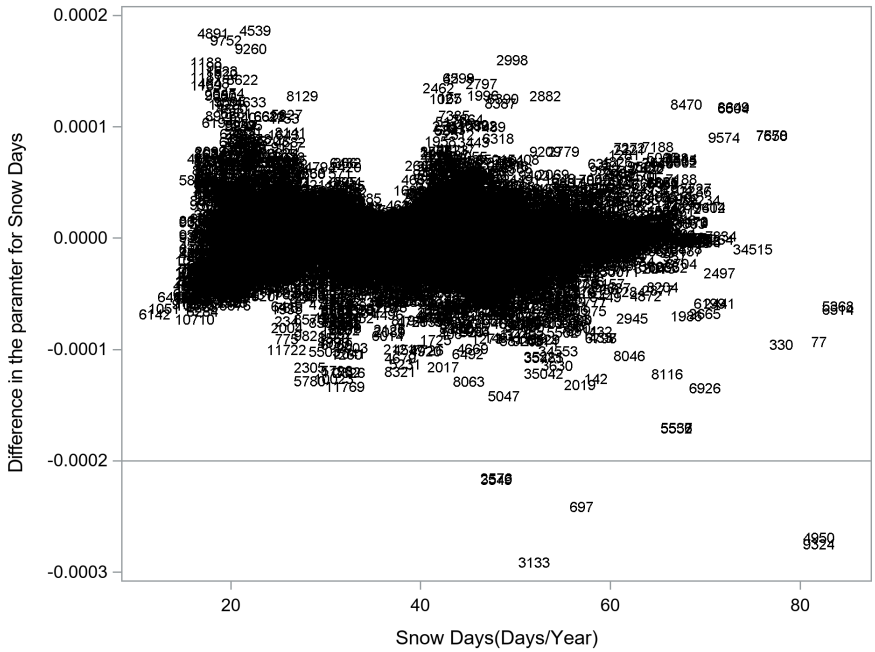

Figure G-13. Plot showing the influence of individual observations on snow days for CIP deck.

The plot of the effect of the influential observations for the interaction term of snow days and salt is shown in Figure G-14. The furthest bridge IDs are 9224 and 4550 with positive values at about 0.00015. Comparing this value with the parameter estimate for the interaction, -0.00599, indicates that including these two points would increase the parameter estimate by 0.00015, or by 2.6% each. Again, the change is not dramatic and therefore it is not an influential observation for this interaction.

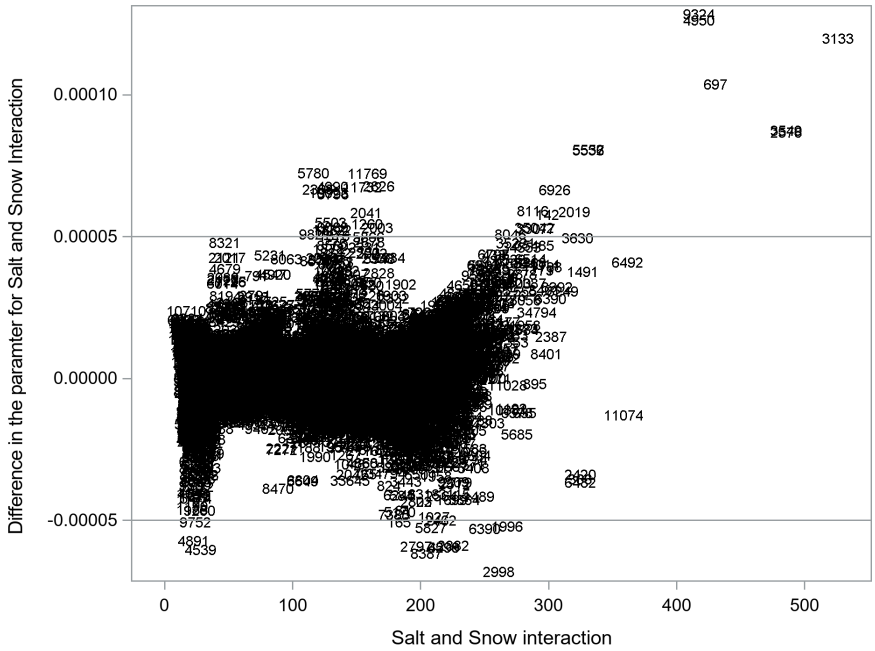

Figure G-14. Plot showing the influence of individual observations on salt and snow interaction for CIP deck.

Overall Fit for CIP Decks

The plot to check for the overall fit of the model is shown in Figure G-15. The vertical axis is the likelihood displacement that "quantifies how much the likelihood of the model, which is affected by all coefficients, changes when the observation is left out." [12] Again, bridge IDs are shown on the plot to find out the bridge which influences the Cox regression's overall fit. But as discussed before, this observation does not have a dramatic influence on the specific parameter, and therefore no observations were deleted, and no new models were fit.

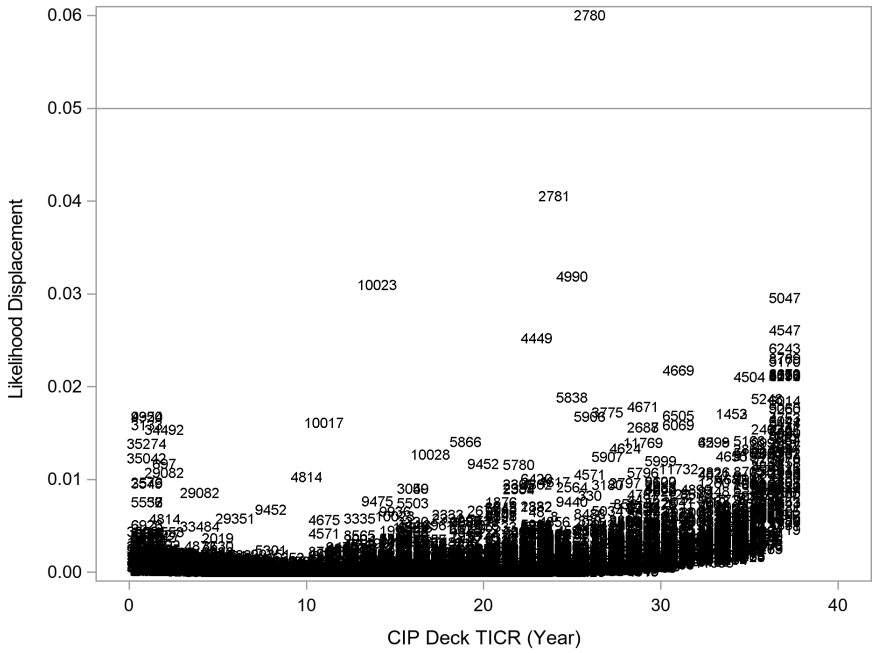

Figure G-15. Plot of likelihood displacement for the overall fit of the model for CIP decks.

Predictive Accuracy of the Cox Regression for CIP Decks

The predictive accuracy of the Cox regression for CIP decks is presented below using the Harrell's C-statistics. For CIP decks data set, there are 85,496,079 concordant pairs, 54,473,993 discordant pairs, and 6,619,931 tied-in-time pairs. Using equation (A-7), the C-statistics for CIP decks is 0.61. The area under the ROC curve (AUC) and the 95% confidence interval for CIP decks is shown in Figure G-16. As shown, the predictive accuracy of the Cox regression is reaching 0.7 for TICR equal to 15 years and increasing for longer TICRs than 15. Typical, or common, values for C-statistics for valid model are in the range of 0.6 to 0.8. As these data show, the C-statistic is within the typical value for statistical models and increases with increasing TICR. This verifies the predictive accuracy of the Cox regression models used in the research.

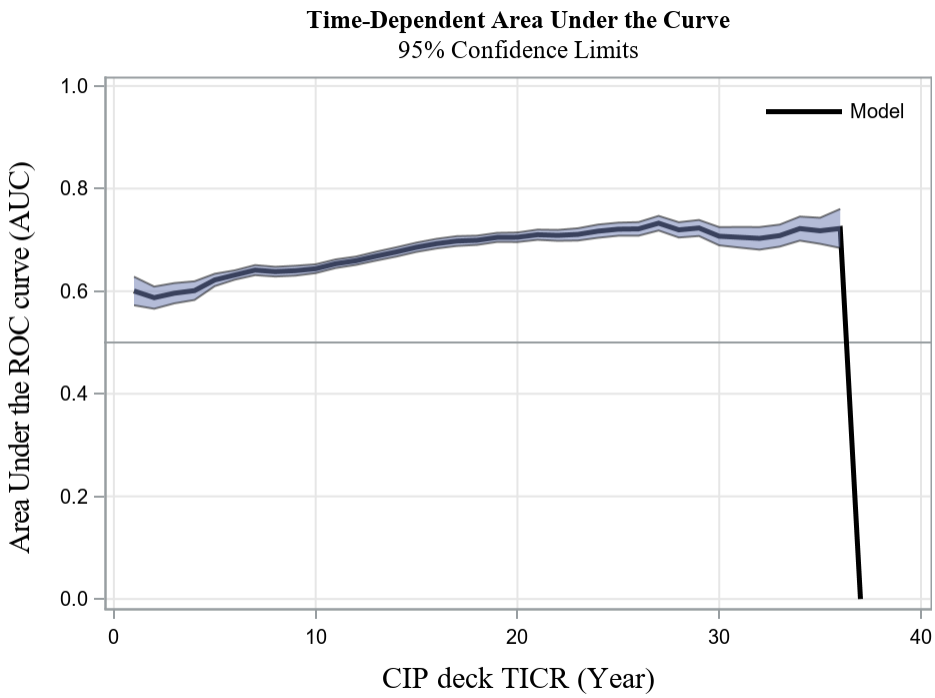

Figure G-16. Plot showing AUC for the time-dependent ROC curve for CIP decks.

Checking Model Assumptions for Superstructures

This section contains the model assumptions for superstructures. Description of each plot is provided for CIP decks and is omitted here.

Functional Form of the Covariates

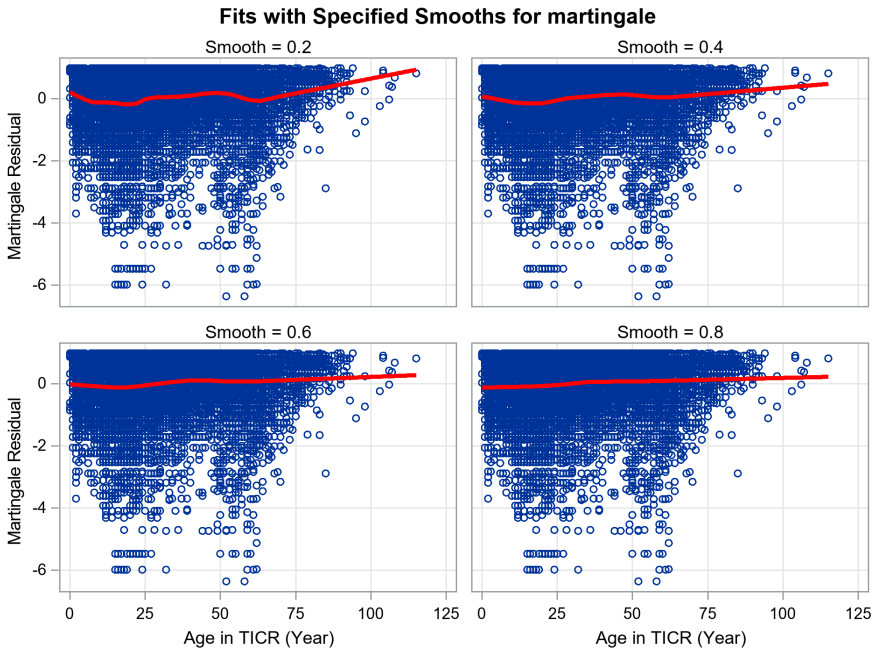

Figure G-17. Plot showing martingale residuals with smooths for age in TICR for superstructures.

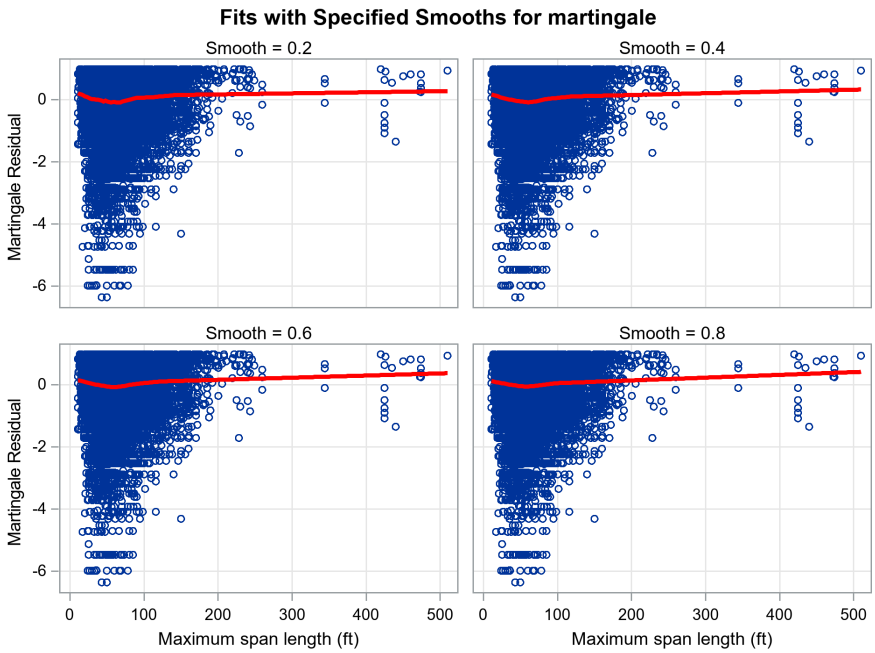

Figure G-18. Plot showing martingale residuals with smooths for maximum span length for superstructures.

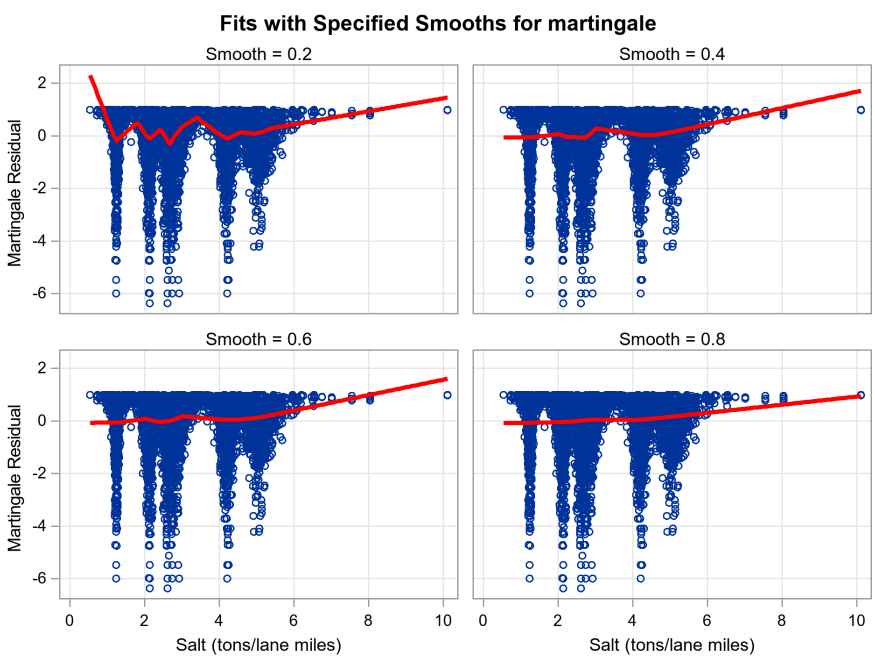

Figure G-19. Plot showing martingale residuals with smooths for salt for superstructures.

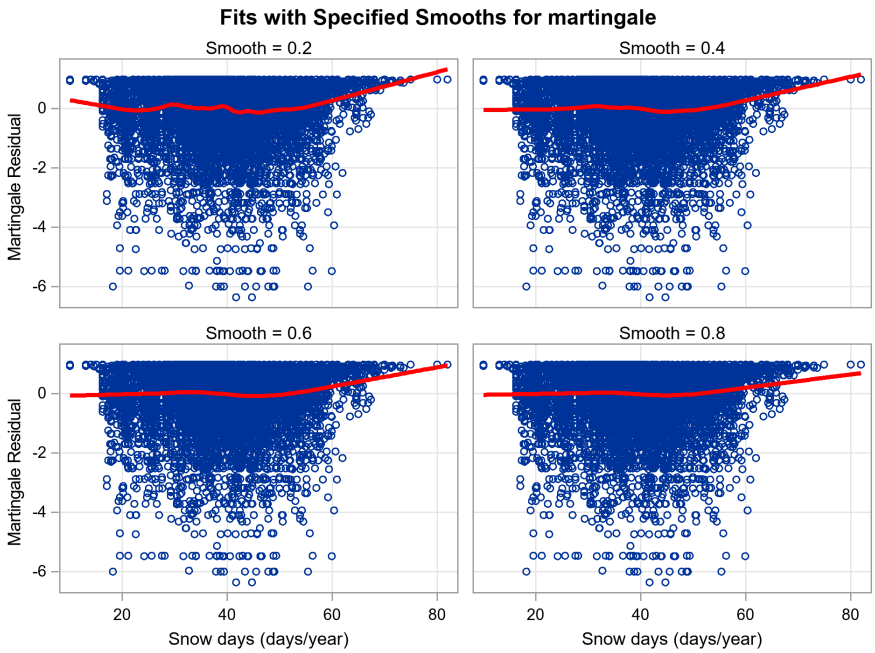

Figure G-20. Plot showing martingale residuals with smooths for snow days for superstructures.

Proportional Hazard Assumption

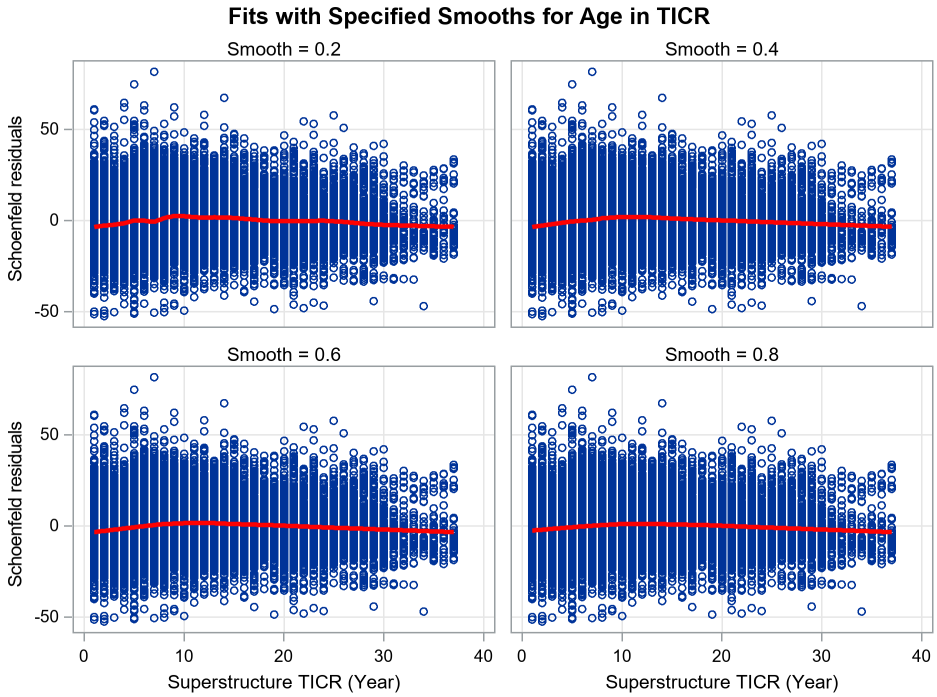

Figure G-21. Plot showing Schoenfeld residuals with smooths for age in TICR for superstructures.

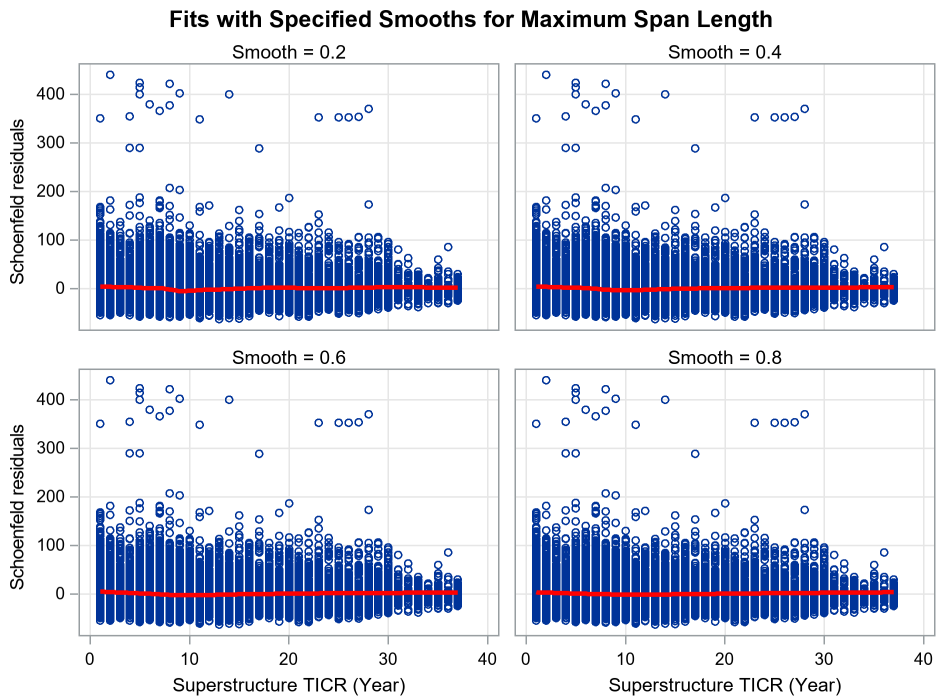

Figure G-22. Plot showing Schoenfeld residuals with smooths for maximum span length for superstructures.

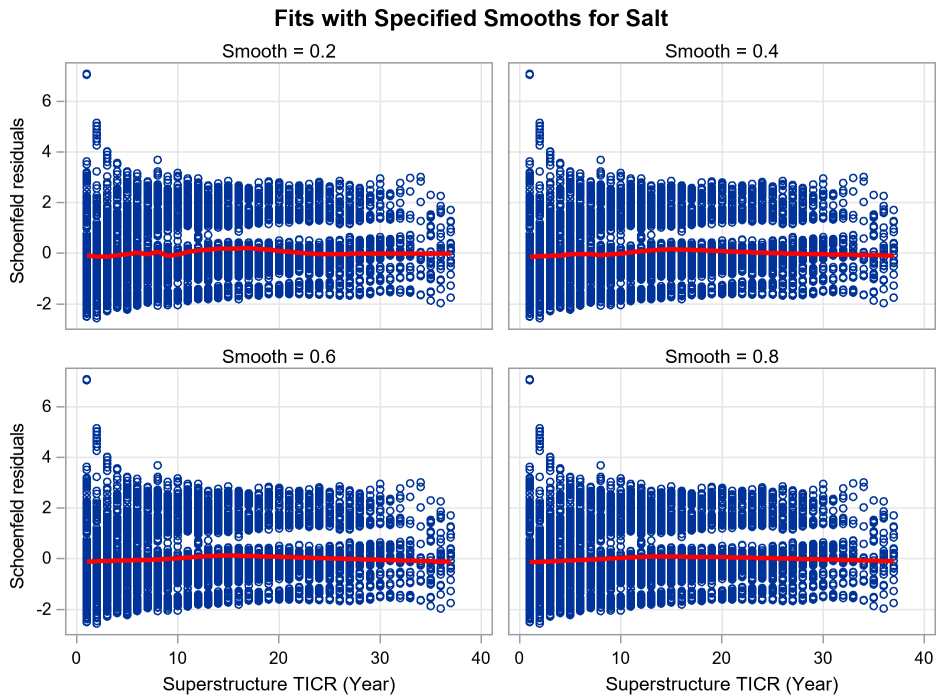

Figure G-23. Plot showing Schoenfeld residuals with smooths for salt for superstructures.

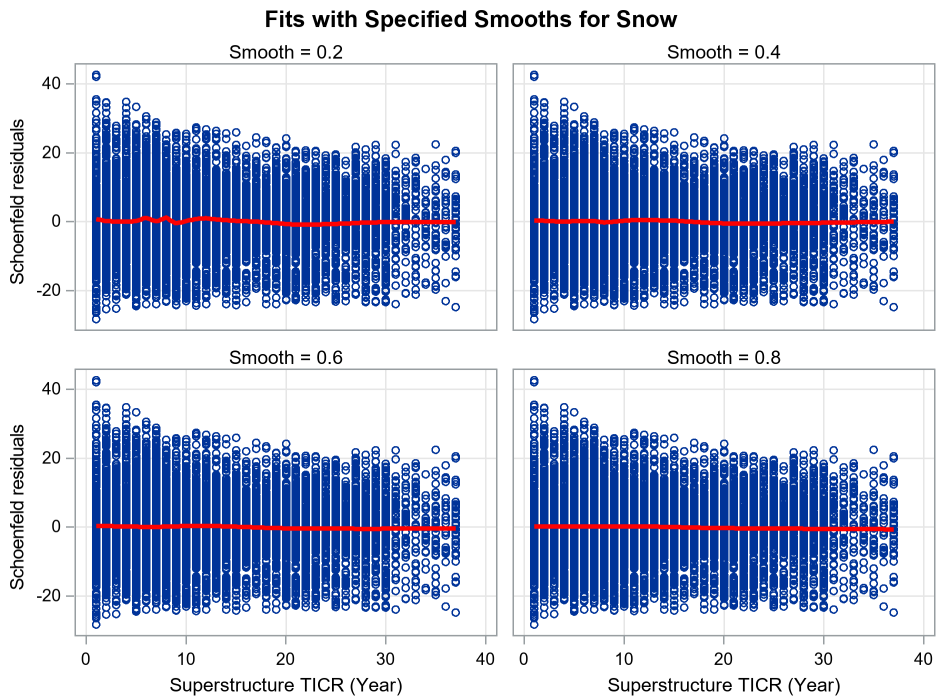

Figure G-24. Plot showing Schoenfeld residuals with smooths for snow for superstructures.

Influential Observations and Outliers

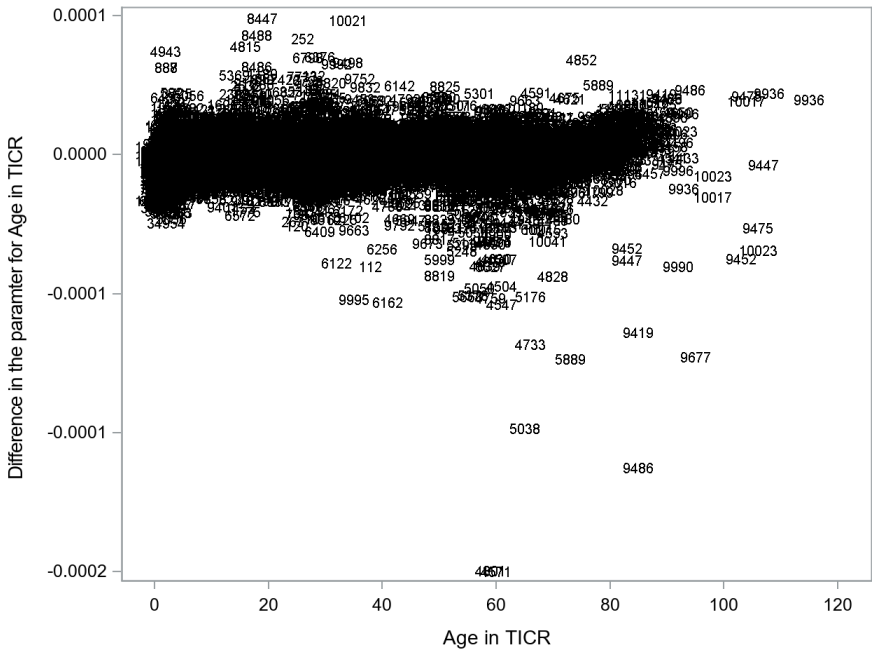

Figure G-25. Plot showing the influence of individual observations on age in TICR for superstructures.

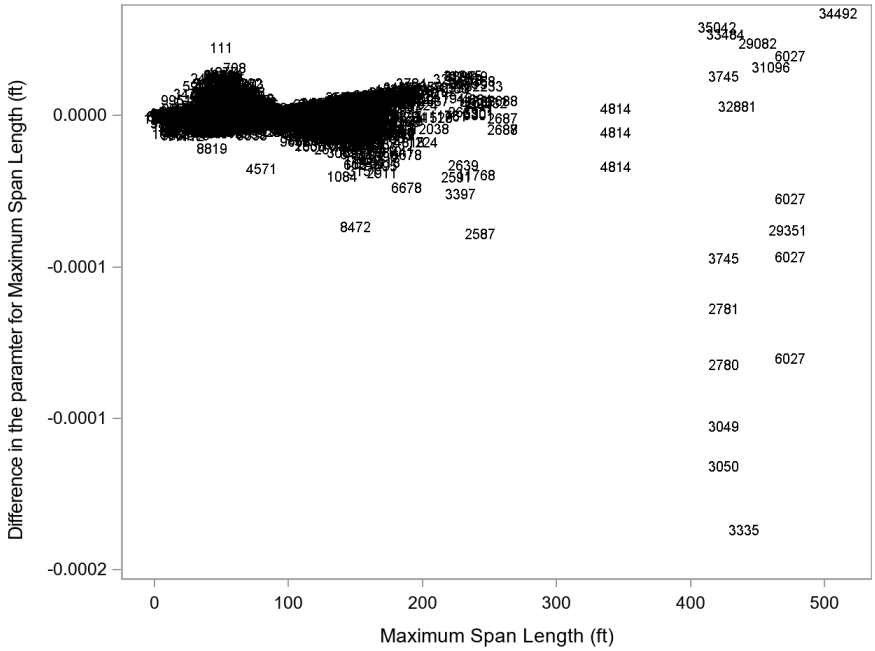

Figure G-26. Plot showing the influence of individual observations on maximum span length for superstructures.

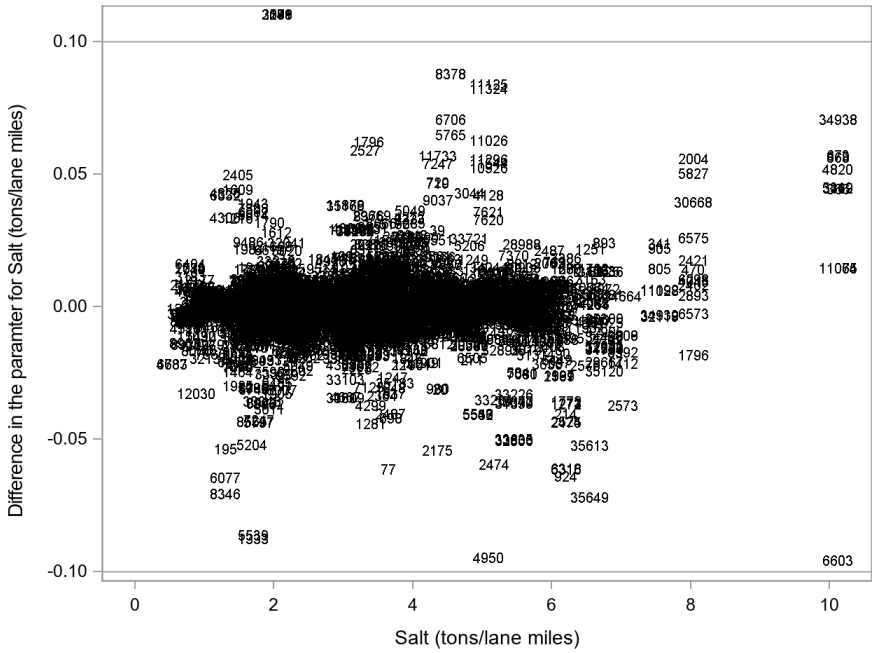

Figure G-27. Plot showing the influence of individual observations on salt for superstructures.

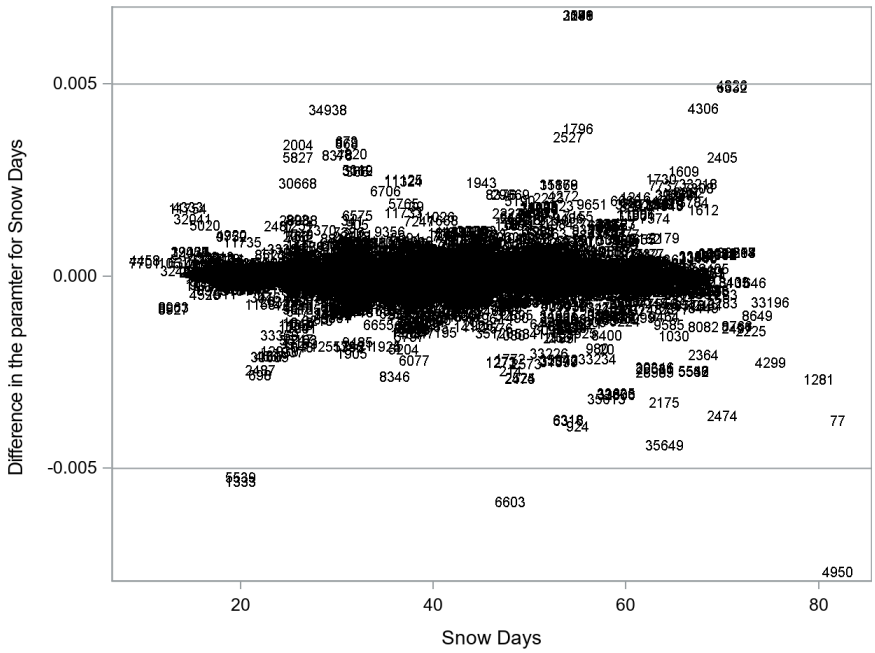

Figure G-28. Plot showing the influence of individual observations on snow for superstructures.

Overall Fit for Superstructures

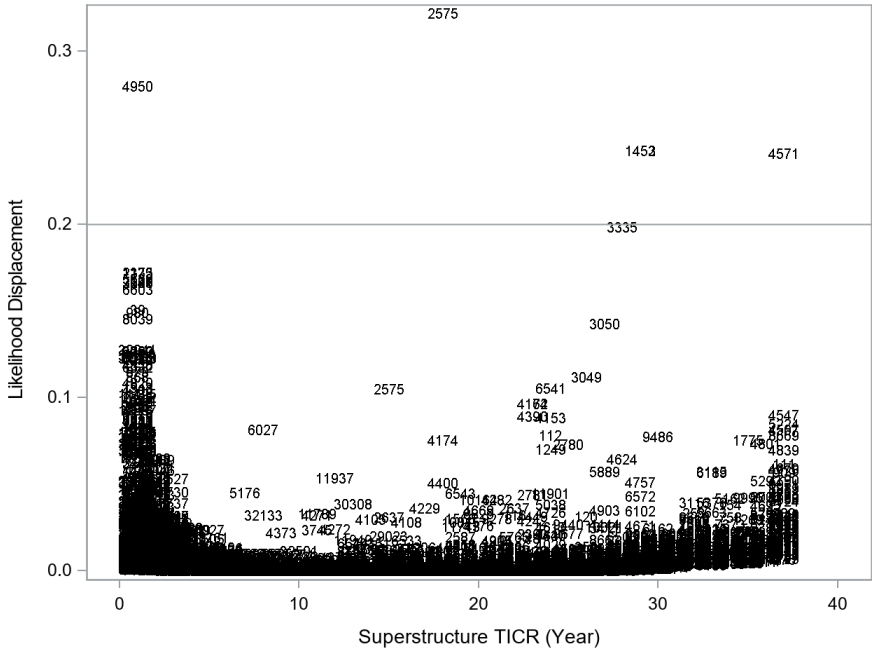

Figure G-29. Plot of likelihood displacement for the overall fit of the model for superstructures.

Predictive Accuracy of the Cox Regression for Superstructures

The predictive accuracy of the Cox regression for superstructures is presented below using the Harrell's C-statistics. For superstructures data set, there are 73,135,361 concordant pairs, 53,982,296 discordant pairs, 4 tied-in-predictor, and 5,800,699 tied-in-time pairs. Using equation (A-7), the C-statistics for superstructures is 0.58. The area under the ROC curve (AUC) and the 95% confidence interval for substructures is shown in Figure G-30. As shown, the predictive accuracy of the Cox regression for superstructures is about 0.6 in the beginning but reaching to 0.7 at TICR 25 to 37.

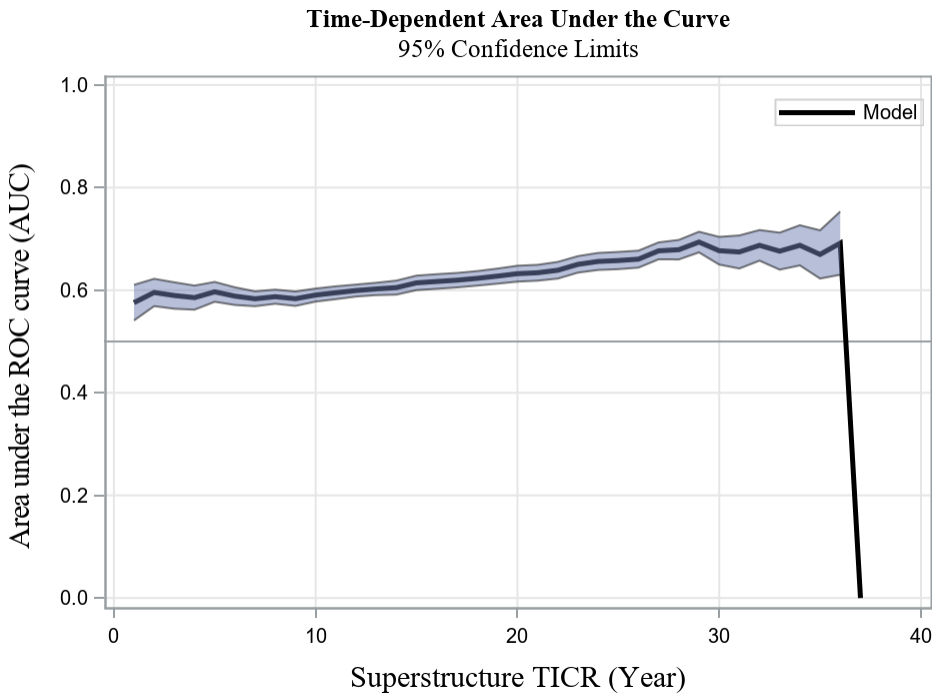

Figure G-30. Plot showing AUC for the time-dependent ROC curve for superstructures.

Checking Model Assumptions for Substructures

Functional Form of the Covariates

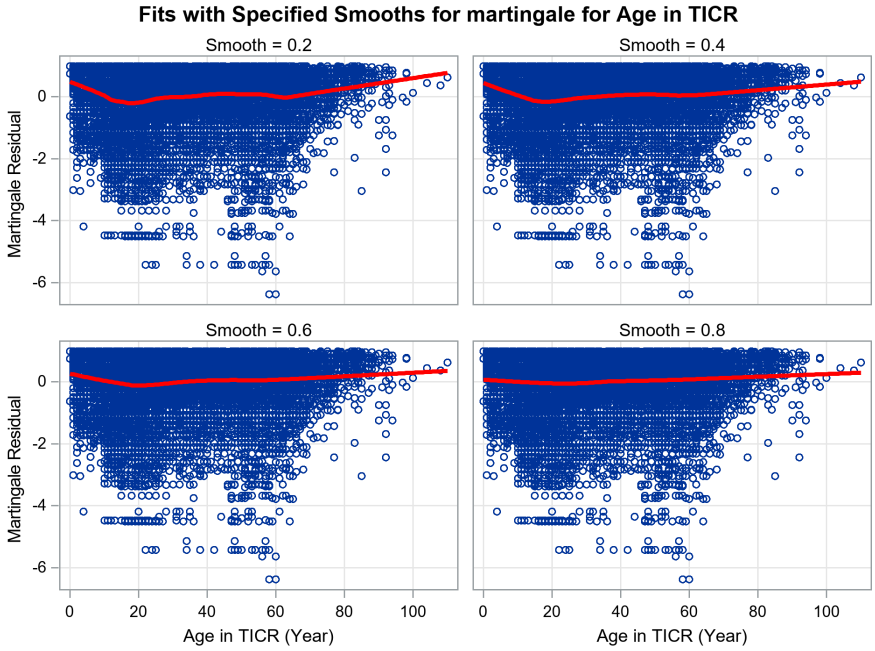

Figure G-31. Plot showing martingale residuals with smooths for age in TICR for substructures.

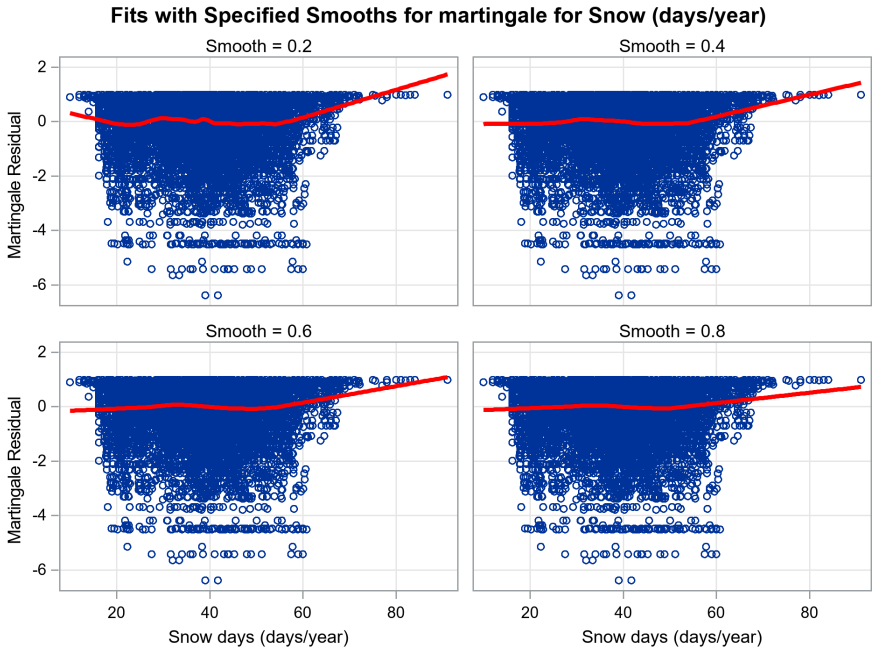

Figure G-32. Plot showing martingale residuals with smooths for snow days for substructures.

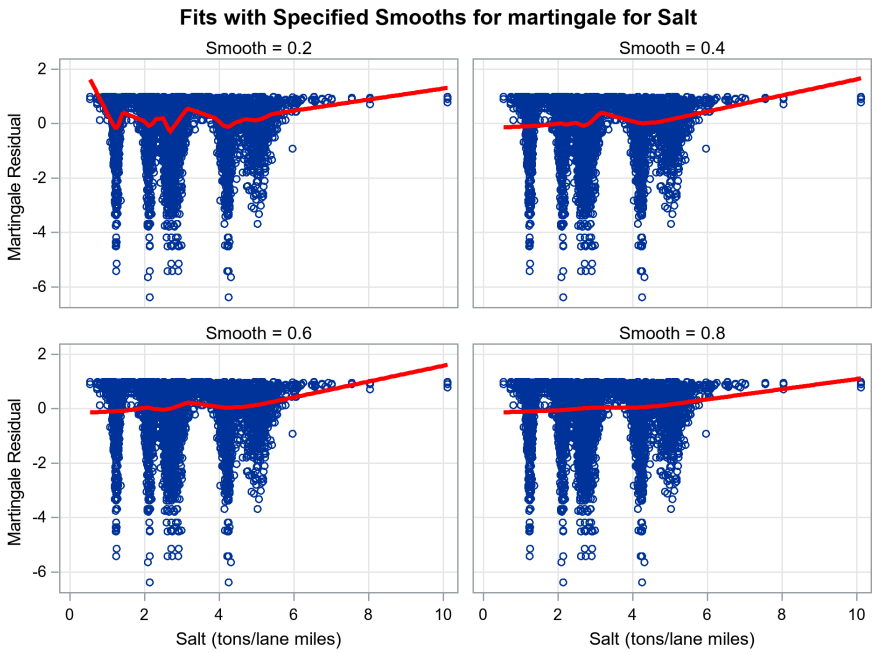

Figure G-33. Plot showing martingale residuals with smooths for salt for substructures.

Proportional Hazard Assumption

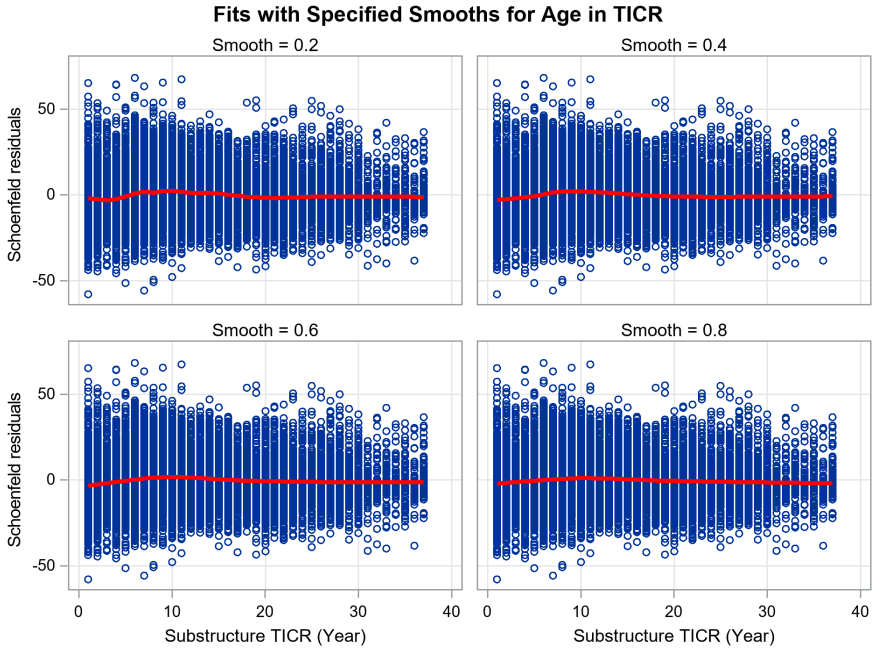

Figure G-34. Plot showing Schoenfeld residuals with smooths for age in TICR for substructures.

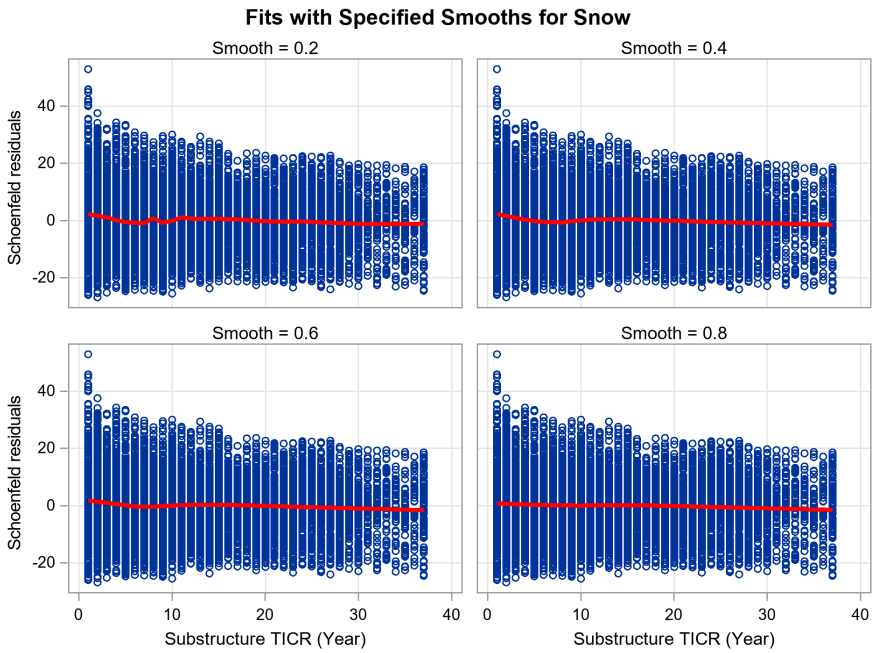

Figure G-35. Plot showing Schoenfeld residuals with smooths for snow for substructures.

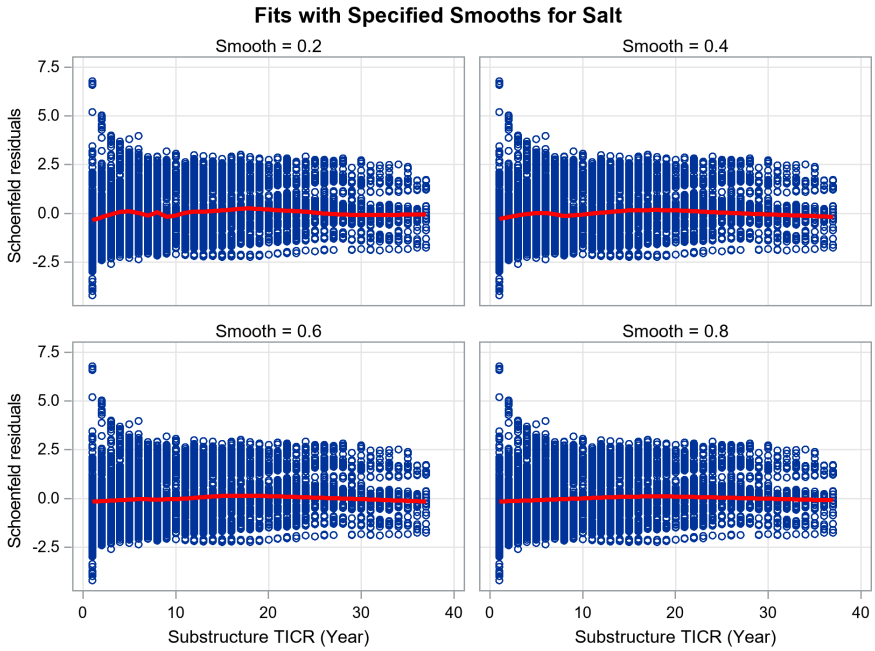

Figure G-36. Plot showing Schoenfeld residuals with smooths for salt for substructures.

Influential Observations and Outliers

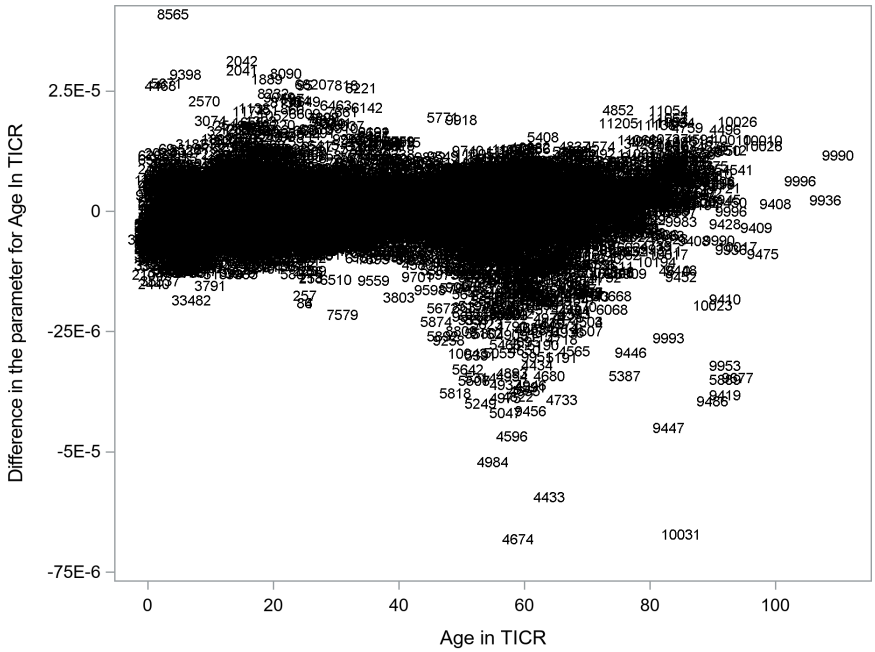

Figure G-37. Plot showing the influence of individual observations on age in TICR for substructures.

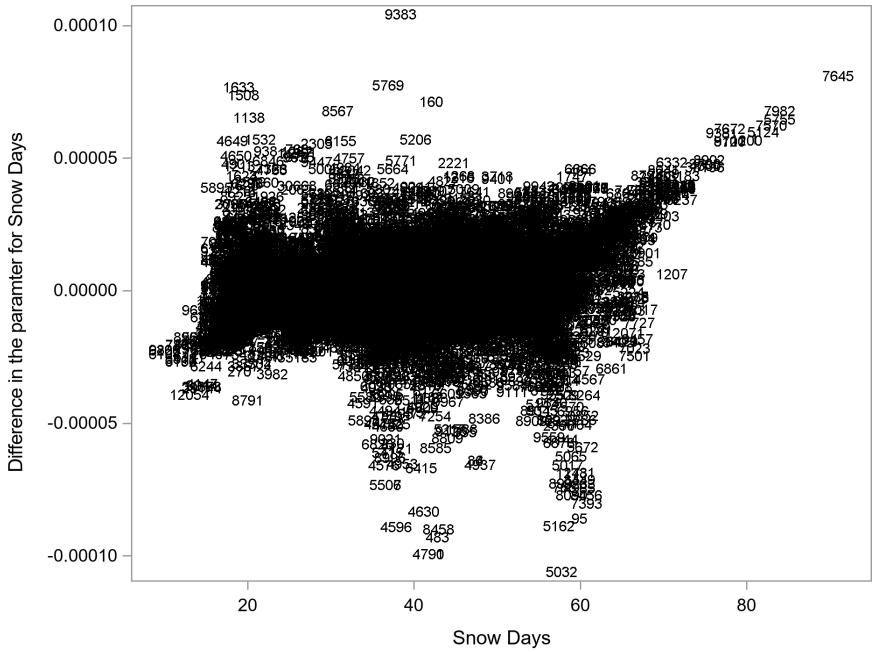

Figure G-38. Plot showing the influence of individual observations on snow days for substructures.

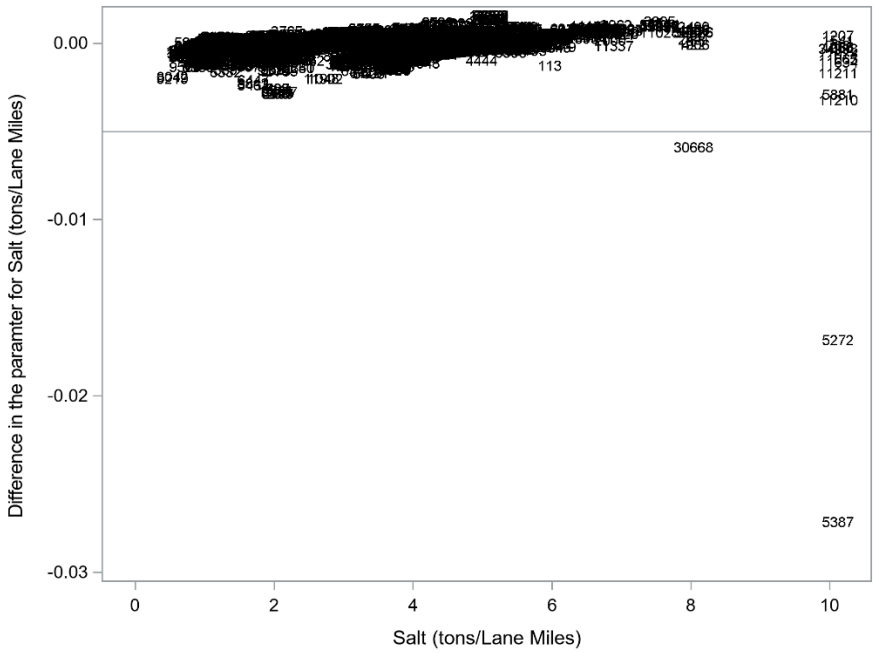

Figure G-39. Plot showing the influence of individual observations on salt for substructures.

Overall Fit for Substructures

As shown in Figure G-40,data for structure number 5387, 5272, and 30668 fall outside of other substructures in the data set, and therefore these three substructures are excluded in the final model presented in Table C-14.

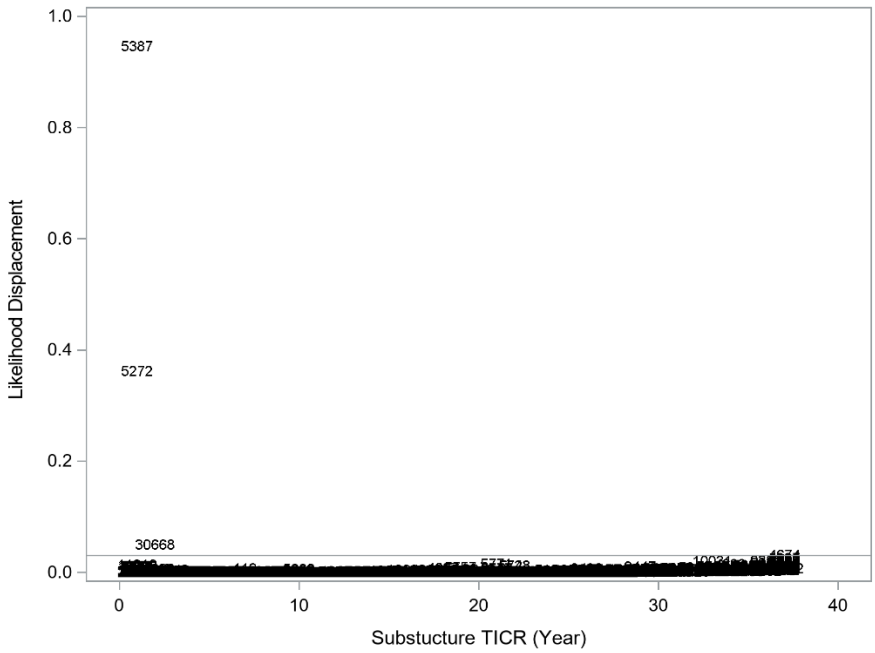

Figure G-40. Plot of likelihood displacement for the overall fit of the model for substructures.

Predictive Accuracy of the Cox Regression for Substructures

The predictive accuracy of the Cox regression for substructures is presented below using the Harrell's C-statistics. For substructures data set, there are 76,923,632 concordant pairs, 61,010,630 discordant pairs, 4 tied-in-predictor, and 5,878,054 tied-in-time pairs. Using equation (A-7), the C-statistics for substructures is 0.56. The area under the ROC curve (AUC) and the 95% confidence interval for substructures is shown in Figure G-41. As shown, the predictive accuracy of the Cox regression is about 0.6 throughout the available data.

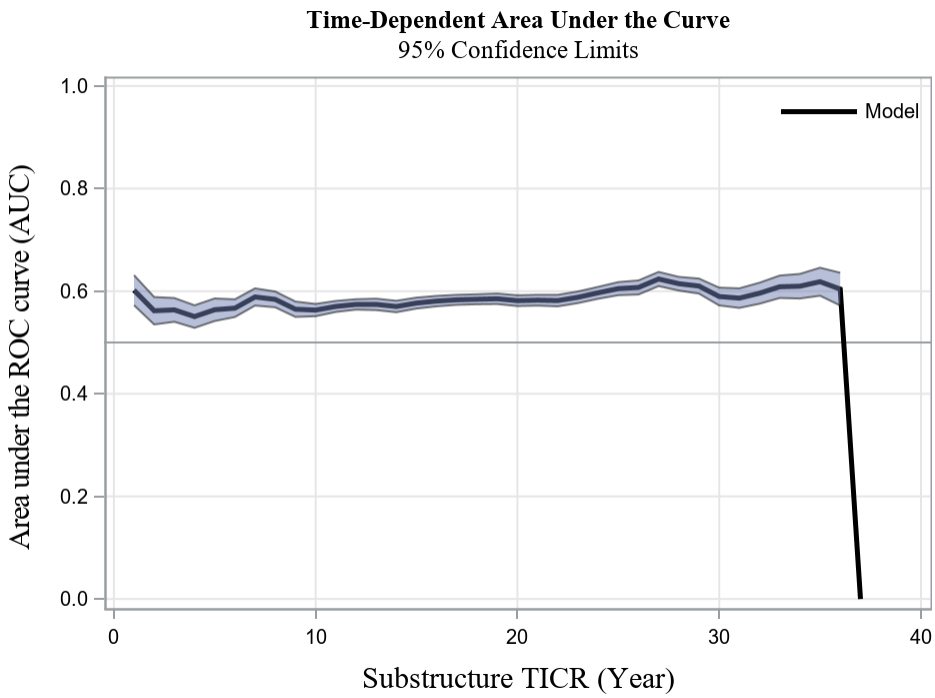

Figure G-41. Plot showing AUC for the time-dependent ROC curve for substructures.

Checking Model Assumptions for Culverts

For reading the graphs for model validation of culverts, the description is similar to those provided for CIP decks.

Functional Form

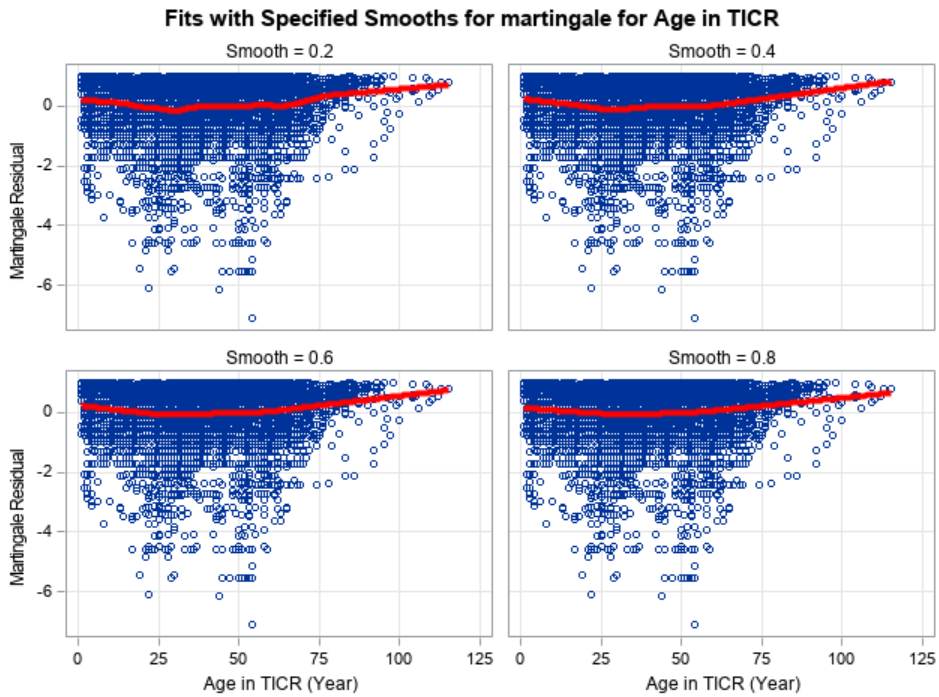

Figure G-42. Plot showing martingale residuals with smooths for age in TICR for culverts.

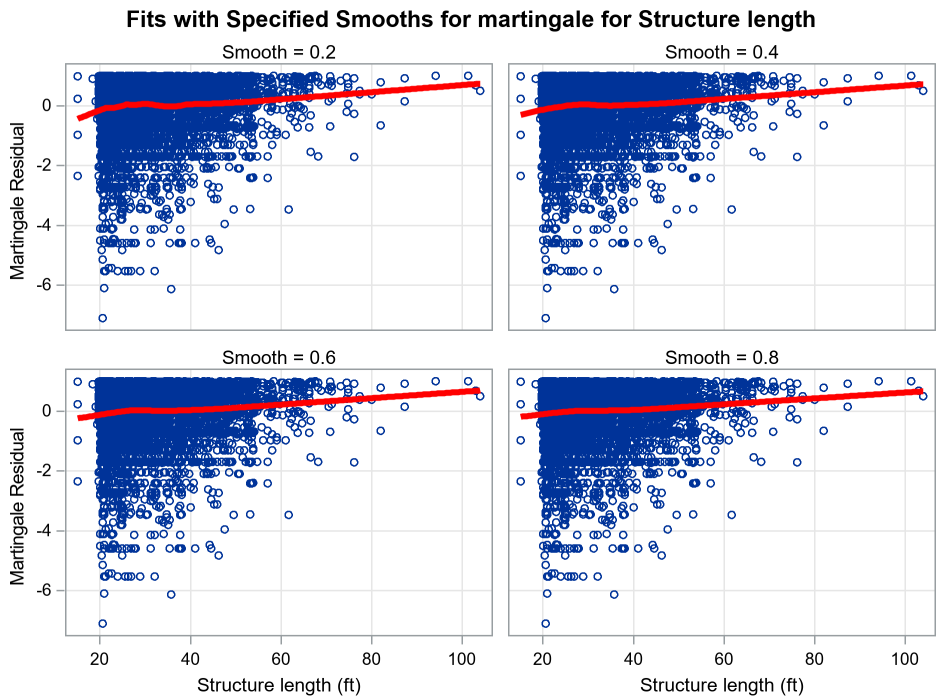

Figure G-43. Plot showing martingale residuals with smooths for structure length for culverts.

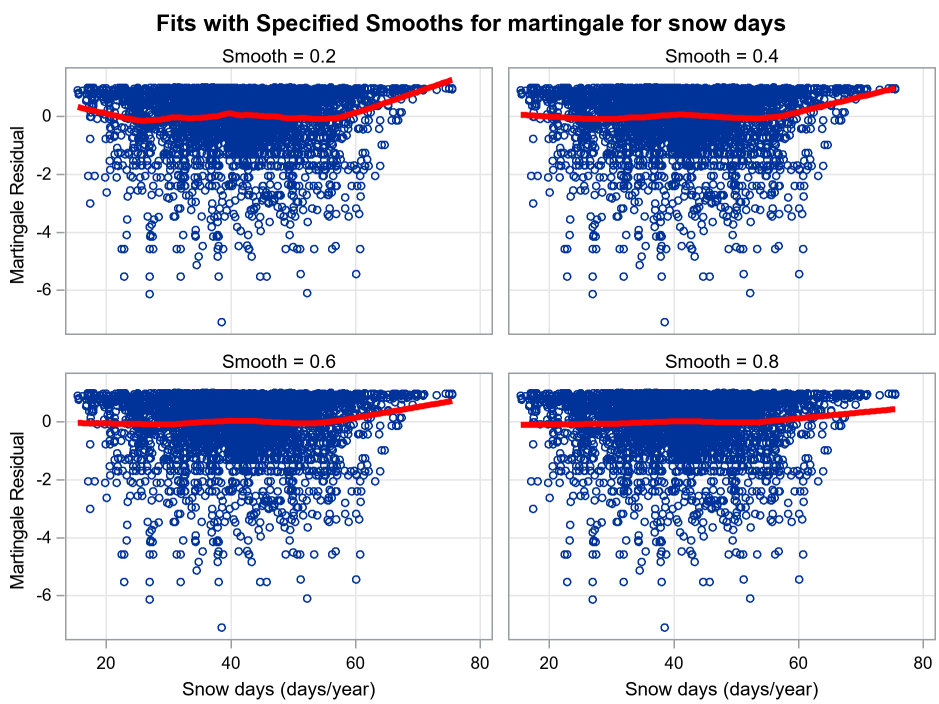

Figure G-44. Plot showing martingale residuals with smooths for snow days for culverts.

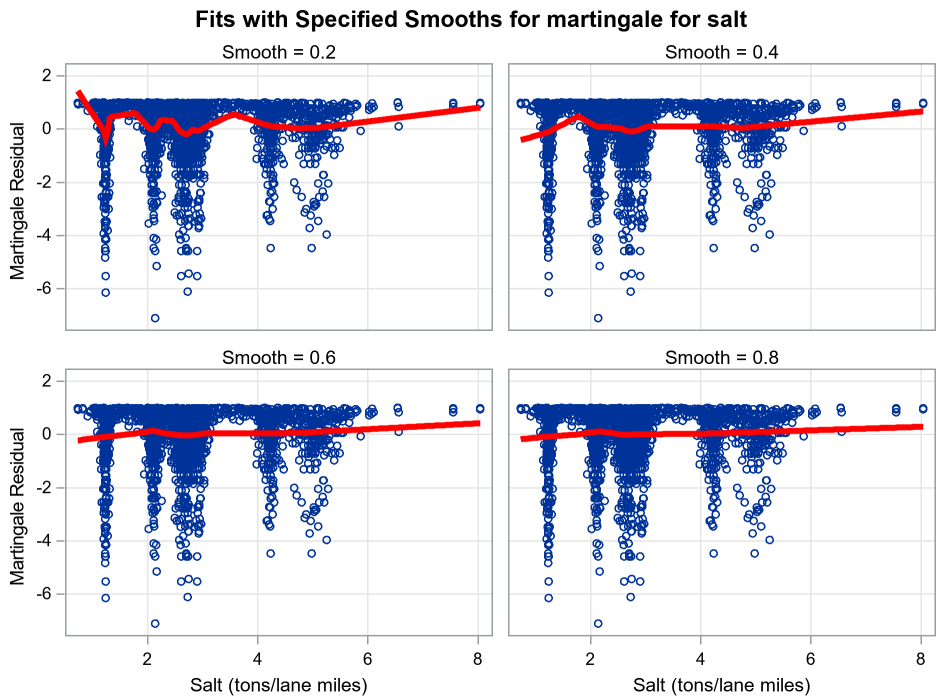

Figure G-45. Plot showing martingale residuals with smooths for salt for culverts.

Proportional Hazard Assumption

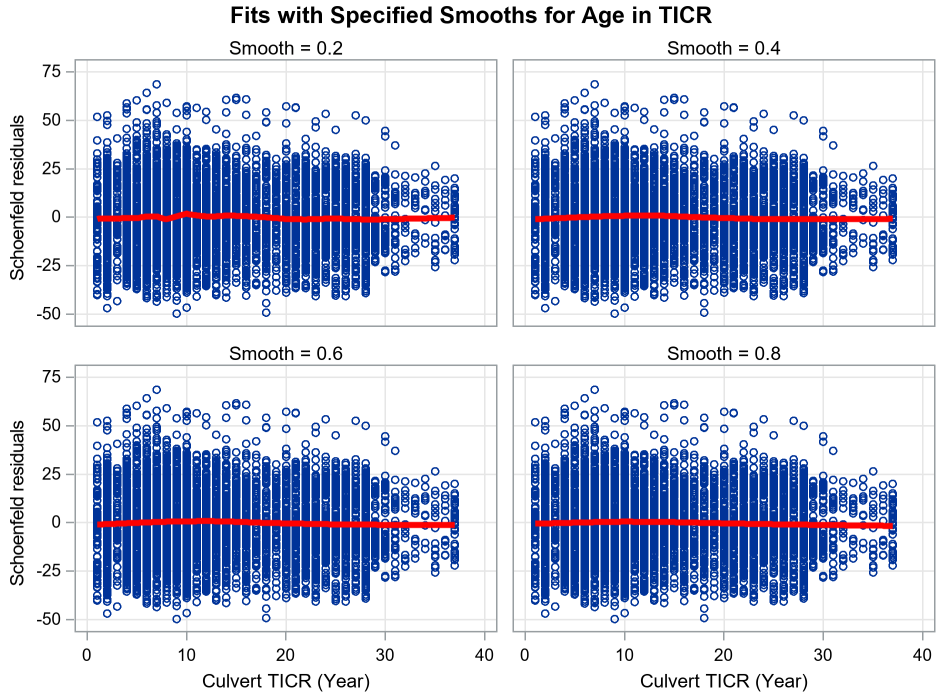

Figure G-46. Plot showing Schoenfeld residuals with smooths for age in TICR for culverts.

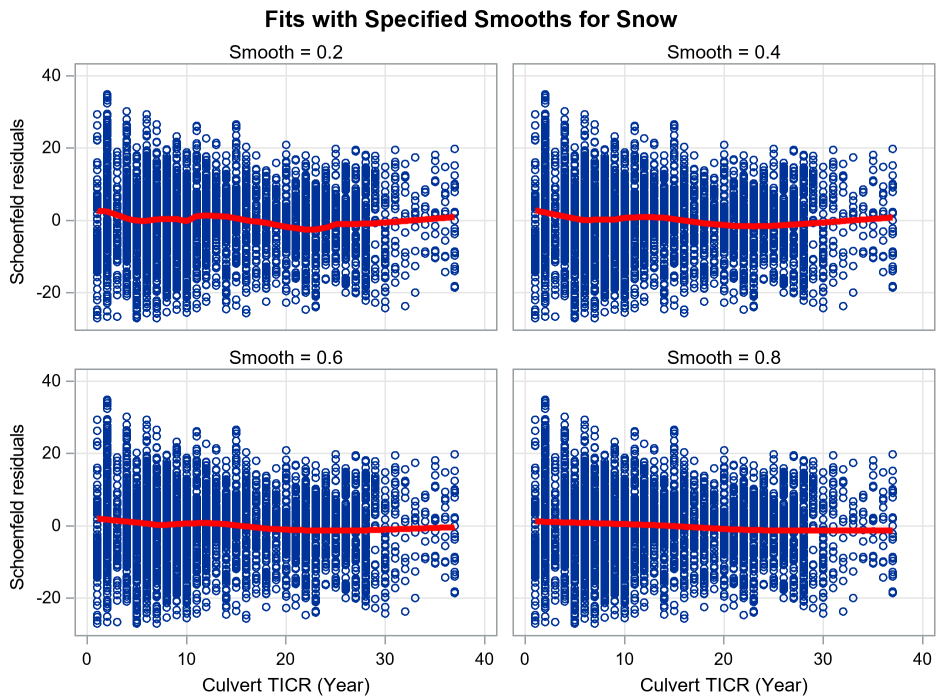

Figure G-47. Plot showing Schoenfeld residuals with smooths for snow for culverts.

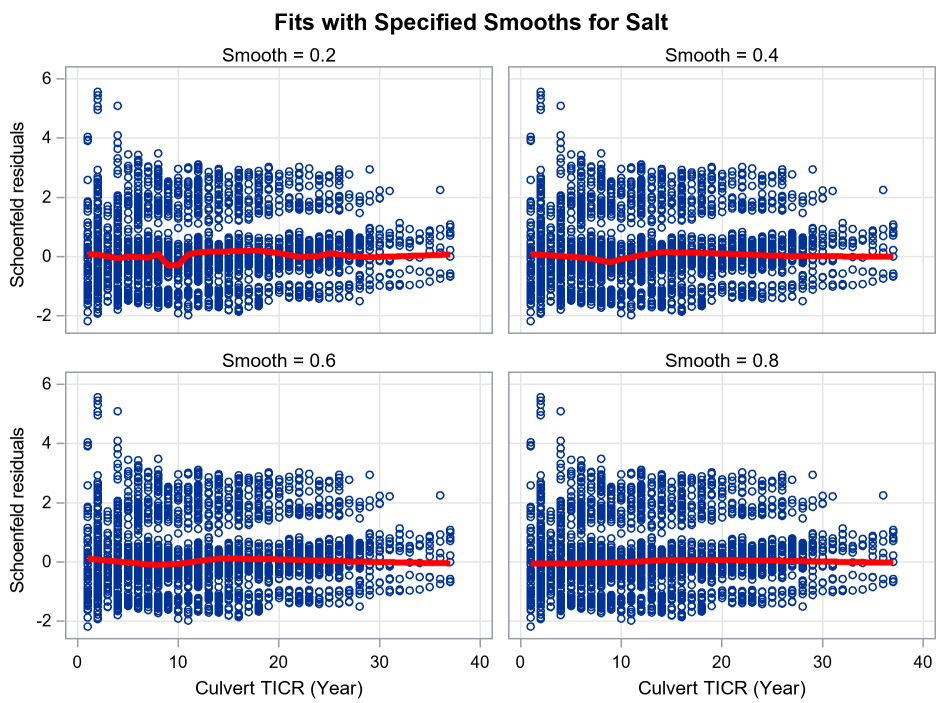

Figure G-48. Plot showing Schoenfeld residuals with smooths for salt for culverts.

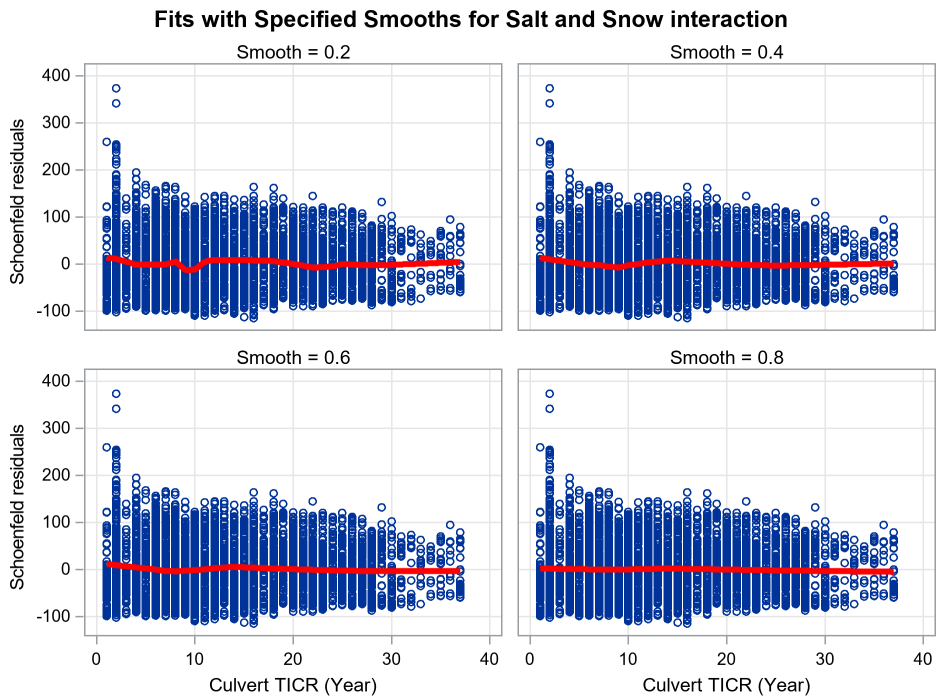

Figure G-49. Plot showing Schoenfeld residuals with smooths for salt and snow interaction for culverts.

Influential Observations and Outliers

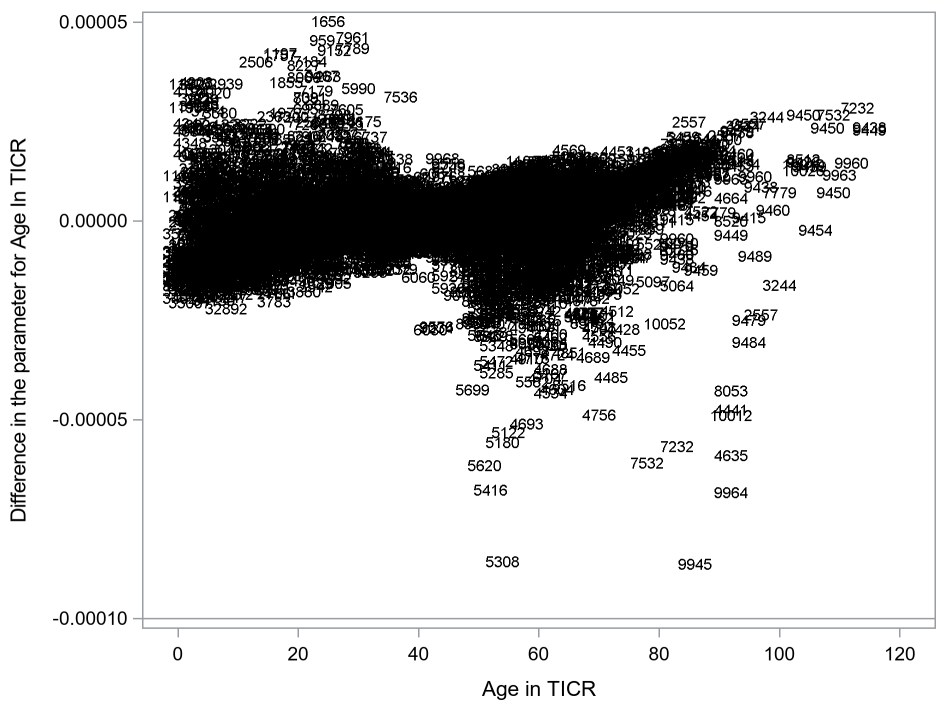

Figure G-50. Plot showing the influence of individual observations on age in TICR for culverts.

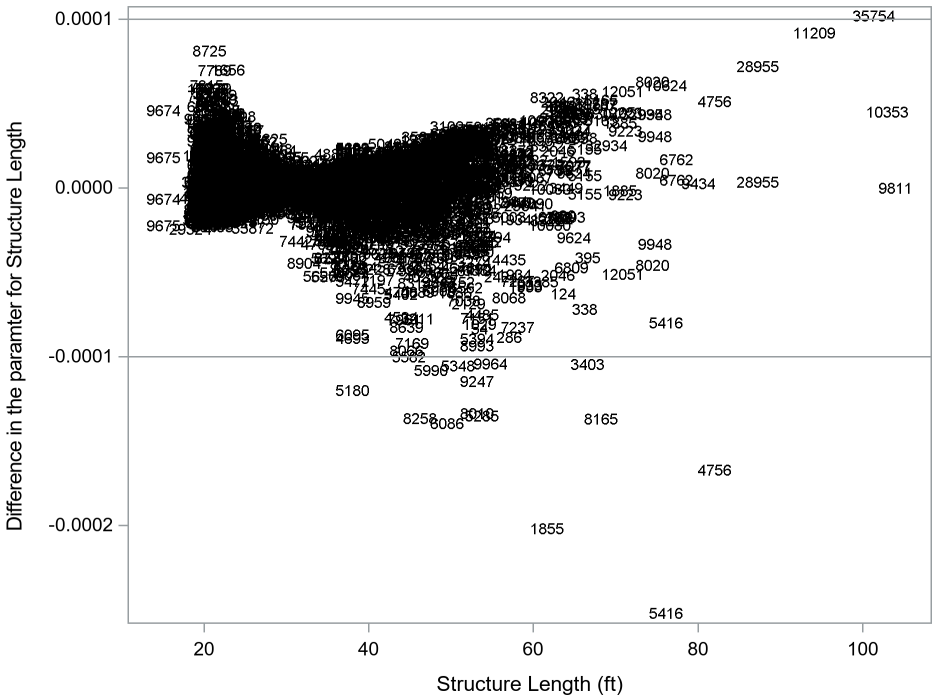

Figure G-51. Plot showing the influence of individual observations on Structure length for culverts.

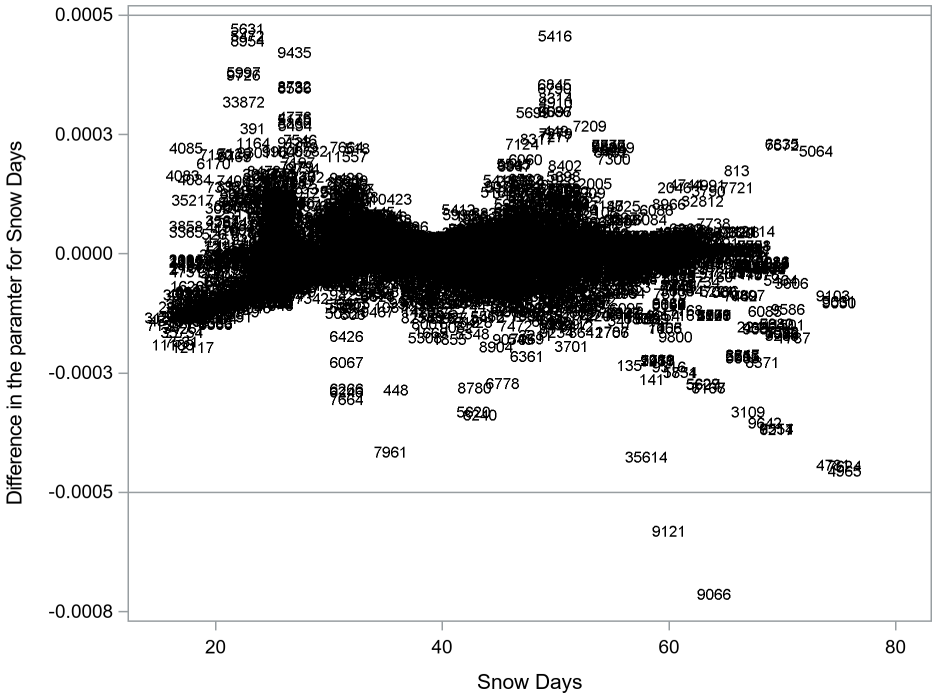

Figure G-52. Plot showing the influence of individual observations on snow days for culverts.

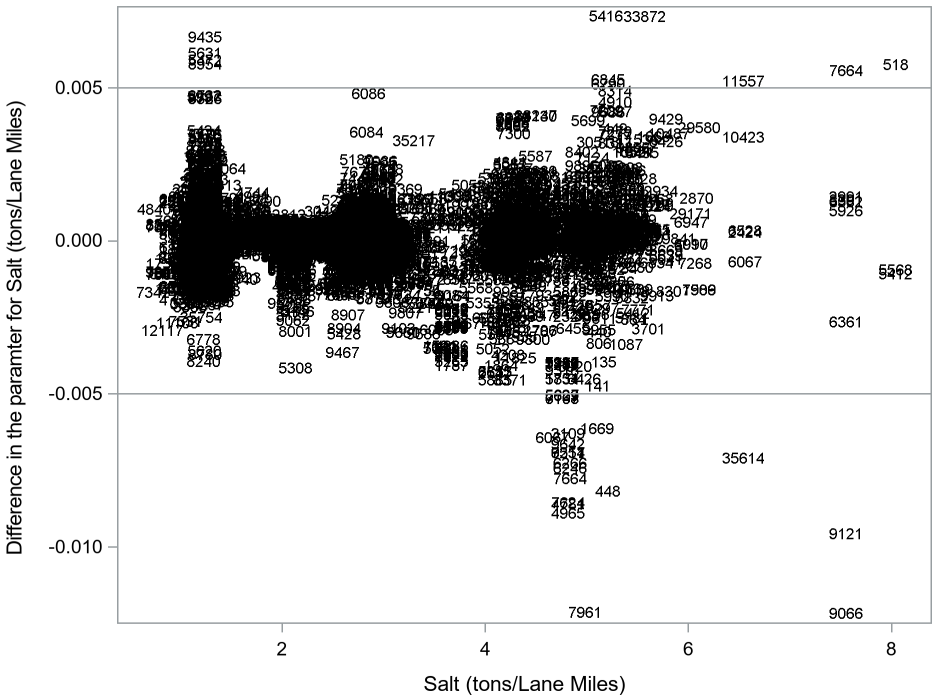

Figure G-53. Plot showing the influence of individual observations on salt for culverts.

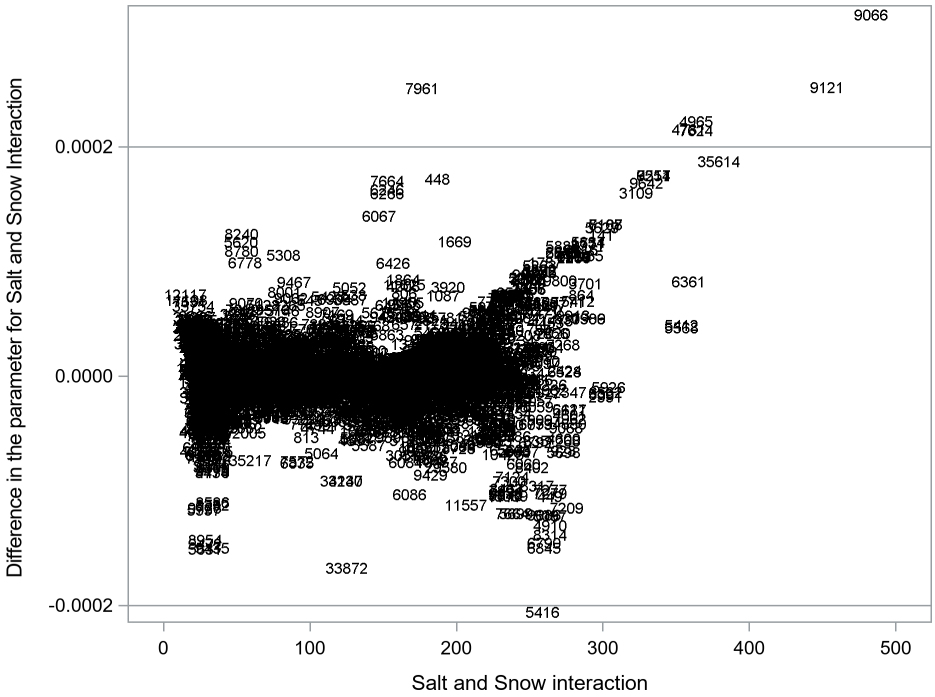

Figure G-54. Plot showing the influence of individual observations on salt and snow interaction for culverts.

Overall Fit for Culverts

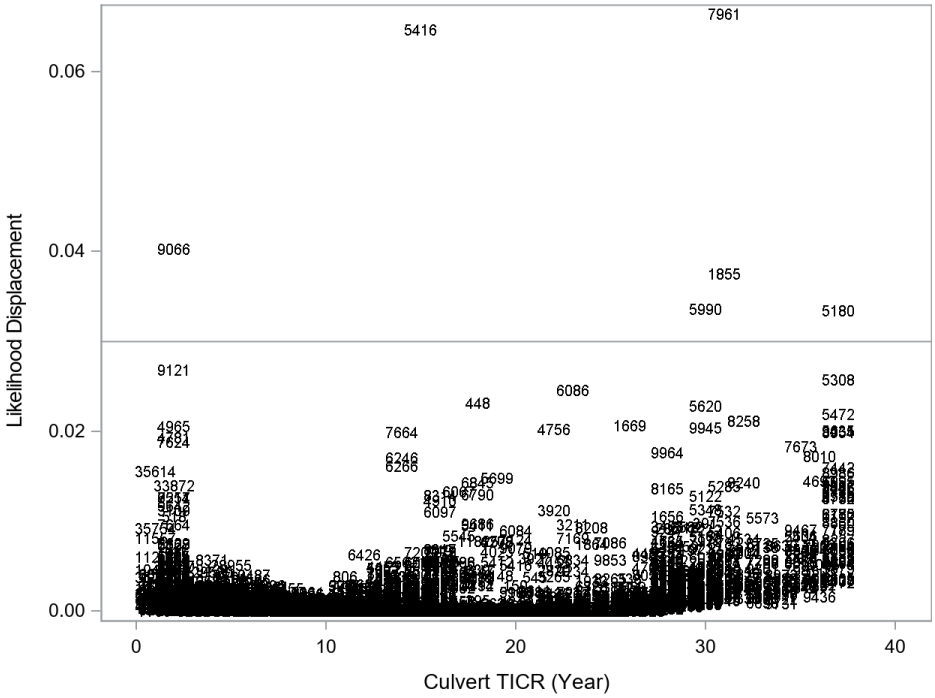

Figure G-55. Plot of likelihood displacement for the overall fit of the model for culverts.

Predictive Accuracy of the Cox Regression for Culverts

The predictive accuracy of the Cox regression for culverts is presented below using the Harrell's C-statistics. For culverts data set, there are 16,835,557 concordant pairs, 11,960,669 discordant pairs, and 1,358,495 tied-in-time pairs. Using equation (A-7), the C-statistics for substructures is 0.58. The area under the ROC curve (AUC) and the 95% confidence interval for substructures is shown in Figure G-56. As shown, the predictive accuracy of the Cox regression for superstructures is about 0.6 throughout the available data for culverts.

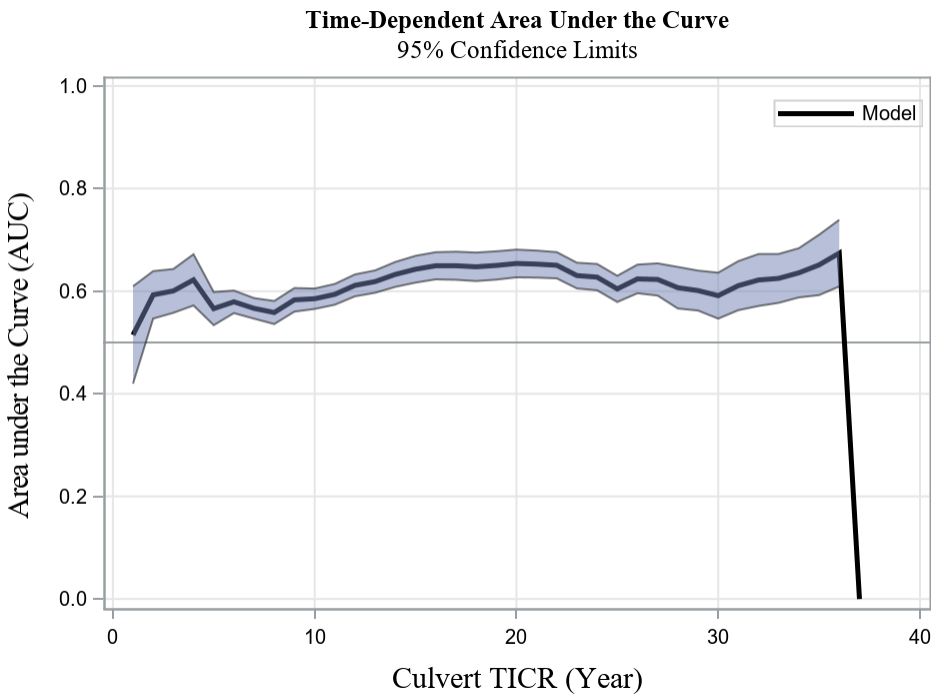

Figure G-56. Plot showing AUC for the time-dependent ROC curve for culverts.

REFERENCES

1. Salkind, N.J., *Encyclopedia of research design*. Vol. 1. 2010: Sage.
2. Allison, P.D., *Survival analysis using SAS: a practical guide*. 2010: Sas Institute.
3. Kaplan, E.L. and P.J.J.o.t.A.s.a. Meier, *Nonparametric estimation from incomplete observations.* 1958. **53**(282): p. 457-481.
4. Tobias, P.A. and D. Trindade, *Applied reliability*. 2011: CRC Press.
5. Collett, D., *Modelling survival data in medical research*. 2015: Chapman and Hall/CRC.
6. Kleinbaum, D.G. and M. Klein, *Survival analysis*. 2010: Springer.
7. Hosmer, D.W. and S. Lemeshow, *Applied survival analysis: regression modelling of time to event data*. 2002: Wiley.
8. Kutner, M.H., et al., *Applied linear statistical models*. Vol. 5. 2005: McGraw-Hill Irwin New York.
9. Minitab-Blog-Editor. *Enough Is Enough! Handling Multicollinearity in Regression Analysis*. 2013 [cited 2020 December 29]; Available from: https://blog.minitab.com/blog/understanding-statistics/handling-multicollinearity-in-regression-analysis.
10. Smith, T. and B. Smith. *Graphing the Probability of Event as a Function of Time Using Survivor Function Estimates and the SAS® System's PROC PHREG*. 2003.
11. Menard, S., *Applied logistic regression analysis*. Vol. 106. 2002: Sage.
12. UCLA, *Introduction to SAS. UCLA: Statistical Consulting Group*.
13. Klein, J.P. and M.L. Moeschberger, *Survival analysis: techniques for censored and truncated data*. 2006: Springer Science & Business Media.
14. SAS, I., *SAS/STAT User's guide, Version 9.2.* SAS Cary, NC, 1999.
15. Sakulich, A.R. and D.P. Bentz, *Increasing the service life of bridge decks by incorporating phase-change materials to reduce freeze-thaw cycles.* Journal of Materials in Civil Engineering, 2012. **24**(8): p. 1034-1042.